ANALYSIS OF THE CELL-ADHESION SIGNALING NETWORK AND ITS CROSSTALK WITH THE EPIDERMAL GROWTH FACTOR PATHWAY IN PRIMARY RAT HEPATOCYTES

by

TSIRISOA SOLON'I AINA ANDRIANARIJAONA

A Dissertation submitted to the

Graduate School-New Brunswick

Rutgers, The State University of New Jersey

and

The Graduate School of Biomedical Sciences

University of Medicine and Dentistry of New Jersey

In partial fulfillment of the requirements

For the degree of

Doctor of Philosophy

Graduate Program in Biochemistry

Written under the direction of

Dr. Charles M. Roth

And approved by

_____

_____

_____

_____

_____

New Brunswick, New Jersey

October 2013

ABSTRACT OF THE DISSERTATION

Analysis of the cell-adhesion signaling network and its crosstalk with the epidermal growth factor pathway in primary rat hepatocytes

By TSIRISOA SOLON'I AINA ANDRIANARIJAONA

Dissertation Director:

Dr Charles M. Roth

Cultured primary hepatocytes provide excellent platforms for the experimental study of the toxicology and the metabolism of various potentially harmful compounds. However, the usefulness of primary hepatocytes is significantly hampered by their loss of specific functions *in vitro* through a process called dedifferentiation. In general, dedifferentiation results from the loss of the normal balance of proliferation and differentiation, which are mutually exclusive in vitro. Therefore, a clear understanding of the mechanisms that drive hepatocyte proliferation in culture would certainly provide valuable information for the design of new cell culture systems.

This doctoral dissertation is focused on understanding the dynamical properties of the rat hepatocyte-adhesion signaling network and its crosstalk with the MAPK/ERK pathway. A major part of this thesis was focused on designing a mathematical model of the coupled integrin and E-cadherin/β-catenin signaling

pathways to analyze the property of their underlying control system. Combining bifurcation analysis with single-cell measurements, this study provided the evidence that the hepatocyte adhesion pathways exhibit a bistability in response to changes in PIP2 cellular levels, and thereby may undergo a switch between a strong integrin-based/weak E-cadherin-based adhesion, and a weak integrin-based/strong E-cadherin-based adhesion. Rat hepatocytes secrete fibronectin in culture, and this study showed that the strong integrin-based adhesion resulted from a fibronectin-mediated activation of the integrin pathway. A strong integrin-based adhesion primes the hepatocytes for a maximal responsiveness to EGF, which was characterized by a sustained activation of the MAPK/ERK pathway in mid G1 and the ensuing full cell commitment to proliferation. The adhesion-dependent priming was characterized by an upregulation of certain MAPK/ERK activators.

The overall results from this dissertation provide a better insight into the design of novel hepatocyte culture systems that will be more conducive to the preservation of hepatocyte differentiation. Additionally, the mathematical model that was designed in this study provides a foundation for future in-depth studies of the cell-adhesion network in various cell types.

ACKNOWLEDGEMENTS

Although my closest family and friends know me as a rather talkative person at times, I am just at loss for the proper words to express my eternal gratitude to all those who have nurtured and helped me to become who I am today. You have all done your best and I am fully appreciative of that.

To everyone, THANK YOU VERY MUCH and MAY YOU BE HAPPY!!!

TABLE OF CONTENTS

LIST OF FIGURES

LIST OF TABLES

Chapter 1

Introduction

1.1. **Liver**

1.1.1**. Anatomy and Histology**

The liver is the second largest and the heaviest organ in the body. Small hexagonal structures, commonly denominated "hepatic lobules" (**Figure 1.1**), constitute the functional unit of the liver. Each lobule is wrapped by connective tissue and surrounded by a system of vessels including the hepatic artery, the hepatic portal vein, and the bile ducts. The vast majority of the liver blood comes through the hepatic portal vein, and the remainder comes from the hepatic artery. The central vein runs through the center of each lobule, and bloods from the central veins are drained into the hepatic veins.

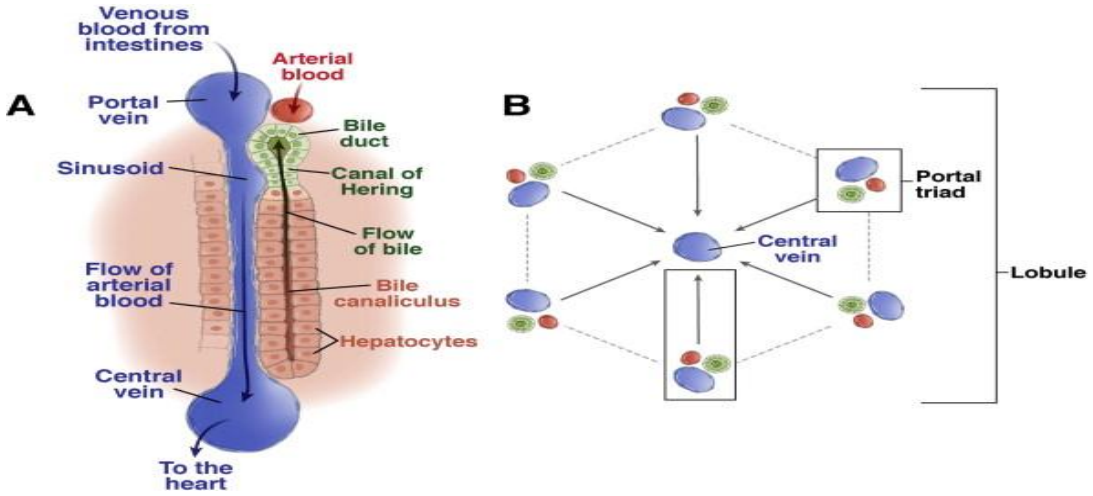

Figure 1.1. **Structure of a hepatic lobule** (Duncan AW, 2009)

Two major groups of cells, parenchymal and non-parenchymal cells, form the functional unit of the liver. The non-parenchymal cells include epithelial cells, smooth muscle cells, endothelial cells, macrophages or Kupfer cells, stellate cells, and Pitt cells. Parenchymal cells or hepatocytes constitute more than 80% of the mass of the normal liver, and perform most of the major functions attributed to that organ. Hepatocytes are arranged in a highly polarized manner into hepatic cords, which resemble two-dimensional sheets radiating from the central vein to the periphery of each hepatic lobule. The hepatic cords are separated by sinusoids, and each faces the space of Disse. Both ends of the hepatocyte are bordered by basal surfaces, where exchanges of metabolites with the blood take place. The apical surface resides halfway between the two opposing basal surfaces, where the secretions of bile and detoxification products take place. The lateral surface wraps around each hepatocyte, where cell-cell interactions through gap junctions and cell-cell adhesions through tight and adherence junctions exist.

1.1.2. **Physiology**

The liver performs several functions that are critical for the maintenance of homeostasis. It is the major site for the synthesis, regulation, and secretion of many critical blood and digestive components. As such, the liver can be classified as both as an endocrine and an exocrine gland.

The liver plays a central role in carbohydrate metabolism that is essential for the maintenance of a homeostatic blood glucose level. The postprandial elevation of

the blood glucose level triggers the glycogenesis (synthesis of glycogen) in the liver, whereas a low blood glucose level long after a meal induces the breakdown of glycogen (glycogenolysis) in the liver. The liver is also the site of gluconeogenesis, which is the synthesis of glucose from non- carbohydrate substrates (e.g. from the glucogenic acids).

Both the energy producing oxidative breakdown of fatty acids (β-oxidation) and their syntheses take place in the liver. The liver also synthesizes a large number of lipids such as triglycerides, cholesterol and many lipoproteins. Another important role of the liver is the synthesis of ketone bodies, which are the major source of energy for many cells such as the heart muscle cells and the renal-cortex cells.

The amino acid deamination, a critical step in the amino acid catabolism, happens in the liver. Similarly, the liver contains the enzymes responsible for the transamination reactions that are essential for the synthesis of new amino acids. Another important role of the liver is the synthesis of all major plasma proteins of (e.g. albumin, clotting factors…), with the exception of immunoglobins.

1.1.3. **Roles of the liver in detoxification**

The liver is central to the removal of most toxic compounds from the body. For example, the removal of free ammonia (a toxic by-product of amino acid breakdowns) through the urea cycle takes place in the liver. The liver is also

responsible for clearing non-hydrosoluble and potentially toxic xenobiotic compounds from the body.

1.2. **Primary hepatocytes**

There are three types of hepatocytes based on the proliferation and differentiation capacities: Type 1 cells or small hepatocytes include cells with high proliferation potential, type 2 cells include cells with limited proliferation capacity, and type 3 cells include terminally differentiated cells that have lost the capacity to proliferate. Type 2 and type 3 cells are qualified as mature hepatocytes; they assume most of the metabolic functions of adult the liver (Mossin L, 1994)

1.2.1. **Isolation and culture**

Rat hepatocytes are isolated using the well-established two-step perfusion process, an initial perfusion of the liver with a calcium-free buffer followed by another perfusion using a buffer containing collagenase. Following the disruption of cell-cell and cell-extracellular matrix (ECM) interactions in the liver, the resulting single cell suspension is subjected to a Percoll gradient centrifugation to isolate and purify the hepatocytes from the other cell types in the liver.

Purified hepatocytes are usually provided with an exogenous extracellular matrix (e.g. collagen, laminin, fibronectin) to facilitate their attachments and thereby promote their survivals. Collagen type I remains the most commonly used extracellular matrix in rat hepatocyte cultures.

1.2.2. **Advantages and limitations**

The usefulness of isolated hepatocytes for clinical cell transplantation and for temporary bioartificial organ support systems has been extensively studied and acknowledged. Furthermore, *in vitro* cultures of hepatocytes present an excellent platform for pharmacological, toxicological, and metabolic studies. One particular important example is the pharmacology and toxicology of xenobiotic compounds.

A major shortcoming of the usefulness of *in vitro* primary hepatocytes is the loss of a large number of liver specific functions, commonly called dedifferentiation. In particular, the levels of phase I Cytochromes P450 (CYP) decline by 80% to 90% within the first 24 hours of culture (Paine, 1990). CYPs assume primordial roles in the detoxification of numerous drugs and many foreign chemicals that may be present in the body.

1.3. **Cell Adhesion-regulated signaling pathways**

The cell adhesion complex is comprised of interacting molecular networks that are involved in the cell attachment to the extracellular matrix and to other surrounding cells (**Figure 1.2**). The preservation of the differentiated state of highly specialized epithelial cells requires a precise spatial organization of the transmembrane receptors mediating cell-ECM and cell-cell interactions. Hepatocytes are highly differentiated cells and their culture provides an excellent *in vitro* model for studying the interplay between signals that may affect cell behaviors in response to changes in their microenvironments. Signaling pathways involving integrins and E-cadherins dictate whether a switch between the hepatocyte differentiation and proliferation programs will take place in the presence of growth factors (Oda H, Cell shape, cell-cell contact, cell-extracellular matrix contact and cell polarity are all required for the maximum induction of CYP2B1 and CYP2B2 gene expression by phenobarbital in adult rat cultured hepatocytes, 2007) (Mizuno K, 1993).

1.3.1. **Cell-Extracellular Matrix associated signaling pathways**

Integrins are heterodimeric transmembrane cell surface receptors that are composed of two non-covalently associated α and β subunits. The binding specificity and the signaling property of each integrin receptor depend on the $\alpha\beta$ combination. Mature adult rat hepatocytes express mostly $\alpha1\beta1$ and $\alpha5\beta1$-integrin

receptors. Hepatocyte attachment to collagen and laminin occurs through the α1β1 integrin; whereas attachment to fibronectin depends on the α5β1 heterodimer.

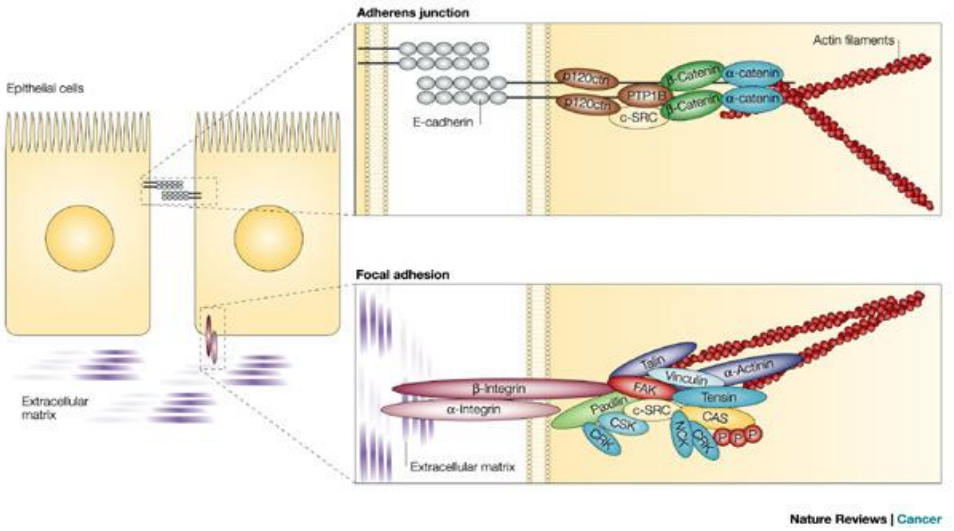

Figure 1.2. **Cell adhesion complexes**. Adherens junctions (cell-cell interaction) and focal adhesion (cell-extracellular matrix interaction) constitute the two main types of cell junction in epithelial cells (Yeatman, 2004).

The binding of the integrin extracellular domains to extracellular matrix molecules induces the clustering of integrins, and the recruitment and activation of mediator proteins via the integrin cytoplasmic tails. The adaptor protein talin, an early mediator of the integrin pathway (Partridge MA, 2006), recruits a phosphoinositide phosphate kinase leading to the synthesis of phosphatidylinositol-4,5-bisphosphate or PIP2 (Ling K, 2002). The enrichment in PIP2 at the adhesion sites facilitates the recruitment and the autophosphorylation (Y^{397}) of the tyrosine kinase FAK, followed by its Src-dependent activation. Active FAK exerts in return a

positive feedback on PIP2 through the tyrosine phosphorylation of the PtdIns Phosphate Kinase (Ling K, 2002), and is also important for the regulation of Rho-family GTPases. PIP2 is a low abundance membrane phospholipid that constitutes a major focal point for many signaling pathways, thus playing a pivotal role in the regulation of the growth/differentiation balance (Kimata T, 2006). Strong FAK activation has been associated to cell cycle progression (Owen KA, 2011) and the loss of hepatocyte specific function (Kim SH A. T., 2007). Nearly all extracellular matrix molecules contain binding sites for syndecans, a transmembrane proteoglycan, in addition to integrins. Full activation of cell-ECM related pathway requires the simultaneous ligations of integrins and syndecans to the extracellular matrix proteins. In particular, strong FAK phosphorylation (Wilcox-Adelman SA, 2002) and stabilization of PIP2 in the plasma membrane (Kwon S, 2009) require the full engagement of Syndecan-4.

1.3.2. **Cell-Cell associated signaling pathways**

Cell-cell junctions play a central role in the establishment and maintenance of cell polarity and tissue integrity in multicellular organisms. Three major types of cell-cell junctions can be found in vertebrates: gap junctions, which permit the communication between adjacent cells; tight junctions or zonula occludens, which play a central role in the establishment of the impermeability of the epithelial barrier; and the adherens junctions or zonula adherens. Adherens junctions play a critical role in the organization of the cytoskeleton, the formation of the other types

of cell junctions, and thereby play a central role in the regulation of cell and tissue behaviors. They can be structurally broken into three major components: transmembrane cadherins, armadillo family members, and cytoskeletal adapter proteins (Green KJ, Intercellular junction assembly, dynamics, and homeostasis, 2010).

E-cadherins are large transmembrane receptors that form homophilic bindings with local neighbors on adjacent cells, and their cytoplasmic domains are indirectly linked to the actin filaments through α-catenin and β-catenin. The expression and cellular distribution of β-catenin are tightly controlled in the liver, and in normal epithelial tissues. β-catenin is predominantly located at the plasma membrane where it interacts with E-cadherin to stabilize cell-cell interactions; additionally, the APC/Axin/GSK-3β-complex regulates the level of free cytoplasmic β-catenin through proteasome-mediated degradation. Conversely, the disruption of cell-cell adhesions combined with the stabilization of the β-catenin protein lead to the internalization of E-cadherin and the increase of free β-catenin. The accumulation of cytoplasmic β-catenin above a certain concentration threshold will induce its nuclear translocation (Kemler R, 2004) (Ramis-Conde I, 2008), where it interacts with TCF and upregulates the transcription of genes involved in cell proliferation. Mechanical stress or cell signaling events leading to tyrosine phosphorylations of the E-cadherin/catenin complex causes the loss of cell-cell adhesions. Growth factors, or abnormal mutations affecting the gene of β-catenin or

any of the components of the β-catenin degradation complex, stabilize β-catenin and potentiates its transcriptional property.

1.3.2. **Crosstalk**

The tyrosine kinases FAK and Src (Avizienyte E, 2005) and the small Rho-GTPases are among the prime candidates for the integration of cell-adhesion dependant signals. Integrin mediated activations of FAK and Src have been shown to disrupt the cadherin-catenin complex (Koenig A, 2006) , and the loss of E-cadherin leads to upregulation of the FAK protein level and its activity (Alt-Holland A, 2011). Mutual regulations also occur between Rho-family GTPases and FAK/Src. FAK may modulate RhoA activity due to its ability to bind to RhoA-GAP and RhoA-GEF (Tomar A, 2009); similarly, FAK may be both an upstream activator of Cdc42 (Myers JP, 2012), and an inhibitor in a paxillin-Nudel dependent manner (Shan Y, 2009). In return, active Cdc42 (Yang L, 2006) and RhoA (Wilcox-Adelman SA, 2002) may also play important roles in the regulation of FAK phosphorylation. Bidirectional signaling also occurs between E-cadherins and the Rho-family GTPases. The establishment and maintenance of E-cadherin-mediated adhesions depend on the activations of small GTPases at the sites of cell-cell junctions. In particular, Cdc42 and Rac1 play important roles in the microtubule-dependent delivery of E-cadherin to new adherens junction sites and the stabilization of the cadherin-catenin complex (Fukata M K. S., 1999) (Izumi G, 2004). De novo cadherin-mediated adhesions lead

to elevations of Cdc42 (Kim SH L. Z., 2000) and Rac1 (Nakagawa M, 2001) activities, and a repression of RhoA (Noren NK N. C., 2001).

1.4. **Growth Factor regulated signaling pathways**

1.4.1. **MAPK - ERK1/2 signaling pathways**

The mitogen-activated protein kinases (MAPKs) belong to a large family of serine/threonine kinases that are activated by certain growth factors, such as the epidermal growth factor (EGF). The binding of EGF to its receptor (EGFR) triggers the onset of a cascade of reactions leading to the activation of different isoforms of mitogen-activated extracellular signal regulated kinases (MEKs), which in turn activate specific MAPKs such as the extracellular signal-regulated kinases (ERKs) or the stress activated protein kinases (SAPKs). Although eight different ERK isoforms are known; ERK1/2 remain the best studied and have been identified as largely responsible for integrating and relaying external signals (from adhesion and growth factors) to the cell cycle machinery (Meloche S, 2007). Therefore, the nature of ERK1/2 activation constitutes a key determinant of whether a highly differentiated cell may or not irreversibly commit to the cell cycle and loses its function. Exposure to growth factor induces a biphasic activation of ERK1/2, a strong but short early activation followed by a second, less intense but sustained, activation. In primary rat

hepatocytes, the onset of the sustained activation also depends on the nature of the extracellular matrix and has been shown to be necessary to allow the crossing of the restriction point and the resulting full commitment to the cell proliferation mode.

ERK1/2 regulates cell growth, which is characterized by an extensive biosynthesis of macromolecules and organelles leading to a significant increase of the mass of the cell before the beginning of the cell division process. ERK1/2 increases the global protein synthesis by enhancing the activation of the mammalian target of rapamycin pathway, leading to a stimulation of the global mRNA translation (Servant MJ, 1996). Active ERK1/2 promotes the *de novo* synthesis of pyrimidine nucleotide by increasing the activity of the multifunctional CAD enzyme (Carbamoyl-Phosphate Synthetase 2, Aspartate Transcarbamylase, and dihydroorotase) (Evans DR, 2004).

The activations of ERK1/2 drive the G1/S transition by inducing the synthesis and accumulation of cyclin D1. Active ERK1/2 promotes the transcription of cyclin D1 by inactivating the antiproliferative transcription factors, such as Tob (Maekawa M, 2002), which recruit histone deacetylase to the cyclin D1 promoter (Yoshida Y, 2003). Furthermore, the promoter of cyclin D1 contains an “enhancer box” (E-Box) that responds to the AP1 (e.g. c-fos, c-jun…) and c-myc transcription factors. The sustained activations of ERK1/2 promote the activation and stabilization of the AP1 transcription factors. The C-terminal domain of AP1 proteins contains a target sequence for phosphorylation by active ERK1/2 leading to a further activation and stabilization (Murphy LO, 2002).

1.4.2. **PI3K/Akt signaling pathway**

The PI3K/Akt signaling pathway plays a central role in cell proliferation and differentiation and is particularly critical for G1/S progression in rat hepatocytes (Coutant A, 2002).

The PI3Ks, or Phosphoinositide 3-Kinases, phosphorylate the hydroxyl group on the D3 position of the inositol ring of membrane phosphoinositides. They are commonly activated by receptor tyrosine kinases (e.g. EGFR, integrin receptors) or by G-protein coupled receptors (GPCR). Phosphatidylinositol -3,4,5- trisphosphate (PIP3) is the main product of PI3K, and remains the most significant effector of the downstream targets of the PI3K/Akt signaling pathway. PI3Ks can be divided into three classes based on their structure and function (Rameh LE, 1999), and each class can be further classified into more subclasses. Class I PI3Ks are of particular importance since they are the only PI3Ks able to synthesize PIP3 from PIP2 in vivo (García Z, 2006).

Akt, also known as protein kinase B, is a serine/threonine kinase with three known families in mammals (Akt 1, 2, and 3). The activation of Akt comprises two distinct steps, translocation to the plasma membrane followed by phosphorylations at two specific amino acid residues (Chen R, 2001). Newly synthesized PIP3 recruit

Akt to the plasma membrane, the PIP3 synthesis involves class IA and class IB PI3Ks. At the plasma membrane, Akt is first phosphorylated by phosphoinositide-dependent kinase 1 (PDK1) at Thr^{308}, which then triggers the phosphorylation of Ser^{473} either through autophosphorylation or by the action of PDK2.

Akt plays a pivotal role in cellular processes such as cell survival, intermediate metabolism, proliferation and differentiation. In particular, the inhibitory effect of Akt on glycogen synthase kinase-3 (GSK-3) affects not only the glucose metabolism but also play a central role in the regulation of cell cycle progression (Luo Y, 2007) and cell survival (Song G, 2005).

1.5. **Hepatocyte dedifferentiation**

The precise molecular mechanism underlying the primary hepatocyte dedifferentiation process remains largely not understood. Dedifferentiation starts during the isolation process, and is rendered irreversible during the ensuing cell culture. The prevailing consensus states that dedifferentiation is caused by the loss of the "normal" balance between proliferation and differentiation, which results from a significant disturbance of the normal hepatocyte gene expression induced by the dramatic change in microenvironments of the cells during isolation and culture. Proliferation and differentiation are mutually exclusive in vitro; therefore, a cell commitment to enter into the proliferation mode will inexorably lead to an

irreversible dedifferentiation. In the intact liver, mature hepatocytes normally exist in the quiescent G0 phase of the cell cycle and remain highly differentiated, whereas they enter into the cell cycle and dedifferentiate during their isolations and cultures.

1.5.1. **Isolation-induced dedifferentiation**

The transcriptional repressions of liver specific genes starts during the isolation process itself (Paine AJ, 2004), whereas the expressions of other "common" genes remain largely undisturbed (Elaut G, 2006). The liver exposure to significant stresses (oxidative stress, loss of normal tissue structure, presence of endotoxins…) induces the release of proinflammatory cytokines such as TNFα and IL-6 (**Figure 1.3**). These cytokines ultimately trigger the process globally named "priming effect", which promotes the cell's exit from G0 and render them subsequently responsive to later exposure to growth factors. Many transcription factors that are associated with the priming effect also exert an inhibitory effect on hepatocyte specific proteins. The inhibition may happen at the protein level through direct protein-protein interactions (Tinel M, 2003) (Nikolaidou-Neokosmidou V, 2006) (Maeda Y, 2006), or at the transcriptional level through their binding to the gene's promoter regions of the liver-specific proteins (Hatzis P, 2006).

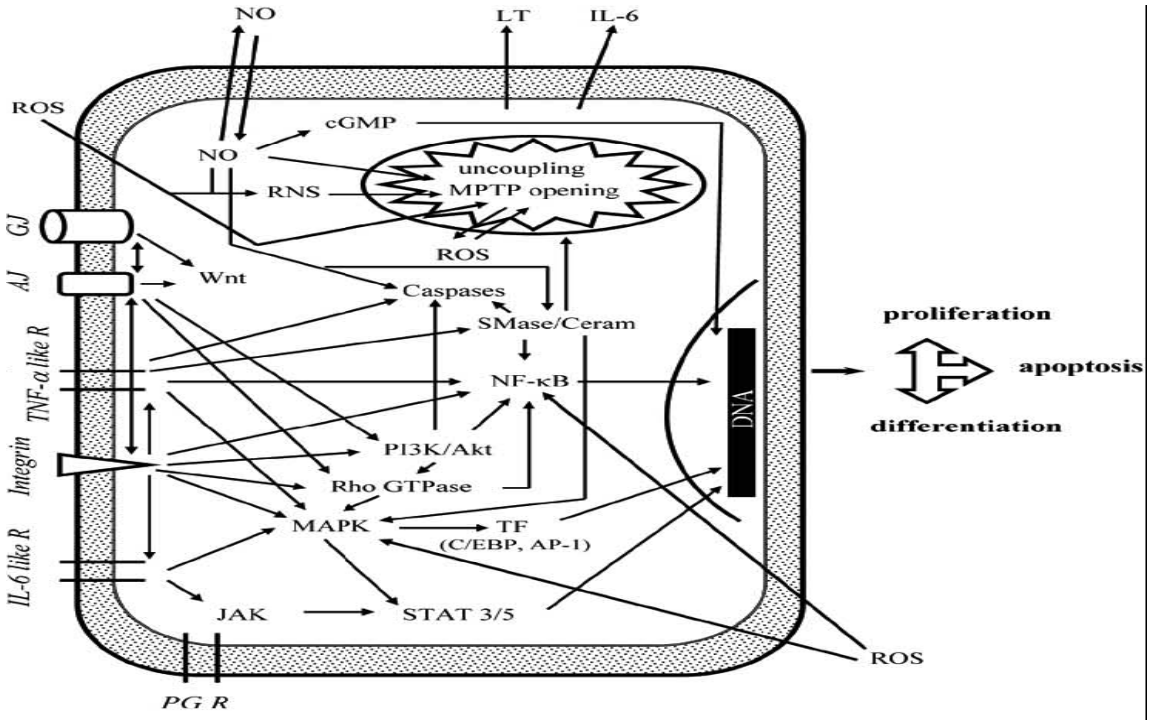

Figure 1.3: **Signaling pathways that are activated during rat hepatocyte isolation**. (Elaut G, 2006)

1.5.2. **Dedifferentiation during culture**

Mature hepatocytes exit the quiescent G0 phase after the isolation, and then undergo a G1 phase progression up to the restriction point located in mid-late G1 (Loyer P, 1996). The cells remain not fully committed to proliferation as long as they do not cross the restriction point; therefore, the crossing of the restriction point constitutes a point of no return beyond which dedifferentiation becomes irreversible. It has been shown in primary rat hepatocytes that the crossing of the restriction point requires the presence of a growth factor (Loyer P, 1996) and a culture on a permissive extracellular matrix.

Being an anchorage-dependent cell, hepatocyte entry into full proliferation mode requires an adhesion to a solid substratum. Primary hepatocytes usually require culture on an exogenous extracellular matrix to promote proper attachment and to ensure survival. Numerous studies have shown that the nature of the extracellular culture is of primary importance in determining how cultured hepatocytes would respond to the presence of growth factors. Cultures on collagen and fibronectin (Hodgkinson CP, 2000) promote the cell entry into full proliferation mode, and thereby are not conducive for the preservation of the hepatocyte differentiated states. Other extracellular matrices, such as laminin (Oda H, Cell shape, cell-cell contact, cell-extracellular matrix contact and cell polarity are all required for the maximum induction of CYP2B1 and CYP2B2 gene expression by phenobarbital in adult rat cultured hepatocytes, 2007) and matrigel (Schug M, 2008), are more amenable to the prevention of dedifferentiation by keeping the cells in a more or less complete growth-arrested state.

At the signaling level, the intensity and the duration of the activation of the MAPK/ERK pathway dictate the ultimate hepatocyte phenotype. In particular, a full commitment to proliferation requires a moderate but sustained activation from early/mid G1 phase to mid/late G1 phase (Fassett JT, 2003). Changes in the expression levels of specific constituents of the pathway usually affect the final output of a signaling pathway. For instance, primary rat hepatocytes can express three isoforms of the EGF receptor and the preferential upregulation of a particular isoform generates very different cellular reactions to the presence of EGF (Scheving LA, 2006). Hepatocytes in the intact liver and during early culture express high level

of EGFR (also called Erbb1), whereas cultured hepatocytes in mid G1 express high level of Erbb2 and a very low level of EGFR. The third isoform Erbb3 is only found in fetal hepatocytes and very briefly in mature hepatocytes during early culture. Numerous studies in various cell lines have shown that the activation of the MAPK/ERK through the Erbb1 receptor is intense but short lived, whereas the Erbb2 receptor can induce a moderate but sustained activation of ERK1/2. The changes in the expressions of certain scaffolding proteins may potentiate (or inhibit) the activation of specific MAPK effectors, such as protein kinases and the small GTPases, and thereby significantly alter the pathway output.

Similar to the effects of TNFα and IL6 in "priming" the cells during the isolation for an entry into the cell cycle, a second priming induced by the cell adhesion network during culture can also be considered. That second priming prepares the cells for an optimal responsiveness to EGF during mid G1, which will ensure the crossing of the restriction point. An ECM-induced "morphological priming" has been proposed (Semler EJ, 2001); changes in the overall shape of the cells define how they will respond to the addition of EGF in the growth medium. Fully spread hepatocytes enter into S phase and dedifferentiate, whereas rounded hepatocytes are growth arrested and maintain their specific functions. The activation of the MAPK/ERK is absent in hepatocytes with limited spreading, which may explain the growth arrest in rounded cells (Fassett J, 2006).

The absence (or scarcity) of cell-cell interaction also promotes higher stimulation of proliferation in the presence of growth factors (Oda H, Cell shape,

cell-cell contact, cell-extracellular matrix contact and cell polarity are all required for the maximum induction of CYP2B1 and CYP2B2 gene expression by phenobarbital in adult rat cultured hepatocytes, 2007). In general, the initial cell seeding density and the nature of the extracellular matrix determine the ultimate extent of cell-cell interactions in primary hepatocyte cultures. Low cell-cell interactions may lead to an increase of free β-catenin leading to its translocation to the cell nuclei. Nuclear β-catenin can facilitate proliferation in various manners; in particular, it can feedback into the MAPK/ERK pathway and promote a sustained activation (Kim D, 2007). Furthermore, active ERK1/2 can stabilize free β-catenin catenin leading to a reciprocal positive feedback between the MAPK/ERK and the β-catenin signaling pathways (Yun MS, 2005).

A better harnessing of the primary hepatocyte potentials requires an improved knowledge of the factors leading to the loss of the proliferation/differentiation balance in culture. The absence of a clear understanding of the interplay between the cell adhesion networks and the MAPK/ERK pathway in cultured hepatocytes constitutes one hurdle that needs be overcome.

1.6. **Dissertation hypothesis and overview**

The objective of this dissertation is to undertake a systematic analysis of the hepatocyte adhesion pathways and their modulatory effects on the MAPK/ERK pathway. The thesis research assigns a strong emphasis on the study of the dynamical properties of the signaling pathways, as well as the crosstalks between them. One goal of special interest is the identification of "important" pathway constituents, which can be specifically targeted in future culture systems. The thesis research aims to address some issues related to the regulation of the proliferation/differentiation balance in cultured primary rat hepatocytes including,

- Correspondence between the activation modes of the primary rat hepatocyte adhesion signaling pathways and the outputs of the MAPK/ERK pathway.

- Identification of potential targets of the primary rat hepatocyte adhesion pathways that may affect the outputs of the MAPK/ERK pathway

- Mechanism of regulation of the underlying control system of the primary rat hepatocyte adhesion pathways that may explain the switch between activation modes.

We hypothesize that a threshold activation of the cell adhesion-signaling network must be achieved in order to properly "prime" the cells for an optimal responsiveness to EGF, and thereby enter into full proliferation mode. The nature of the extracellular matrix and the magnitude of cell-cell interactions would

determine whether the aforementioned threshold could be reached or not. We further hypothesize that signaling induced by endogenous fibronectin constitutes a major cause of hepatocyte dedifferentiation. Primary rat hepatocytes secrete fibronectin (Hodgkinson CP, 2000), which can be rapidly adsorbed onto the original matrix and triggers dedifferentiation-inducing pathways.

In order to achieve the objective of the dissertation, an integrative approach combining experimental investigations and mathematical analysis was utilized. The need for such integrative method first arises from the inherent complexity of the signaling pathways of interest. We used cultures of freshly isolated rat primary hepatocytes at different culture conditions, such as varying seeding density or cultures on different extracellular matrices that are known to elicit distinct phenotypes. Specific signaling pathway components were also targeted, either through the use of specific activators/inhibitors, gene silencing, or plasmid transfections, in order to elucidate their mechanism of regulation and/or to identify their roles within their host pathways. Mathematical models provide valuable support for experimental designs, and help to detect unexpected mechanism that could not be determined through reductionist experimental approaches. Furthermore, the use of mathematical models provides a mean to gain an intuitive understanding of the principles underlying the signaling network properties within a more restricted context. We designed a simplified mathematical model of the cell adhesion pathways using a system of coupled ordinary differential equations (ODE) ; bifurcation theory was used to gain an insight into the specific properties of the cell

adhesion pathways that may explain the loss of specific functions of primary rat hepatocytes in culture.

The overall thesis aims are as follows:

1. To investigate the adhesion-dependent regulation of the MAPK/ERK pathway around the G1/S transition in primary rat hepatocytes.

2. To characterize the properties of the cell adhesion signaling networks in primary rat hepatocytes.

3. To analyze the dynamical properties of the cell adhesion pathways in primary rat hepatocytes

Chapter 2

Materials and Methods

2.1. **Materials**

Male Sprague Dawley rats were purchased from Taconic Farm. Ketamine and Xylazine were obtained from Henry Schein. Collagenase type IV, and Percoll were purchased from Sigma. Collagen type 1 (from rat tail), and matrigel were supplied by BD Biosciences. William E media, penicillin, fetal bovine serum (FBS), insulin, dexamethasone, epidermal growth factor (EGF), and proline were also supplied by Sigma. Glutamax® and sodium pyruvate were ordered from Life Technologies. PF-562271 was supplied by AdooQ BioScience. Silencer® Select Myc siRNA, integrin α1 siRNA, integrin α5 siRNA, syndecan-4 siRNA, Lipofectamine RNAiMax, and Lipofectamine LTX were ordered from Life Technologies. The phospho-Erk1/2 (T^{202}/Y^{204}) antibody, ERK1/2 antibody, phospho-FAK (Y^{397}) antibody, FAK antibody, cdc42 antibody, and RhoA antibody were ordered from Cell Signaling Technology. The anti-β-catenin antibody was purchased from Sigma. The phospho-FAK (Y^{576}, ^{577}) antibody was supplied by Abcam.

2.2. **Methods**

2.2.1. **Hepatocyte isolation**

Krebs-Ringer Bicarbonate (KRB) buffer was prepared by the dissolving of 14.27 g NaCl, 4.2g $NaHCO_3$, 2g glucose, 9.53 HEPES, and 0.84g KCl in 2000 ml of distilled water, with the final pH adjusted to 7.4.

Hepatocytes were isolated from male Sprague Dawley rats, weighting between 150-200g, using the widely established double-perfusion system (Seglen, 1976). The rat was first anesthetized through an intraperitoneal injection of 0.2 ml of ketamine/xylazine mix (1:9 v/v). A two-stage perfusion through the hepatic portal vein was then performed at 37^{o}C in the continuous provision of oxygen. In the initial stage of, the liver was perfused with 300 ml of KRB buffer containing 5 mM of ethyleneglycol-bis(aminoethylether)-tetraacetic acid (EGTA) to break cell-cell interactions and facilitate the cell dispersions. In the second stage, collagenase type IV (1 mg/ml) in 200 ml of KRB buffer supplemented with $CaCl_2$ (10 mM) was used to dissolve the extracellular matrix.

To isolate the hepatocytes from the other cell types, the liver was shaken very gently in a fresh and ice-cold KRB buffer to free the cells from the dissolve liver capsules, then filtered through a sterile 100μm nylon mesh followed by a gentle centrifugation (50g for 5 min) at 4^{o}C. The cell pellets were resuspended in a Percoll buffer diluted with fresh KRB (final concentration ~44% v/v), and centrifuged at 1000g for 5 min at 4^{o}C to collect the intact hepatocytes in the pellet. The pellet was

rinsed two times with fresh ice-cold KRB, and the cells were resuspended in Williams E culture medium. The cell count and viability were evaluated using Trypan blue (0.4%).

2.2.2. **Hepatocyte culture**

Basal Medium: William E medium supplemented with Glutamax® (1mM), sodium pyruvate (1 mM), L-Proline (30 mg/l), dexamethasone (50 nM), penicillin (100 U/ml), streptomycin (0.1 mg/ml).

All cell cultures were done in a humidified 10% CO_2 incubator at 37°C. Freshly isolated hepatocytes were cultured on collagen film-coated dishes (5 μg /cm^2) or on matrigel gel-coated dishes in basal medium supplemented with 5% FBS. The cells were left for about 3 h, and then the culture medium was replaced with a serum-free basal medium with or without insulin (50 mU/l) and EGF (50 ng/l). Unless stated otherwise, the cells were seeded at a density of 70,000 cells/cm^2.

2.2.3. **Western blotting**

At the indicated time points, the plates were washed two times with ice cold PBS and the cells were lysed in RIPA buffer (50 mM Tris-HCl, 1% NP-40, 0.5% sodium deoxycholate, 0.1 % SDS, at pH 7.8) supplemented with protease inhibitors (cOmplete® inhibitor cocktail, Roche) and phosphatase inhibitors (Phosphatase

inhibitor cocktails 2 and 3, Sigma). The cell lysates were clarified by centrifugation at 15,000g for 15 min at 4°C, and the total protein concentrations were evaluated using the BCA assay (Pierce™ BCA Protein Assay Kit). The clarified lysates were diluted in Laemmli sample buffer (Sigma) supplemented with 5% (v/v) β-mercaptoethanol, and boiled for 15 min.

Proteins were separated by sodium dodecyl sulfate polyacrylamide gel electrophoresis (SDS-PAGE), using 10 % or 12% resolving gel, and then transferred to polyvinylidene fluoride (PVDF) membranes. The membranes were incubated with specific primary antibodies from rabbit overnight at 4°C. For detection, goat anti-rabbit IgG conjugated with horse peroxidase (Santa Cruz Biotechnology, CA) and electrochemiluminescence (Pierce ECL Plus®) method were used according to the manufacturer's instructions.

Chapter 3

Analysis of the adhesion-dependent regulation of the growth factor pathway in primary rat hepatocytes

3.1. Introduction

EGF is one of the major inducers of hepatocyte proliferation both *in vivo* and *in vitro*. The EGF-dependent activation of the MAPK/ERK pathway is necessary for the onset of the G1/S transition. Numerous studies have shown that molecular structure and the physical property of the extracellular matrix have a significant impact on how hepatocytes respond to the presence of EGF in culture. Cultures on laminin, matrigel, and collagen gel (soft and malleable) do not induce a G1/S transition; whereas cultures on the rigid collagen film do. A sustained activation of the MAPK/ERK pathway from mid to late G1 is required for the crossing of the restriction point . Such activation depends on the levels of expression (and possibly the degree of activation) of specific pathway components, which might be directly or indirectly modulated by the cell adhesion-priming effect from early to mid G1.

The EGF receptors constitute a very likely target for the cell adhesion-induced priming. Mature hepatocytes can express three different isoforms, EGFR (or Erbb1), Erbb2, and Erbb3. Erbb3 is only expressed for a very short time during early culture, and does not have a noticeable impact on the activation of the pathway. EGFR is abundant in the intact liver but its level decreases significantly during culture. Hepatocytes in the intact liver do not express Erbb2; however, its level of expression increases significantly starting from early/mid G1. The activation of the EGF receptors involves a binding to EGF followed by a dimerization. EGFR transmits signals either as a homodimer (EGFR-EGFR) or as a heterodimer with Erbb2 (EGFR-Erbb2), while Erbb2 can only work as a heterodimer with EGFR. Active EGF

receptor dimers undergo internalization and can be either recycled back to the plasma membrane for a new round of activation or shipped to the lysosomes for a full proteolysis. EGFR homodimers undergo fast internalization and a lower rate of recycling, whereas the heterodimers are internalized at slower rates and recycled back to the plasma membrane at much higher rates (Hommelgaard AM, 2004).

The family of scaffold proteins IQGAPs constitutes another potential target for cell adhesion priming. The IQGAPs belong to a conserved group of small GTPase-binding proteins. Three known isoforms, IQGAP1, IQGAP2, and IQGAP3, are expressed in mammalian cells with two of them directly linked to the cell adhesion system. The downregulation of IQGAP1 impedes the activation of the MAPK/ERK pathway (Roy M, IQGAP1 is a scaffold for mitogen-activated protein kinase signaling, 2005). IQGAP1 interacts with the EGFR receptor (McNulty DE, 2011), Raf (Ren JG, 104), and ERK (Roy M, IQGAP1 binds ERK2 and modulates its activity, 2004). It also interacts with the active forms of Cdc42 and Rac1, which is crucial for the formation and the stabilization of the E-cadherin-mediated cell-cell adhesion (Fukata M W. T., 2002). Active Cdc42 (and/or Rac1) prevents the IQGAP1-induced disassembly of the E-cadherin/α-catenin/β-catenin trimeric complex and thereby prevents the disruption of cell-cell interactions (Fukata M K. S., 1999). IQGAP2 binds to Cdc42 and stabilizes its active form (Cdc42-GTP); it is largely believed to be a tumor suppressor (Xie Y, 2012) . IQGAP3 binds to Ras and also stabilizes its GTP-bound form (Nojima H, 2008), and is considered to be a MAPK/ERK activator.

The connection between the cell adhesion pathways and the MAPK/ERK pathway likely occurs through molecules with at least two specific properties. First, their level of expression (and/or activity) must be tightly regulated and cell adhesion-related. And second, they should be involved in both the growth phase and the division phase of the cell cycle. The transcription factor c-myc appears to be a near perfect candidate as a connector between the cell-adhesion and the MAPK/ERK pathways. The integrin pathway can regulate the transcription of c-myc in a β1 integrin-dependent manner (Benaud CM, 2001). The c-myc mRNA and protein have very short half-lives and their expressions are tightly regulated at multiple levels; very small changes in c-myc expression are enough to induce a significant phenotypic switch. Furthermore, the knockdown of c-myc has been shown to significantly extend the duration of the pre and post-restriction stages of the cell cycle (Schorl C, 2003).

Herein, we report on the effects of the hepatocyte adhesion pathways on the MAPK/ERK pathway. We hypothesize that a strong integrin-based adhesion would cause the induction of the second and sustained activation of the MAPK/ERK pathway. Cell cultures on different extracellular matrices, which elicit opposing phenotypes, were used to provide a general overview of the relationship between the pathways. A cell permeable specific FAK inhibitor was used to evaluate the direct and specific impact of the integrin pathway, whereas the calcium chelator EGTA was utilized to evaluate the impact of the E-cadherin pathway. Our findings suggest the cell adhesion-dependence of the sustained ERK activation, which occurs through the upregulation of specific MAPK/ERK pathway activators.

3.2. **Materials and methods**

3.2.1**. Protein analysis**

Rabbit anti-Erk 1/2, rabbit anti-phospho Erk 1/2, or rabbit anti-cyclin D1were used in western blot analysis as described in chapter 2.

3.2.2. **Gene expression analysis by Real Time PCR**

All reagents, except the specific primers for the amplification/detection step, were purchased from Qiagen (Qiagen, CA). Total RNA were prepared using Qiagen Miniprep, and the reverse transcription step was performed using the QuantiTect® Reverse Transcription kit. All specific primers (Supplementary information) were designed using the freeware Primer3, and were synthesized by Integrated DNA Technologies. The amplifications, detections, and data collections were performed using QuantiFast SYBR Green PCR Kit on Roche Cycler 480 (Roche Diagnostics, IN). Data analysis were performed on Microsoft Excel using the Pfaffl method (Pfaffl, 2001)

3.2.3. **RNA silencing**

The silencing of c-myc was performed using a validated c-myc specific siRNA (Silencer® Select siRNA), and Lipofectamine RNAiMax®, which were both purchased from Life Technologies.

3.3. Results

3.3.1. Kinetics of the MAPK/ERK pathway activation

To investigate the effects of the extracellular matrix on the activation of the MAPK/ERK pathway, the phosphorylations of p42/p44 ERK were analyzed in rat hepatocytes on collagen film or matrigel at varying times following the addition of EGF. An early transient activation of p42/p44 ERKs occurred on both extracellular matrices, and a low activation level was maintained in hepatocytes on matrigel for all remaining time points. However, the cells on collagen expressed a second phase of moderate p42/p44 ERK phosphorylations that lasted for more than twenty-four hours (**Figure 3.1**).

The expressions of cyclin D1 were also evaluated to correlate the activation of MAPK/ERK with the crossing of the restriction point, which is characterized by a strong upregulation of cyclin D1. As expected, the hepatocytes grown on matrigel did not express cyclin D1 whereas those on collagen expressed significant amount of cyclin D1 after 48 hours of culture (**Figure 3.1**).

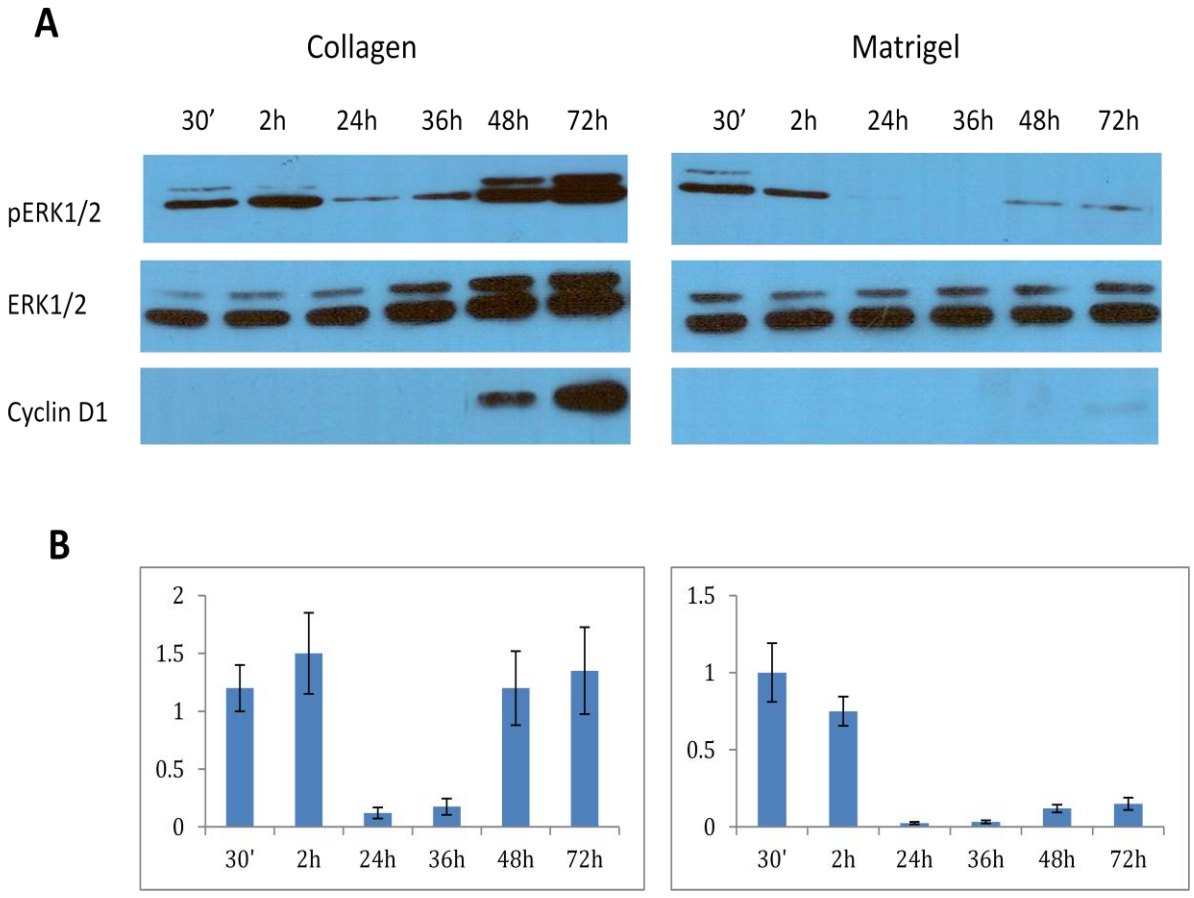

<u>Figure 3.1</u>. Activation profiles of the MAPK/ERK signaling pathway in rat hepatocytes on collagen and matrigel. **(A)** Rat hepatocytes were seeded onto collagen-coated or matrigel-coated plates. At the indicated time points, total cell lysates from hepatocytes on collagen or matrigel were collected and analyzed by western blot using rabbit anti-phospho Erk 1/2, rabbit anti-Erk 1/2, and rabbit ant--cyclin D1. **(B)** Densitometries were performed for all time points. The bars represent the ratios between active Erk1/2 and total Erk1/2, each bar was obtained from three independent experiments.

In order to establish the relationship between the sustained phase of MAPK/ERK activation and the integrin pathway, hepatocytes on collagen were exposed to the specific FAK inhibitor PF-562271 (Stokes JB, 2011) in an EGF-free culture medium for at least 24 hours before switching to a fresh medium containing EGF. Primary rat hepatocytes progress from early G1 to the restriction point in an EGF-independent manner; therefore, all cells had not crossed the restriction point at the time of their first exposure to EGF (48 hours after plating). Hepatocytes in the control group (no FAK inhibition), expressed a sustained phosphorylations of p42/p44 ERKs after the addition of EGF to the culture media. However, prior exposure to the FAK inhibitor induced a decrease in the intensity of the MAPK/ERK pathway following EGF addition (**Figure 3.2**). These results suggest that the sustained MAPK/ERK activation in mid/late G1, and the ensuing crossing of the restriction point, requires a strong activation of the integrin pathway.

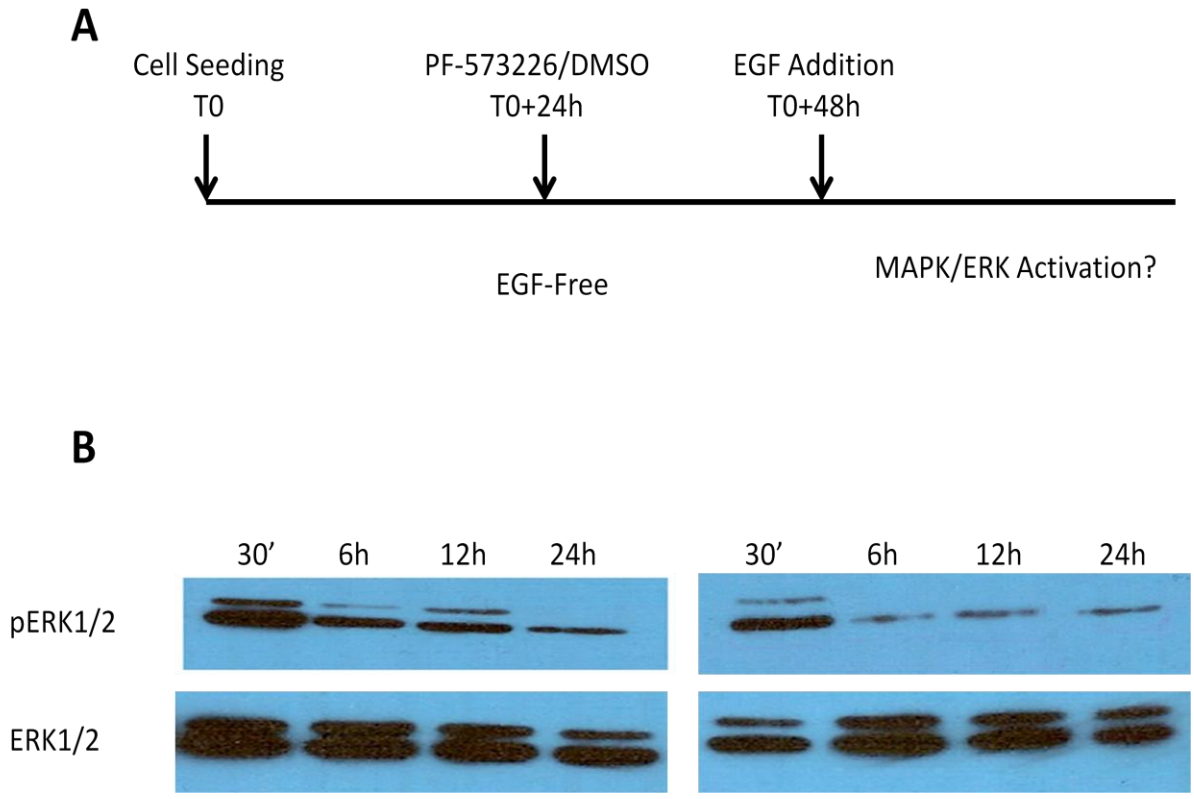

<u>Figure 3.2</u>. Effects of FAK inhibition on the activation of MAPK/ERK pathway in rat hepatocytes on collagen. **(A)** Schematic of the experimental approach. Rat hepatocytes were left to attach on collagen in EGF-free culture media. After 24 hours, either DMSO (control) or PF-573226 was added to the culture media. EGF was added after 24 hours, and the activations of the MAPK/ERK were evaluated. **(B)** At the indicated time points after EGF addition, cell lysates from the DMSO control (left) and the cells treated with PF-573226 (right) were collected and analyzed by western blot using rabbit anti-phospho Erk 1/2, rabbit anti-Erk 1/2.

3.3.2. **Cell adhesion effects on the gene expressions of the MAPK/ERK pathway effectors**

The gene expressions of MAPK/ERK effectors, which are also known to be directly or indirectly involved in the cell adhesion pathway, were evaluated in rat hepatocytes on collagen and matrigel. Higher gene expressions of effectors with cell growth-inhibiting properties were observed in hepatocytes on matrigel compared to those on collagen. Compared to hepatocytes on collagen, the gene expression of the scaffolding protein IQGAP2 on matrigel was more than two times higher after 48 hours and more than four times higher after 72 hours (**Figure 3.3**). Similarly, the gene expressions of Tob1 (an Erbb2 inhibitor) were approximately three times higher after 48 and 72 hours in hepatocytes on matrigel compared to those cultured on collagen (**Figure 3.3**). Nevertheless, the gene expressions of IQGAP2 and Tob1 underwent a sharp decline on both extracellular matrices when compared to the levels in freshly isolated hepatocytes (**Figure 3.3**).

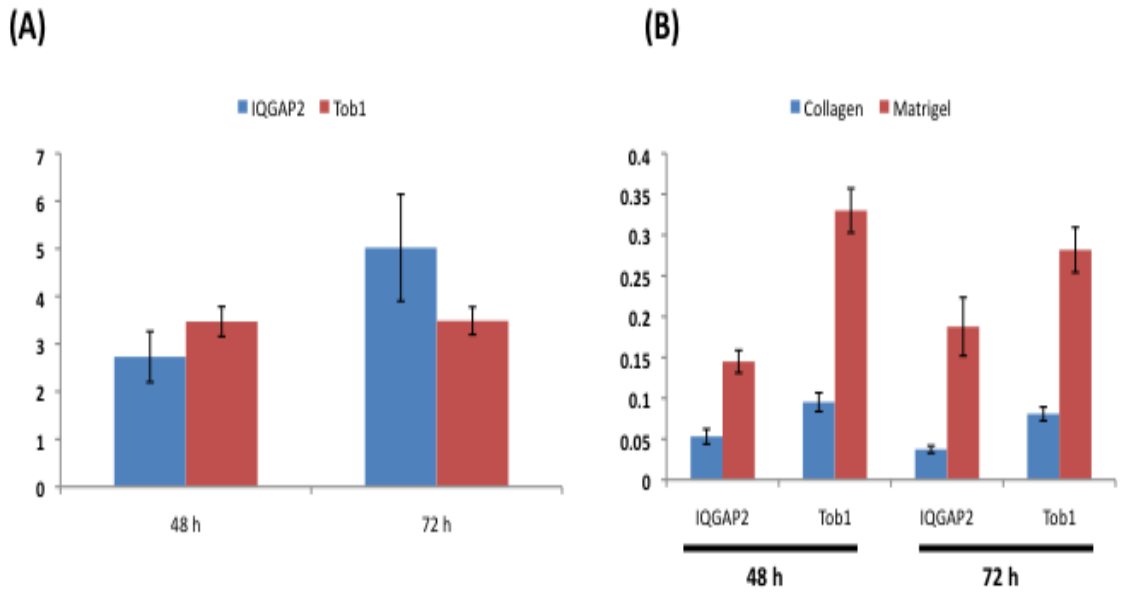

Figure 3.3. **Gene expression kinetics of MAPK/ERK pathway inhibitors in hepatocytes on collagen and matrigel**. Rat hepatocytes were seeded on collagen-coated or matrigel-coated plates. The gene expressions of IQGAP2 and Tob1 were evaluated by real-time PCR at the indicated time points. **(A)** Gene expressions of IQGAP2 and Tob1 on matrigel compared to their corresponding expression levels on collagen. **(B)** Gene expressions of IQGAP2 and Tob1 on matrigel or collagen compared to their corresponding expression levels in freshly isolated hepatocytes.

Contrary to the trend of the gene expressions of growth-inhibiting effectors, hepatocytes on collagen showed higher gene expressions of cell growth-promoting properties than those on matrigel. While no significant difference in IQGAP1 gene expression was observed in hepatocytes on matrigel compared to freshly isolated hepatocytes, increases of four times or more were found in hepatocytes on collagen.

Similarly, cultures on matrigel did not affect the expression of Erbb2 whereas cultures on collagen upregulated the gene expression of Erbb2 by more than 20 times. Finally, hepatocytes on matrigel showed about 70% downregulation in the expression of IQGAP3 compared to freshly isolated hepatocytes. On the contrary, an about eight-fold increase in the gene expression of IQGAP3 was observed in hepatocytes on collagen (**Figure 3.4**).

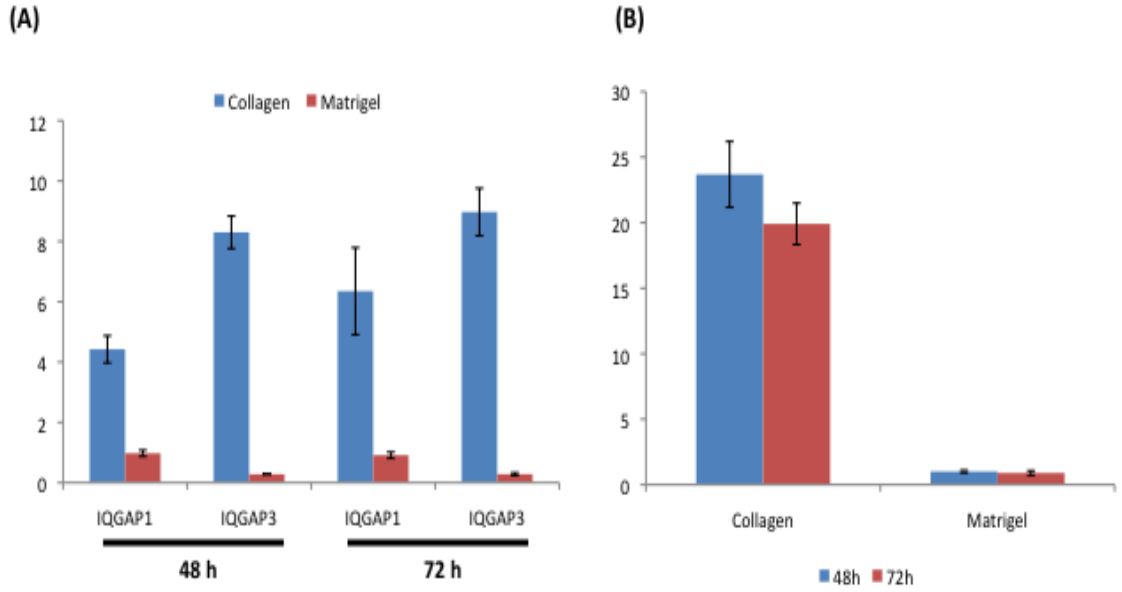

Figure 3.4. **Gene expression kinetics of MAPK/ERK pathway activators in hepatocytes on collagen and matrigel**. Rat hepatocytes were seeded on collagen-coated or matrigel-coated plates. The gene expressions of IQGAP1, IQGAP3, and Erbb2 were evaluated by real-time PCR at the indicated time points. (A) Gene expressions of IQGAP1 and IQGAP3 on matrigel or collagen compared to their corresponding expression levels in freshly isolated hepatocytes. (B) Gene expressions of Erbb2 on matrigel or collagen compared to its corresponding expression levels in freshly isolated hepatocytes.

While the expressions of Erbb2, IQGAP1, IQGAP2, and Tob1 were not affected by the presence of EGF; the transcription of IQGAP3 appeared to be EGF-dependent where significant upregulations started in mid-G1 phase (48 hours post seeding). In order to further confirm the EGF-dependence of IQGAP3 transcription, the cells were cultured in EGF-free media for 48 hours then switched to culture media containing EGF. An upregulation of IQGAP3 gene expression occurred 24 hours after the addition of EGF, with a more substantial increase after 48 hours (**Figure 3.5**).

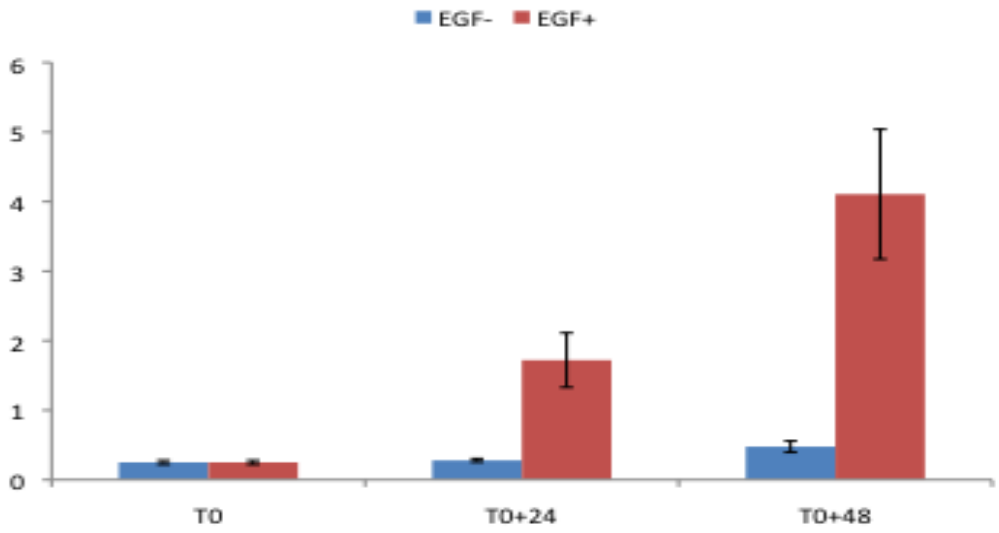

Figure 3.5. EGF-dependence of IQGAP3 transcription. Rat hepatocytes were seeded on collagen, and maintained in EGF-free culture media. After 48 hours (T0 on the figure), the cells were switched to culture media containing EGF and the gene expressions of IQGAP3 were quantified by real-time PCR at the indicated time points.

Because of the apparent influence of the extracellular matrix on the gene expressions of the MAPK effectors mentioned above, it was of interest to investigate

the involvement of integrin pathway in the regulation of their gene expressions by using a specific inhibitor of focal adhesion kinase (FAK). The inhibition of FAK did not exert any effect on the expression of IQGAP1, IQGAP2 and Tob1 (**Figure 3.6**). However, the inhibitor induced a small decrease in the expression of Erbb2 (about 30 %), and a significant downregulation of the scaffolding protein IQGAP3 (about 90 %) (**Figure 3.6**).

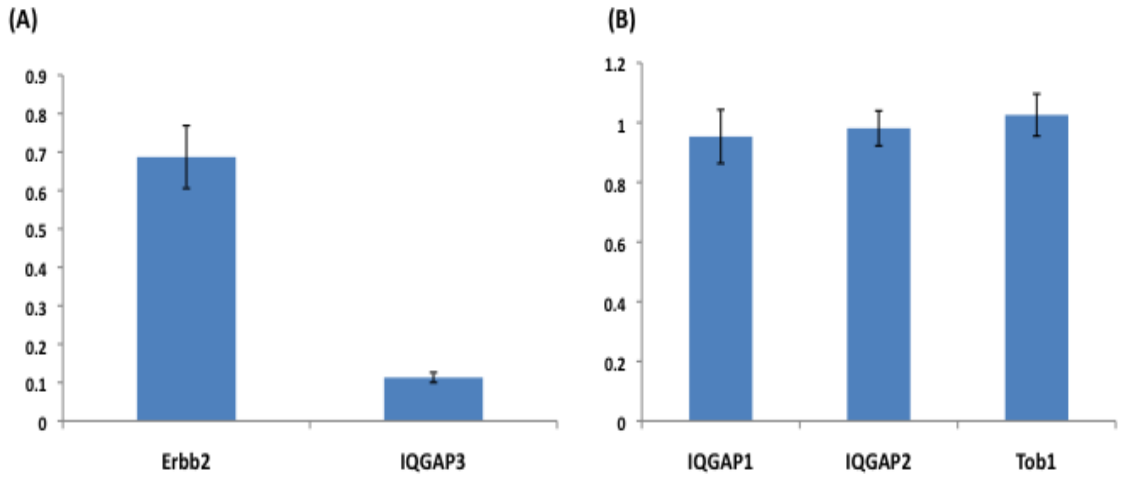

Figure 3.6. **Effects of FAK inhibition on the transcription of the MAPK/ERK pathway effectors**. Rat hepatocytes were cultured on collagen. After 24 hours, the cells were switched into culture media containing either DMSO (control) or PF-573226 (0.5 μM) and left to incubate for another 24 hours. The gene expressions of the MAPK/ERK pathway effectors were quantified by real-time PCR. **(A)** Gene expressions of Erbb2 and IQGAP3 in hepatocytes exposed to PF-573226,

standardized to their corresponding expressions levels in hepatocytes treated with DMSO alone. **(B)** Gene expressions of IQGAP1, IQGAP2, and Tob1 in hepatocytes exposed to PF-573226, standardized to their corresponding expressions levels in hepatocytes treated with DMSO alone.

3.3.3. **Cell adhesion effects on the induction of c-myc**

The hepatocytes adhesion-priming effect on the MAPK/ERK pathway may occur through the transcription factor c-myc. To investigate the effects of the extracellular matrix on c-myc transcription, the gene expressions of c-myc were evaluated in hepatocytes on collagen and on matrigel (**Figure 3.7**). At all time points, the transcription levels of c-myc in hepatocytes on collagen were at least two-times higher compared to the transcription levels on matrigel, which suggested an effect of the extracellular matrix on c-myc expression. Furthermore, the c-myc RNA levels in hepatocytes on collagen, in the presence or absence of growth factor, were consistently about twice higher compared to hepatocytes from the intact liver with an unexpected stronger expression levels in hepatocytes not exposed to any growth factor. The protein levels of c-myc were initially identical regardless of the growth factor conditions; however, a more significant protein expression of c-myc only occurred in hepatocytes exposed to EGF after 48 hours of culture (**Figure 3.8**). To further establish a direct link between the integrin pathway and c-myc transcription, hepatocytes on collagen were exposed to a FAK inhibitor.

Surprisingly, the addition of FAK inhibitor, even at very high concentration, did not affect the transcription levels of c-myc (**Figure 3.9**).

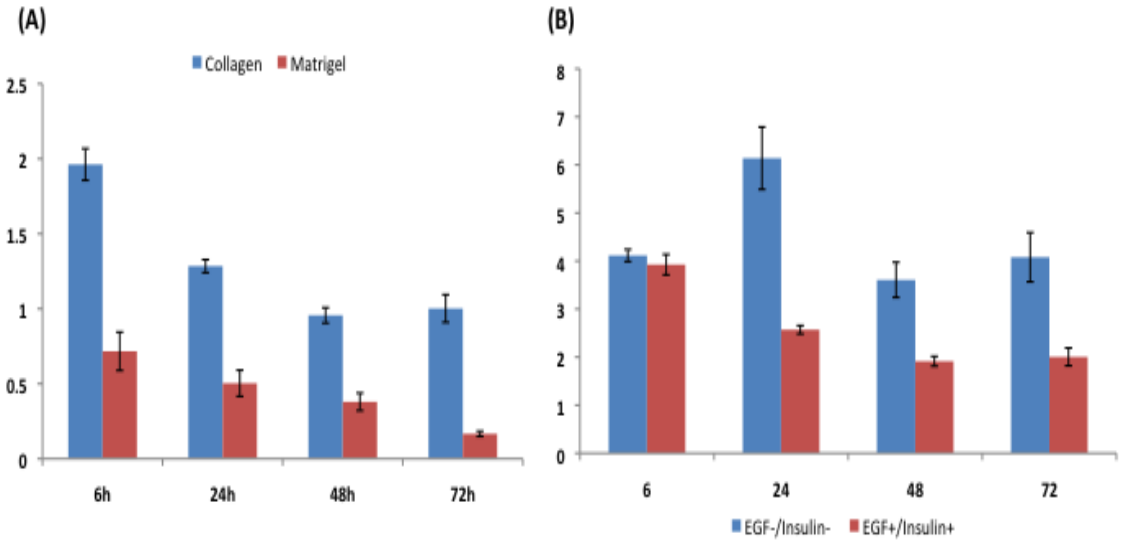

Figure 3.7. Gene expressions of c-Myc in rat hepatocytes on collagen and on matrigel. Rat hepatocytes were cultured on collagen or matrigel, and the gene expressions of c-myc were evaluated at the indicated time points by real-time PCR. (A) Gene expressions of c-Myc on collagen or matrigel, standardized to the c-myc mRNA level in the intact liver. (B) Gene expressions of c-Myc in hepatocytes on collagen that were cultured either in basal culture media (EGF-/Insulin+) or in the standard culture media (EGF+/Insulin+), standardized to the c-myc mRNA level in the intact liver.

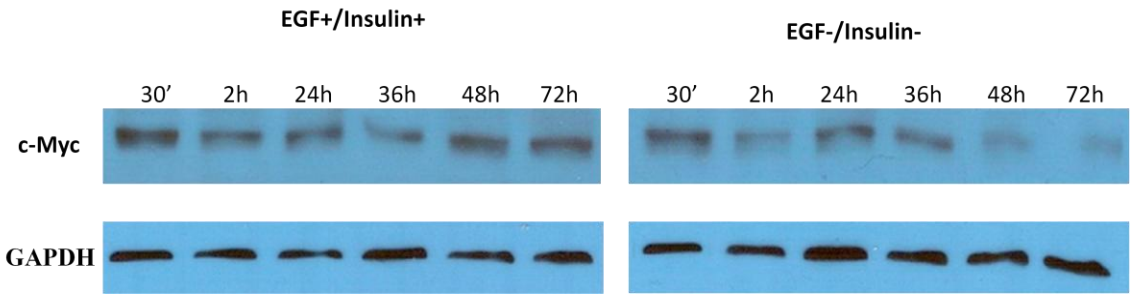

Figure 3.8. c-myc protein expressions in rat hepatocytes on collagen. Primary rat hepatocytes were seeded on collagen and maintained in EGF and insulin free media (left) or in media containing EGF and insulin (right). At the indicated time points, the cell lysates were collected and analyzed by western blot using rabbit anti-myc. GAPDH was used to standardize the protein loads.

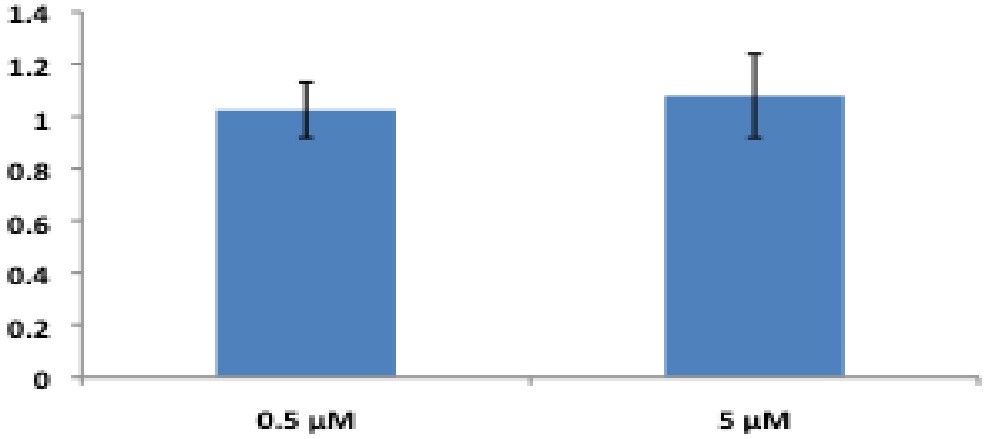

Figure 3.9. Effects of FAK inhibition on the transcription of c-myc. . Rat hepatocytes were cultured on collagen. After 24 hours, the cells were switched into culture media containing either DMSO (control) or PF-573226 (0.5-5 µM) and left to incubate for another 24 hours. The gene expressions of c-myc were quantified by

real-time PCR, and standardized to expressions levels in hepatocytes treated with DMSO alone.

In order to establish a link between c-myc and the expressions of MAPK effectors, hepatocytes on collagen were transfected with a specific c-myc siRNA that resulted into about 40 % (± %) downregulation of c-myc transcription. The silencing of c-myc did not have any effect on the expression of the IQGAP1, and the growth inhibitors (Tob1, IQGAP2). However, it induced a modest downregulation of Erbb2 mRNA (~20%) and a strong downregulation of IQGAP3 (>60%) (**Figure 3.10**)

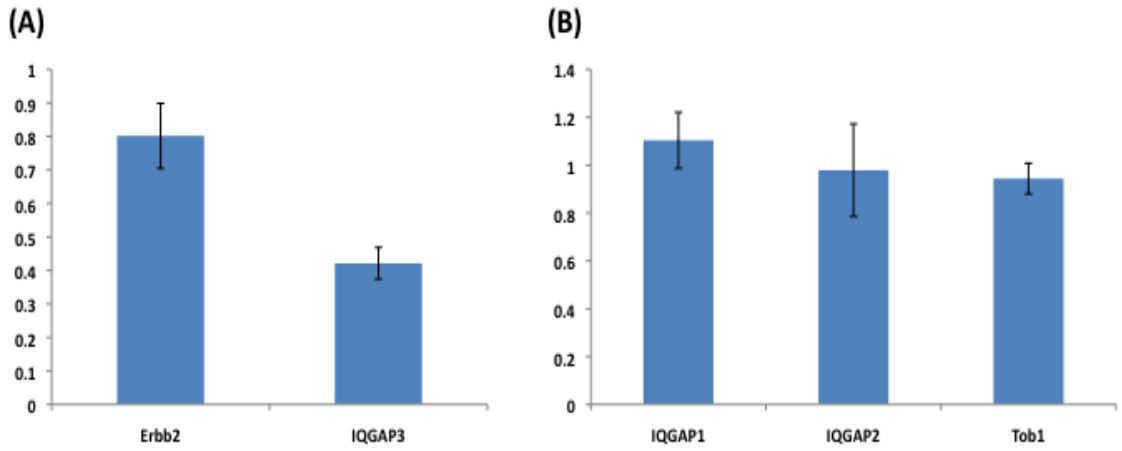

Figure 3.10. Effects of c-myc silencing on the gene expressions of MAPK/ERK pathway effectors. Rat hepatocytes were cultured on collagen for 12 hours, and then transfected with a specific siRNA for c-myc. The gene expressions of MAPK/ERK pathway effectors were quantified 48 hours after the transfections, and standardized to their corresponding expression levels in hepatocytes that were

transfected with a scrambled siRNA (negative control). **(A)** Gene expressions of Erbb2 and IQGAP3 **(B)** Gene expressions of IQGAP1, IQGAP2, and Tob1.

3.4. **Discussion**

Numerous studies have reported on the overall effects of the cell adhesion-signaling pathway on the activation of the MAPK/ERK pathway; however, the nature of the crosstalks between them remains largely unknown. To address this issue, we evaluated the kinetics of MAK/ERK pathway activation and the gene expressions of certain MAK/ERK pathway effectors in hepatocytes that were cultured under different adhesion conditions.

Significant differences of the MAPK/ERK activation profiles were observed in hepatocytes cultured on different extracellular matrices. While the initial response to EGF remained identical during early culture (intense but transient MAPK/ERK activation), a moderate and sustained MAPK/ERK activation was observed on collagen but not on matrigel. Cell density was found to have a minor impact on the intensity but not on the duration of the second peak, and no effect at all on the transient early peak. Higher gene expressions of MAP/ERK activators were observed on collagen than on matrigel, while the opposite trend occurred with regard to the gene expressions of growth inhibitors. Myc transcription was upregulated in a growth factor-independent manner, with a much higher gene expression on collagen than on matrigel. The potential involvement of c-Myc in the extracellular matrix-priming phase was partially substantiated by the downregulation of some MAPK/ERK positive effectors following the induced knockdown of c-Myc.

The quasi-similar profiles of the early MAPK/ERK activation on different extracellular matrices suggest that the transient activation during early G1 was not adhesion-dependent. Furthermore, the results on the kinetics of EGF receptor expressions in culture support the conclusion that the early activation is EGFR-dependent. The EGFR homodimer-dependence partially explains the transient nature of the activation, EGFR homodimers undergo fast internalization and slower recycling rate when compared to other EGF receptor isoforms. Conversely, the adhesion-dependence of the second activation phase was more evident with a much stronger effects from the integrin-dependent pathway. The growth factor switch in the presence of a specific FAK inhibitor (PF-562271) further supported the preponderance of the integrin pathway, with a significantly lower (and less sustained) MAPK/ERK activation in hepatocytes previously exposed to PF-562271 before the addition of EGF in the culture media.

We also found that the gene expressions of the EGF receptor Erbb2 and the scaffolding proteins IQGAP1 and IQGAP3 were higher in hepatocytes cultured on collagen than those on matrigel. The transcription of Erbb2 and IQGAP1 appeared to be growth factor-independent, whereas IQGAP3 transcription required the presence of EGF. However, the adhesion-dependence of IQGAP3 transcription was confirmed by the substantial decrease in its gene expression level following a sustained exposure to the FAK inhibitor. The presence of FAK inhibitor also caused a modest decrease in the gene expression of Erbb2 and no significant effect on IQGAP1 mRNA level. These outcomes may result from the likely fast metabolism of the inhibitor, or they imply the involvement of cell adhesion-related effectors other than FAK. The

protein tyrosine kinase Pyk2, which is activated following the integrin receptor attachment to the extracellular matrix and shares numerous structural similarities with FAK, is a very likely candidate as an alternative to FAK for the cell-adhesion-dependent priming of the MAPK/ERK pathway.

The relatively high c-myc gene expression levels in hepatocytes on collagen regardless of the presence of growth factor, and the significant differences between c-myc gene expression levels in hepatocytes on collagen and those on matrigel supported the hypothesis of the cell adhesion-dependence of c-myc transcription. On collagen, the higher gene expression levels in the absence of any growth factor mostly likely resulted from a low feedback control of c-myc transcription in the absence of growth factor. The unexpected absence of any significant change in c-Myc transcription in the presence of FAK inhibitor may have resulted from the fast metabolism of FAK or suggests a non-FAK related regulation of c-Myc gene expression by the integrin pathway. The significant downregulation of c-Myc induction on IQGAP3 gene expression supported the idea that the cell adhesion-related priming effect on the MAPK pathway may in part happens through the upregulation of c-Myc. The knockdown of c-Myc did not exert any effect on IQGAP1 expression, and only induced a very modest decrease on Erbb2 gene expression. It can be speculated that the cell adhesion-dependent upregulation of IQGAP1 and Erbb2 might not involve c-myc. Nevertheless, it is noteworthy to speculate that a more efficient c-myc knockdown (we only observe about 40% silencing) may have allowed us to establish the connection between c-myc and those two MAPK effectors.

In conclusion, a mid-G1 phase sustained activation of the MAPK/ERK pathway was observed in hepatocytes on collagen that was followed by a crossing of the restriction point whereas only an early and transient activation occurred on matrigel. The sustained activation was linked to an extracellular matrix-dependent upregulation of certain MAPK/ERK pathway activators. The loss of the sustained activation in the presence of a specific FAK inhibitor supports the hypothesis that the mid-G1 hepatocyte response to EGF is under the regulation of the cell adhesion pathways.

3.5. **Supplementary information**

Supplementary Table 3.1. Primer sequences of MAPK/ERK effectors

GAPDH	Forward: 5'- ATCACCATCTTCCAGGAGCGAG-3' Reverse: 5'- GCCAGTAGACTCCACGACATAC-3'
Tob1	Forward: 5'-TCTGGACATTGACGATGTTC-3' Reverse: 5'-TACAGCACCTTCACTGGTC-3'
IQGAP1	Forward: 5'-CCAACAATACCAACGACGGTTG-3' Reverse: 5'-GCTGGGCTTCAGGATTCATTAG-3'
IQGAP2	Forward: 5'-AGAATACGCTGCTTGCACTG-3' Reverse: 5'-GCCAAGTAGTTCATGGTGTTC-3'
IQGAP3	Forward: 5'-ATCTCCCTGTCTCTCACTTCAG-3' Reverse: 5'- CTTGGCATTGACGGCGAAC-3'
Erbb2	Forward: 5'- TGTGGTCATCCAGAACGAGG -3' Reverse: 5'-TTCAGCGTCTACCAGGTCAC-3'
c-myc	Forward: 5'-AACAGATCAGCAACAACCGC-3' Reverse: 5'-TTCTCCTCTGACGTTCCAAGAC-3'

Chapter 4

Characterization of the adhesion-signaling network in primary rat hepatocytes

4.1. Introduction

Cell adhesion is a generic term that is used to describe the binding of a cell to the extracellular matrix (cell-ECM) or to another cell (cell-cell). The cell adhesion to the extracellular matrix induces the activation of the integrin pathway. The activation of the cytoplasmic protein tyrosine kinase FAK, or focal adhesion kinase, is a hallmark of the integrin pathway activation. FAK activation occurs through a sequential phosphorylation of specific tyrosine residues following its translocation to the plasma membrane. An autophosphorylation at Y^{397} is followed by a Src-dependent phosphorylation of two additional tyrosine residues (Y^{576} and Y^{577}). A reciprocal positive feedback occurs between FAK and the phospholipid PIP2. The recruitment of FAK and its autophosphorylation are facilitated by PIP2; in return, active FAK promotes the localization as well as the activation of the enzyme phosphatidylinositol 4-phosphate 5-kinase (PIP5K) which leads to an increase of PIP2 at the focal contact.

The formation of E-cadherin homophilic interactions between neighboring cells is the prerequisite for the formations of other types of cell-cell interactions (Green KJ, 2009), and thereby plays a critical role in the maintenance of cell polarity and function. Moreover, E-cadherins in homodimeric interactions sequester β-catenin at the plasma membrane and prevent its translocation to the nuclei. The amount of E-cadherin at the plasma membrane results from the balance between its internalization following the disruption of the E-cadherin/α-catenin/β-catenin

complex, and the plasma membrane translocation of recycled or newly synthesized E-cadherins.

A two-way signaling occurs between the integrin and the E-cadherin pathways. The stability of the E-cadherin/α-catenin/β-catenin trimeric complex, and thereby the localizations of E-cadherin and β-catenin, can be affected by a FAK/Src-mediated tyrosine phosphorylations. The integrin-dependent actomyosin contraction can also induce the scattering effect, which may lead to the disruption of E-cadherin homophilic interactions (de Rooij J, 2005). On the other hand, studies from various cell types have shown that strong cell-cell interactions induce the expression or the activation of various tyrosine phosphatases that may inactivate FAK. The small GTPases cdc42, Rac1, and RhoA constitute a highly likely focal point in the integration of signals from the integrin and the E-cadherin pathways. They can alternate between an inactive GDP-bound and an active GTP-bound states, and are involved in numerous cellular processes such as cytoskeleton remodeling and receptor trafficking. Cdc42 and RhoA can be either activated or inhibited by the active FAK depending on specific conditions; and they can exert feedback by modulating FAK activity. Similarly, functional relationships between E-cadherin and these small GTPases have been reported. Homophilic E-cadherin dimers activate cdc42 and Rac1, and inactivate RhoA. In return, active cdc42 and Rac1 promote the formation of new E-cadherin homodimers by facilitating the translocation of cytoplasmic E-cadherin to new cell-cell contact sites. Moreover, active Cdc42 and Rac1 stabilize cell-cell interactions by inhibiting the IQGAP1-dependent disruption of the E-cadherin/α-catenin/β-catenin trimeric complex. On the contrary, active

RhoA induces the breaking of E-cadherin homodimers most probably through the scattering effect.

The coupled integrin and E-cadherin pathways may conceptually settle into two distinct and non-overlapping states: a strong integrin-based/weak E-cadherin-based adhesion, and a weak integrin-based/strong E-cadherin-based adhesion. In this chapter, culture on different extracellular matrices as well as specific inhibitors and plasmid transfections were used to gain a deeper knowledge of the critical interactions that affect the activation of the hepatocyte adhesion network. Such knowledge is necessary in order to acquire a clear understanding of the switch between the dominant integrin-based and the dominant E-cadherin-based in primary rat hepatocyte culture.

4.2. **Materials and methods**

4.2.1. **Protein analysis**

Rabbit anti-FAK, rabbit anti-phospho FAK (Y^{397}), rabbit anti-E-cadherin, and rabbit anti-β catenin were used in western blot analysis as described in chapter 2.

4.2.2. **Small GTPase activation assay**

RhoA and cdc42 activation levels were evaluated using either a G-LISA® kit or pull-down assays.

For the G-LISA® kit (Cytoskeleton Inc. Denver, CO), snap frozen lysates containing the same amount of total protein (250 μg) were thawed and added to either a cdc42 or a RhoA plate, containing a protein that could bind to either cdc42-GTP or RhoA-GTP, and incubated at 4°C for 30 min. The plates were washed at least three times, and the bound cdc42 or RhoA was detected using colorimetric method using reagents that were provided in the kit.

Pull-down assay using Rhotekin-GST (binds RhoA-GTP) or PAK1-GST (binds cdc42-GTP) beads, both purchased from Cytoskeleton (Cytoskeleton Inc. Denver, CO), was also used to evaluate the activation levels of cdc42 and RhoA according to the manufacturer's instructions. The cells were lysed in an ice-cold buffer (50 mM Tris pH 7.5, 10 mM MgCl2, 0.3 M NaCl, 2% IGEPAL) and the lysate was clarified for 1 min at 15,000 g at 4°C. Lysate containing 700 μg of proteins were added to 20 μg

of beads, and the mixture was left to incubate at 4°C with gentle rotation for 30 min. After three washes using an ice-cold wash buffer (25 mM Tris pH 7.5, 30 mM MgCl2, 40 mM NaCl), the beads were resuspended in Laemmli sample buffer (Sigma) supplemented with 5% (v/v) β-mercaptoethanol, and boiled for 15 min. The boiled samples were analyzed by western blot using rabbit anti-cdc42 and rabbit anti-RhoA (Cell Signaling Technology, CA).

4.2.3. **RNA silencing**

The gene knockdowns were performed using validated siRNAs (Silencer® Select siRNA) for integrin α1, integrin α5, and syndecan-4, and Lipofectamine RNAiMax®, which were purchased from Life Technologies.

4.3. **Results**

4.3.1. **Kinetics of the integrin pathway activation**

To evaluate the activation of the integrin pathway, the phosphorylation levels of FAK (Y^{397}FAK) were evaluated in hepatocytes on matrigel and on collagen at different time points. A continuous increase in FAK phosphorylation level, reaching its peak after about 48 hours, was observed on collagen whereas hepatocytes on matrigel expressed very low FAK phosphorylation levels at all time points (**Figure 4.1**). However; while the total FAK protein levels remained fairly stable on collagen, a very significant upregulation was observed on matrigel.

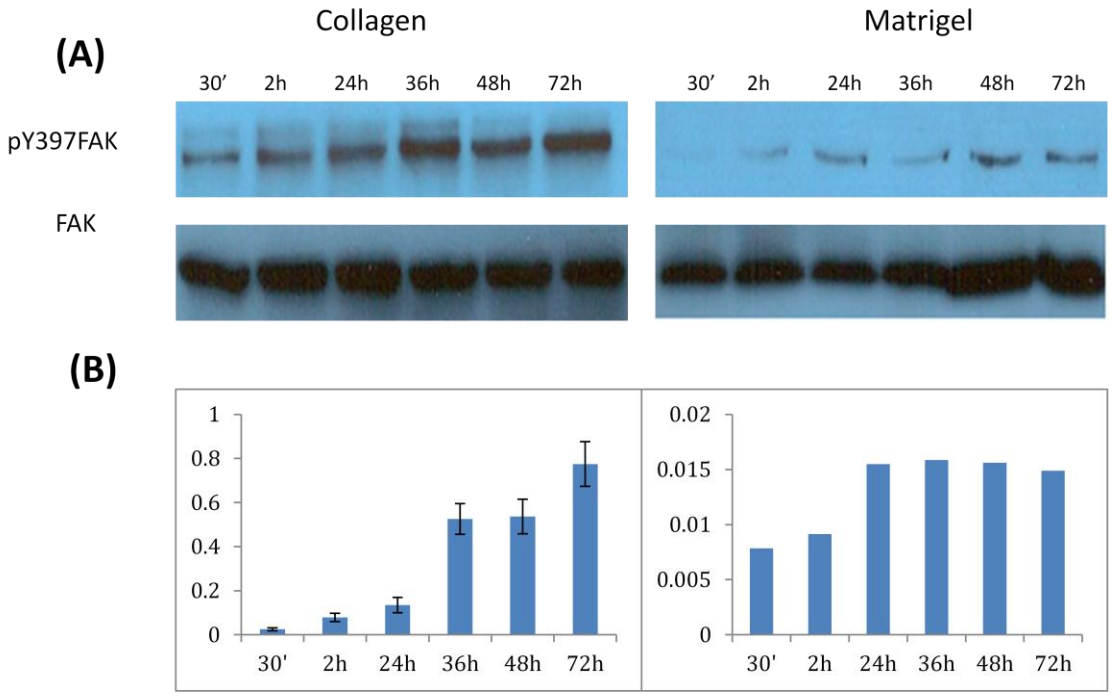

Figure 4.1: **FAK activations in rat hepatocytes on collagen and matrigel**. **(A)** At the indicated time points, total cell lysates from hepatocytes on collagen or matrigel were collected and analyzed by western blot using rabbit anti-phospho FAK (Y^{397}),

and rabbit anti-FAK. **(B)** Densitometries were performed for all time points. The bars represent the ratios between tyrosine (Y^{397}) phosphorylated FAK and total FAK protein.

The levels of active Cdc42 sharply increased during the early stage of cell attachment, declined to slightly below its initial activation level before cell seeding after 24 hours. The decline stopped after 24 hours, but Cdc42 remained in a low activation state throughout the remainder of the experiment (**Figure 4.2**). Conversely, RhoA activity quickly declined following cell seeding and remained at a low activation state until a reactivation occurred after about 24 hours of culture. The reactivation phase lasted for about 24 hours, and a sustained high activity steady state level was observed thereafter (**Figure 4.2**).

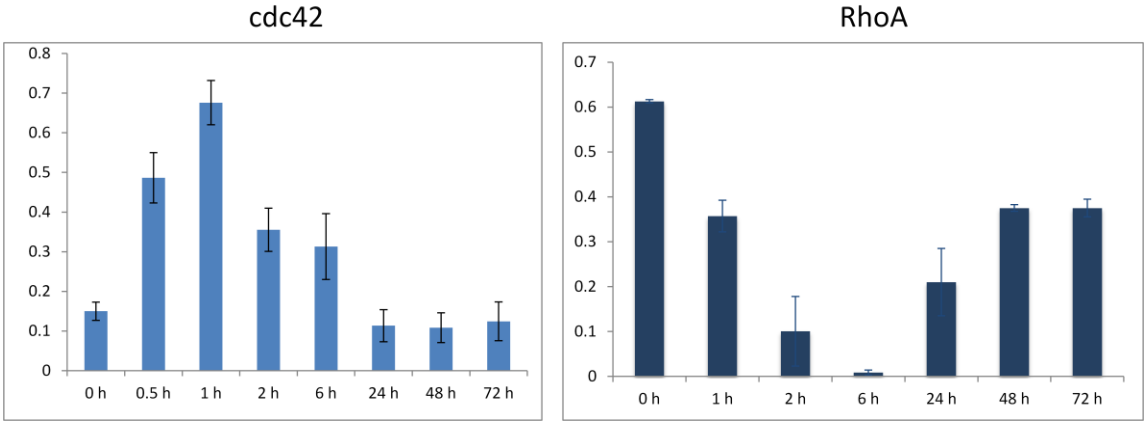

<u>Figure 4.2</u>: Kinetics of cdc42 and RhoA activations in primary rat hepatocyte on collagen. Primary rat hepatocytes were cultured on collagen in serum free, hormone-free, and EGF-free conditions. At the indicated time points, the cells were lysed and the lysates were flash frozen in liquid nitrogen after clarification. Thawed cell lysates containing 250 µg of total proteins were used to evaluate the activation

levels of cdc42 (left) and RhoA (right) using the G-LISA® kit (Cytoskeleton Inc, MA). Each bar was obtained from three independent experiments, values on the Y-axis (arbitrary units) are proportional to the amount of active cdc42 or RhoA detected in each well of the kit.

4.3.2. **Effects of fibronectin on the integrin pathway**

Primary rat hepatocytes attach to the extracellular matrix either through the α1β1 or the α5β1 integrin heterodimers (Hansen LK, 2006). In order to characterize the receptors and the extracellular constituents that were responsible for the full activation of the integrin pathway, the activation levels of FAK were analyzed by western blot in hepatocytes on collagen that were transfected with either the siRNA for α1 integrin, for α5 integrin, or for syndecan-4. While none of the transfection had an effect on the expression of FAK, the knockdowns of α5 integrin and syndecan-4 caused a decrease in FAK activation while α1 integrin silencing did not have any effect (**Figure 4.3**).

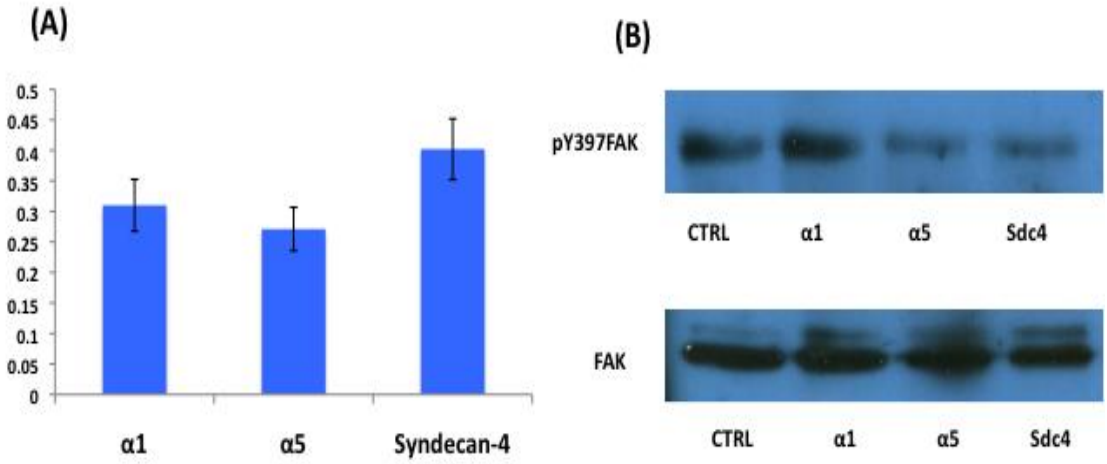

Figure 4.3. **Full activation of FAK requires fibronectin-mediated signaling in rat hepatocytes**. Rat hepatocytes were cultured on collagen for 48 hours, and then transfected with a specific siRNA for either integrin α1 (α1), integrin α5 (α5), or syndecan-4 (Sdc4). **(A)** Efficiencies of the RNA silencing, compared to the corresponding mRNA levels in cells transfected with a scramble siRNA **(B)** 48 hours after transfections, the cell lysates were collected and analyzed by western blot using rabbit anti-phospho FAK (Y^{397}), and rabbit anti-FAK.

4.3.3. **Crosstalk between the integrin and the E-cadherin/β-catenin pathways**

Hepatocytes were cultured at different seeding densities on collagen to evaluate the effects of the cell-cell interactions (E-cadherin pathway) on the activation of FAK, cdc42, and RhoA.

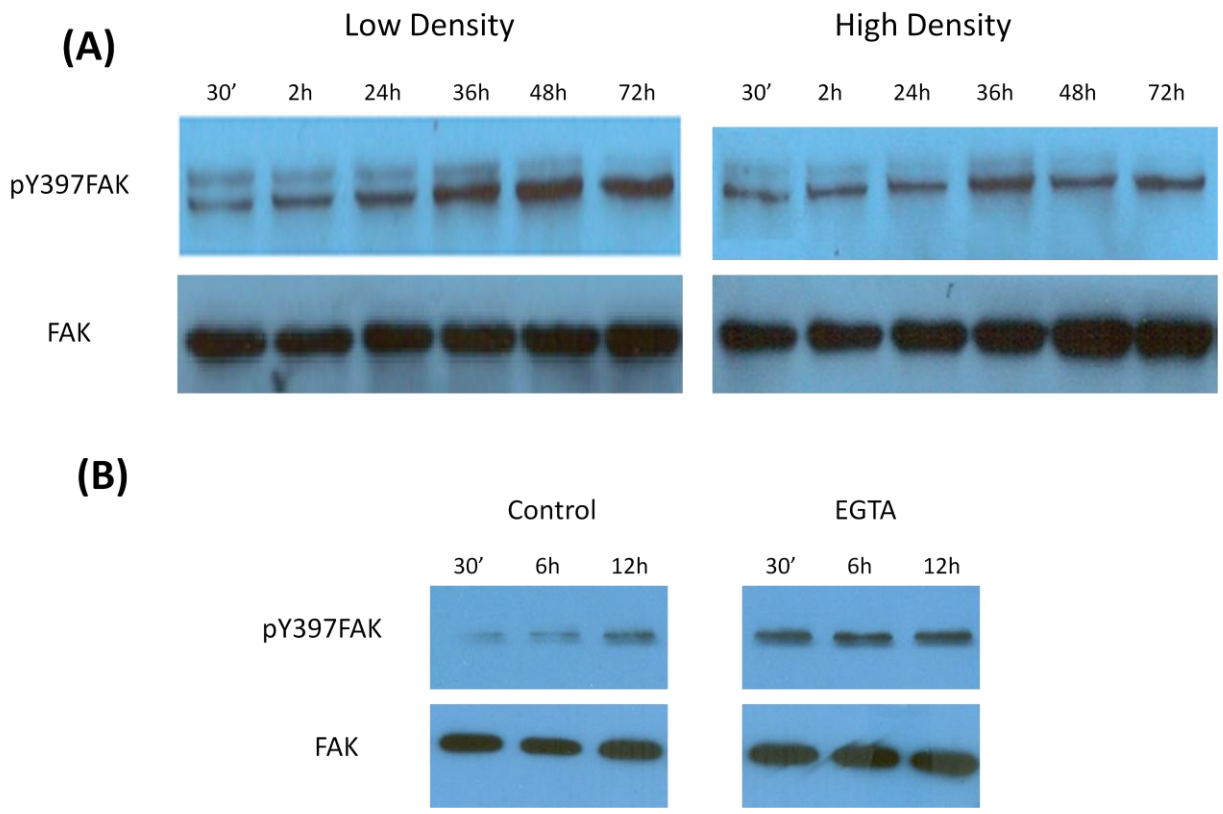

Figure 4.4: **Effects of cell-cell interactions on the activation of FAK**. Rat hepatocytes were cultured on collagen either at low seeding density (17,500 cells/cm^2) or high seeding density (150,000 cells/cm^2). **(A)** At the indicated time points, total cell lysates from hepatocytes on collagen at low density (left) or high density (right) were collected and analyzed by western blot using rabbit anti-phospho FAK (Y^{397}), and rabbit anti-FAK. **(B)** Rat hepatocytes were seeded at high density on collagen. After 48 hours of culture, the cells were exposed to 2 mM EGTA (left) and the cells lysates were collected at the indicated time points after EGTA addition and analyzed by western blot using rabbit anti-phospho FAK (Y^{397}), and rabbit anti-FAK.

Cell density did not significantly affect the initial phase of FAK activation (from 0 to 24 hours of culture), where a steady increase of FAK activation occurred. However, an apparent cell-dependence of FAK activation was observed during late culture (48 to 72 hours). While no significant late (48-75 hours) change in FAK phosphorylation levels was observed at high density, noticeable increases occurred in hepatocytes at low density. The differences in cell density did not appear to have an effect on the expression of total FAK proteins, but the phosphorylated FAK to total FAK ratio generally increased with the increase in cell density (**Figure 4.4**). In order to confirm that the difference in FAK phosphorylation levels was due to cell-cell interactions, hepatocytes at high density were exposed to EGTA to break the E-cadherin homodimers . The presence of EGTA induced a clear increase in FAK phosphorylation, which lasted for up to 12 hours (**Figure 4.4**).

During early culture, the activations of cdc42 and RhoA were not affected by changing cell densities. However, while a low cdc42-GTP levels and a reactivation of RhoA occurred in hepatocytes at low density, the opposite trend was observed at high density where more than two-fold increase in cdc42-GTP level and a drop by more that 75% of RhoA activity occurred (compared to low density). These results suggested a cell-cell-dependence of cdc42 and RhoA activation at late time points (**Figure 4.5**). Similar to FAK activation, the use of EGTA further confirmed the effects of the E-cadherin pathway on cdc42 and RhoA activations in rat hepatocytes after 48 hours. The exposure to EGTA prohibited the reactivation of cdc42 at high density, and instead induced a reactivation of RhoA as it occurred in hepatocytes at low density (**Figure 4.5**).

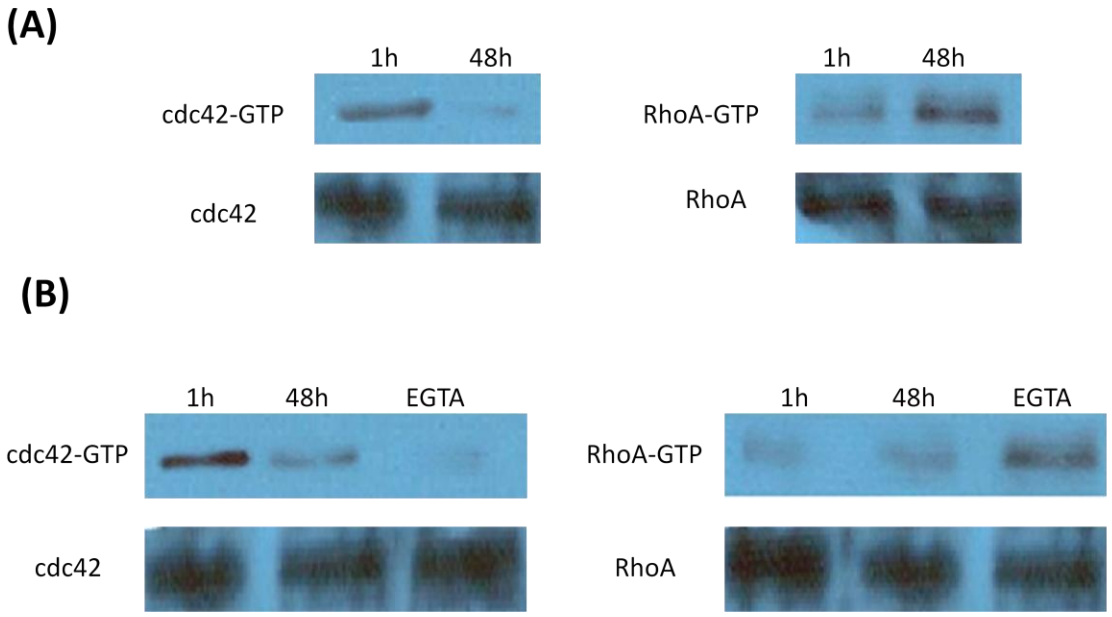

Figure 4.5: **Effects of cell-cell interactions on the activations of cdc42 and RhoA.** Rat hepatocytes were cultured on collagen either at different seeding densities. Total cell lysates were collected at the indicated time points, and the activation levels of cdc42 and RhoA were evaluated using pull down assays as mentioned in the chapter on Materials and Methods. **(A)** Low density seeding (17,500 cells/cm^2). (B). High seeding density (150,000 cells/cm^2). EGTA exposure were started at the 44-hour time point and lasted for 4 hours.

4.4. Discussion

The states of activation of the cell-adhesion signaling pathways can be evaluated by assessing the phosphorylation status of FAK (cell-ECM/integrin pathways) at three tyrosine residues (Y^{397}, Y^{576}, Y^{577}), and by tracking the cellular localization of E-cadherin and/or β-catenin (cell-cell/E-cadherin pathway). In this chapter, we aimed to understand the specific property of each of the two aforementioned pathways in rat hepatocyte culture and to gain deeper insights into the crosstalk between them.

The activation of FAK remained low on matrigel, where a significant increase in total FAK expression was observed. The low active FAK/total FAK ratio on matrigel, with the clear upregulation of total FAK protein, may partly explain the growth inhibitory effect of matrigel. High levels of inactive FAK have been shown to play a role in maintaining the cells in a growth-arrested state. A two-phase activation of the integrin pathway was observed on collagen, an initial cell density-independent activation of FAK followed by a cell density dependent activation where FAK activation was found to be inversely proportional to the cell density.

The knockdown of the α1 integrin did not affect the activation of FAK, whereas the knockdowns of the α5 integrin and syndecan-4 induced a marked downregulation of FAK activity. Rat hepatocytes adhere to collagen through the α1β1 integrin, and to fibronectin through α5β1. Besides its interaction with α5β1 integrin, fibronectin also binds to the transmembrane proteoglycan Syndecan-4 through its heparin-binding domain. It has been shown that simultaneous

fibronectin interaction to α5β1 integrin and Syndecan-4 is required for the completion of normal cell spreading and the strengthening of cell-extracellular matrix interaction (Woods A, 1986). These results suggest that fibronectin-mediated signaling may be responsible for the full activation of the integrin pathway in rat hepatocytes.

Shortly after cell seeding and regardless of the seeding density, a fast and transient activation of Cdc42 followed by a rapid decline was observed. At later time points, a sustained low level of Cdc42 activation was observed in hepatocytes that were seeded at low density whereas a small but noticeable reactivation occurred in cells at high density. Contrary to Cdc42, RhoA activity quickly declined following cell seeding, and remained at low level for approximately 24 hours. A significant reactivation of RhoA was observed at low cell density after 48 hours of culture, whereas no noticeable reactivation took place at higher seeding density.

The plasma membrane pool of E-cadherin comes from recycled and newly synthesized E-cadherin, which are translocated to the plasma membrane in a microtubule-dependent manner. Microtubules form the eukaryotic cell cytoskeleton with actin and intermediate filaments, and they are involved in various cell processes such as cell migration, cell division, and intracellular transports. There is a rather long delay before significant E-cadherins and β-catenins can be found at the plasma membrane may because of the possible slow rate of microtubule polymerization in rat hepatocytes (Mooney DJ, 1995).

The initial phase of FAK activation (cell density-independent phase) is purely integrin-mediated since it likely referred to a period when no E-cadherin-mediated cell-cell interaction had been formed yet. Following the plasma membrane translocation of E-cadherin and the resulting formation of cell-cell adhesion, the activation of FAK became density-dependent and resulted from the crosstalk between the E-cadherin and the integrin pathways. The E-cadherin-dependence of the second phase of FAK activation was further supported by a higher FAK phosphorylation in high-density cells that were treated with EGTA.

Various tyrosine phosphatases, such as the tumor suppressor PTEN (Tamura M, 1999), can induce an inactivation of FAK. Higher E-cadherin homophilic interactions at higher cell densities induce the upregulations, and the activations of certain cell density-dependent tyrosine phosphatases that can inactivate FAK. One likely candidate is the leucocyte common antigen-related phosphatase (LAR) (Serra-Pagès C, 1995) (Symons JR, 2002). The Density-enhanced protein tyrosine phosphatase 1 (DEP-1) can also be considered as another potential candidate (Holsinger LJ, 2002).

The early Cdc42 activation and RhoA inactivation are necessary for the initiation of cell-ECM attachments and the cell spreading (Yang L, 2006) (Partridge MA, 2006) (Arthur WT, 2001). Active Cdc42 promotes the polymerization of actins and the filopodial formation, which is important for the transport of integrin receptors and the formation of new cell-ECM contacts. The deactivation of RhoA induces the disassembly of stress fibers, which facilitates the formation of new

filopodia and the cell spreading (Arthur WT, 2001). The early activation profiles of Cdc42 and RhoA explains the kinetics of microfilament assembly and the cell spreading in rat hepatocytes observed by Mooney et al. (Mooney DJ, 1995).

Similar to FAK activation, the activations of Cdc42 and RhoA also happened in a two-phase manner. An integrin-mediated and cell density-independent phase was observed, followed by a second cell density-dependent phase where the net Cdc42 and RhoA activities depended on the crosstalk between the integrin and the E-cadherin pathways. FAK is most likely one of the major players in the integrin-dependent regulation of Cdc42 and RhoA. Previous reports have shown that FAK can function either as an activator or as a repressor with regards to Cdc42 and RhoA (Sinha S, 2008) (Shan Y, 2009) (Shen Y, 2008) (Tomar A, 2009). Cell-cell interactions activate Cdc42 in an E-cadherin-dependent manner (Kim SH L. Z., 2000) (Noren NK N. C., 2001). E-cadherin engagements induce the recruitment of a Cdc42 activator, the guanine nucleotide exchange factors (GEF) β-Pix, to areas of cell-cell contacts (Liu F, 2010). Furthermore, the translocations of β-Pix and the downstream Cdc42 effector Pak1 to areas of cell-cell contacts are also involved in the establishment of contact inhibitions (Zegers MM, 2003). The E-cadherin-dependent inhibition of RhoA has been shown to involve a tyrosine phosphorylation of the GTPase-activating protein p190RhoGAP (Noren NK A. W., 2003), which inactivates RhoA. The changes in FAK phosphorylation and E-cadherin localization, in response to transfections using active and inactive forms of cdc42 and RhoA, confirmed their central roles in the regulation of the cell adhesion pathways. The increase in active cdc42 promotes the formation of new E-cadherin homodimers and preserves the

integrity of existing homodimers. The increase in E-cadherin homodimers further accentuates the inhibition of RhoA that would lead to a decrease in FAK activation.

In summary, the two states of activation of the hepatocyte adhesion signaling pathway are characterized by opposing activation states of the integrin and E-cadherin pathways, as well as distinct and again opposing patterns of activation of the small GTPases cdc42 and RhoA. The first state is characterized by a strong integrin-based adhesion, a weak E-cadherin-based adhesion, and a low cdc42/high RhoA activation. The second state corresponds to a weak integrin-based adhesion, a strong E-cadherin-based adhesion, and a high cdc42/low RhoA activation. The priming effects of the cell adhesion network on the MAPK/ERK pathway very likely depends on which of the two states above prevail during hepatocyte culture.

4.5. **Supplementary information**

Supplementary Table 4.1. Primer sequences of integrin α1, integrin α5, and syndecan-4

Integrin 1	Forward: 5′- ATACTGATCTGCTTCTCGTC-3′ Reverse: 5′- ACCTTGTCTGATTCACAGC-3′
Integrin 5	Forward: 5′-ACCTCACCTATGGCTATGTCAC-3′ Reverse: 5′-ATTGGTATCAGTGGCAGCTACG-3′
Syndecan-4	Forward: 5′-AGTGTCCATGTCCAGCACTTCC-3′ Reverse: 5′-CACAATCAGAGCTGCCAAGACC-3′

Chapter 5

Analysis of the dynamical property of the adhesion-signaling network in primary rat hepatocytes

5.1. Introduction

The two opposing states of the hepatocyte adhesion network in culture induce two distinct impacts on how the cells respond to the presence of EGF. A strong integrin-based/weak E-cadherin-based adhesion causes a sustained MAPK/ERK activation, whereas a weak integrin-based/strong E-cadherin-based adhesion leads to a transient activation. A sustained MAPK/ERK activation is associated with passage of the restriction point and entry into S phase and irreversible loss of hepatocyte differentiation.

Multiple layers of control systems ensure a very stringent regulation of the crossing of the restriction point in eukaryotes. Such control systems involve numerous pathways such as the MAPK/ERK (Meloche S, 2007) and the pRb-E2F pathways (Giacinti C, 2006). A common property of the MAPK/ERK and the pRb-E2F pathways is the well-documented existence of two distinct states of activation (and expression). The first state corresponds to an inactive MAPK/ERK (which likely results from a transient activation) and the absence of the expression of the transcription E2F1; whereas the second state is characterized by an active (likely following a sustained activation) MAPK/ERK and a high expression of E2F1. The first state will keep the cells in the pre-restriction point stage (and therefore more conducive for the preservation of differentiation), while a full transition into full proliferation mode (post-restriction point stage) will automatically result from the second state. The hierarchical nature of its control system also ensures the irreversibility of the restriction point crossing.

The use of mathematical models allows the derivation of the cellular physiology from the molecular network that comprises a biological control system (Tyson JJ, 2001). More precisely, mathematical approaches allow a deeper and more precise analysis of the dynamical relationships between the molecular components of a regulatory network. The topological properties of the network can be translated into a set of simple mathematical equations that captures the dynamical relationships between molecular components (state variables). Ordinary differential equations (ODE) are appropriate to model most biochemical control systems. The state variables reflect theoretical changes affecting the concentration of the pathway constituents, whereas kinetic parameters are used to simulate the effects of diverse factors on the system of interest (e.g. input from an external control system, rate of synthesis or degradation of a given protein…).

Bifurcation theory provides a tool for analyzing the effects of the kinetic parameters on the properties of state variables at equilibrium (or steady state). Steady states can be classified as unstable or stable. Unstable steady states disappear readily following a small perturbation (or perturbations), whereas a stable steady state remains unaffected. The application of smooth changes to the value of a specific parameter (or parameters), which is fittingly denominated the bifurcation parameter, simulates the perturbation. Although only stable steady states can be experimentally observed (and quantified), both stable and unstable steady states may have significant physiological importance.

The capability to toggle between two discrete stable steady states, or bistability, is at the center of cell cycle progression and is involved in the generation of mutually exclusive phenotypes like cell proliferation and differentiation. Numerous reports have shown that both the MAPK/ERK (Markevich NI, 2004) and the pRb-E2F (Swat M, 2004) pathways exhibit a bistability, which very likely explain the irreversibility of the restriction point. Another interesting property of a bistable control system is the implicit existence of a threshold property that allows the transition between the two stable steady states. For example, a critical threshold of mitogenic stimulation (which corresponds to a ERK activation) must be achieved in order to induce a stable expression of the transcription factor E2F.

Although strong correlations between FAK phosphorylation/nuclear β-catenin levels and Erk activation have been established, no report on the possible bistability of the integrin/E-cadherin pathways under different adhesion conditions is available yet. We can hypothesize the existence of that such bistability based on the hierarchical nature of the control systems regulating the crossing of the restriction point. In this chapter, we constructed a simple mathematical model of the integrin and E-cadherin pathways, using ordinary differential equations, to analyze their underlying control mechanisms. In order to reduce complexity and facilitate the experimental validation of the theoretical predictions, the model was constrained to the interactions that are included in the supplementary figures 5.1 and 5.2. The model does not account for all known physical or functional interactions within the cell-adhesion pathways. Other important events such as, integrin clustering, protein turnovers or specific transcriptional regulations, occur

at different time scales or involve additional control systems and were left for future study.

Based on the mathematical predictions that were validated by flow cytometry analysis, we observed that the hepatocyte adhesion network could settle into two stable steady states: a strong integrin-based adhesion which would lead to a complete dedifferentiation of the cells, and a strong E-cadherin-based adhesion which would induce a growth arrest. We also concluded that the steady state level of PIP2 is one of the potential major factors that control the switch between the aforementioned steady states.

5.2. **Materials and methods**

5.2.1. **Mathematical modeling**

Ordinary differential equations (ODEs) were used to design a mathematical model of the integrin and E-cadherin/β-catenin signaling pathways. Parameter optimizations were performed using the stochastic ranking evolution strategy algorithm (Ji X, 2006), which was implemented using MPI-C++. Time-course simulations and sensitivity analysis, using the Multiparametric Sensitivity Analysis (MPSA) algorithm (Zi Z, 2005), were implemented using Matlab™ (MathWorks, MA). Bifurcation analysis was performed using the freeware AUTO (Doedel, 1981). Detailed description of the model is included in the supplementary information.

5.2.2. **Purification of isolated nuclei**

Purified intact nuclei, which were subsequently used in western blot analysis and in flow cytometry analysis, were purified according to the method proposed by Rosner et al. (Rosner M, 2013) with some modifications. Hepatocytes were cultured in T150 flasks were washed two times with warm PBS, and the cells were retrieved by incubation with 1.5 ml of Accutase™ (Sigma, MO) for 2 min at 37°C. After the Accutase™ treatment, the resulting hepatocyte suspension was washed with 2mM EGTA in ice-cold PBS. After two washes, the hepatocyte pellets were suspended in an ice-cold lysis buffer (20 mM Tris at pH 7.6, 2 mM $MgCl_2$) and incubated on ice to induce hypotonic cell swelling. After 20 minutes, Nonidet P-40 substitute (Sigma,

MO) was added to the cell suspension for a final concentration of 1% (v/v) to induce the disruption of the plasma membrane, and the resulting suspension was homogenized by pipetting up and down ten times using a 200 μl tip. The intact nuclei were separated from the cytoplasmic extract by centrifugation at 200 g for 3 min at 4^{o}C. The pellet was washed by adding 300 μl of the lysis buffer containing 0.5% (v/v) of Nonidet P-40 substitute, followed by gentle pipetting, and was centrifuged at 200 g for 3 min at 4^{o}C. After the last wash, the clean pellet was resuspended in ice-cold PBS with 5 mM $MgCl_2$. The integrity and the purity of the nuclei were evaluated by phase contrast microscopy before any subsequent usages of the pure nuclei.

5.2.3. **Phospholipid (PIP2) intracellular delivery**

Freshly isolated rat hepatocytes were cultured on matrigel. After 72 hours of culture, phosphatidylinositol-4,5-bisphosphate diC16 (PIP2) mixed with a phosphatidylinositol phosphate shuttle system was added to the culture media. 50 μM of PIP2 (Echelon Incorporation, UT) was mixed with a histone carrier (Echelon Incorporation, UT) at a molar ratio of 5:1, and the complexes were allowed to form at room temperature with gentle vortexing for 15 minutes. The PIP2-Histone complex was further diluted in fresh culture media and added to cultures. For 10 hours, the culture media were replaced every hour with new culture media containing fresh PIP2-Histone complexes.

5.2.4. **Flow cytometry analysis**

Evaluation of FAK phosphorylation

Dispase (BD Biosciences, NJ) was used to harvest the hepatocytes that were cultured on matrigel in 12-well plates. The cells were suspended in ice-cold PBS containing 5 mM sodium vanadate (Sigma, MO) and washed by centrifugation (200 g, 4^{o}C) for 2 min. For fixation, the cells were suspended in 1.5% paraformaldehyde with 5 mM sodium vanadate in PBS on ice for 30 min. After fixation, the cells were permeabilized on ice for 20 min using 0.1% saponin in PBS (w/v) in the presence of 5 mM sodium vanadate and 0.5% BSA. After permeabilization, the cells were quickly pelleted by centrifugation, resuspended in ice-cold 5% goat serum in PBS supplemented with 5 mM sodium vanadate and rabbit anti-phospho FAK Y^{576,577} (Abcam, MA) at 1:50 dilution, and left to incubate on ice for 1 hour with periodic pipettings. After the primary antibody incubation, the cells were washed four times in ice-cold 0.5% BSA (w/v) PBS, and pelleted by centrifugation. The pellets were afterward resuspended in 5% goat serum in PBS with Alexa Fluor® 488 Goat Anti-Rabbit Antibody (Life Technologies, CA) at 1:500 dilution, and left to incubate at room temperature. After 30 min of incubation, the cells were washed four times in (w/v) PBS, and resuspended in ice-cold 0.5% BSA in PBS after the last wash. The states of FAK phosphorylation in the stained hepatocytes were thereafter analyzed by flow cytometry. In general, 10000 cells within a specific gate were measured using a BD FACScan flow cytometer (BD Biosciences, NJ).

Evaluation of nuclear β-catenin

Purified nuclei were fixed in 1.5% paraformaldehyde for 15 min at room temperature, pelleted by centrifugation (200g, 5min), and then permeabilized on ice for 30 min using ice-cold methanol. The permeabilized nuclei were pelleted by centrifugation, then incubated in 5% goat serum in PBS with rabbit anti-β-catenin (Sigma, MO) at a dilution of 1:100 for 30 min at room temperature. After the primary antibody incubation, the nuclei were washed four times with 0.5% BSA in PBS. After the centrifugation step in the last wash, the nuclei were resuspended in 5% goat serum in PBS with Alexa Fluor® 488 Goat Anti-Rabbit Antibody (Life Technologies, CA) at 1:500 dilution, and left to incubate at room temperature for 30 min. After four washes with 0.5% BSA in PBS, the stained nuclei were resuspended in a 0.5% BSA in PBS and analyzed by flow cytometry. Generally, 10000 nuclei within a specific gate were measured using a BD FACScan flow cytometer (BD Biosciences, NJ).

5.2.5. **Small GTPase activation assay**

RhoA and cdc42 activation levels were evaluated using the pull-down assay that is described in chapter 4.

5.3. **Results**

In order to analyze the dynamical property of the rat hepatocyte adhesion control system, we designed a model of the integrin and the E-cadherin/β-catenin pathway. The model did not take into account all known details pertaining to the cell adhesion network, such as integrin clustering, and E-cadherin transcriptional control. Instead, our simplified model was intended to provide a proper framework to understand the inherent properties of the hepatocyte adhesion control system. The theoretical kinetic profiles of the integrin and the E-cadherin/β-catenin pathways displayed a similar trend with the corresponding experimental measurements (**Supplementary figures 5.5 and 5.6**).

5.3.1. **Sensitivity analysis of the hepatocyte adhesion network**

Strong FAK activation and nuclear localization of β-catenin induce hepatocyte proliferation in response to growth factors. Multiparametric Sensitivity Analysis (MPSA) was used to identify properties of the cell-adhesion pathways that exert the most significant controls on FAK activation and β-catenin cellular localization. Kinetic parameters related to physical or functional interactions, which are known to hold critical role in the cell adhesion pathways, were selected for the proposed parametric sensitivity analysis. Complete MPSA results for all selected parameters are included in the supplementary information.

The MPSA simulation predicted that parameters related to PIP2 degradation, PIP2-mediated FAK phosphorylation, microtubule polymerization, plasma membrane E-cadherin/β-catenin complex formation and disruption were the most important on the regulation of FAK activation and the nuclear localization of β-catenin. The predicted most sensitive parameters are listed in Table 1, and the diagrams of their corresponding cumulative frequency distributions in figure 5.1. A complete list of the predicted parameter sensitivity is given in the supplementary information.

Table 5.1. MPSA results for the most sensitive parameters

Rate Constant	Description	Reference value	Range of variation	K-S
k_{d1}	PIP2 degradation	0.25	0.025-2.5	0.117039593
K_{f2}	FAK activation_PIP2 feedback	0.375	0.0375-3.75	0.201827267
k_{MT}	Microtubule polymerization	0.35	0.035-3.5	0.510348895
K_{MTmx}	Microtubule polymerization	0.5	0.05-5	0.141477639
k_{C2P}	E-cadherin/b-catenin formation at the plasma membrane	2.5	0.25-20.5	0.170205439
K_{P2C}	E-cadherin/b-catenin disruption at the plasma membrane	1	0.1-10	0.134081384

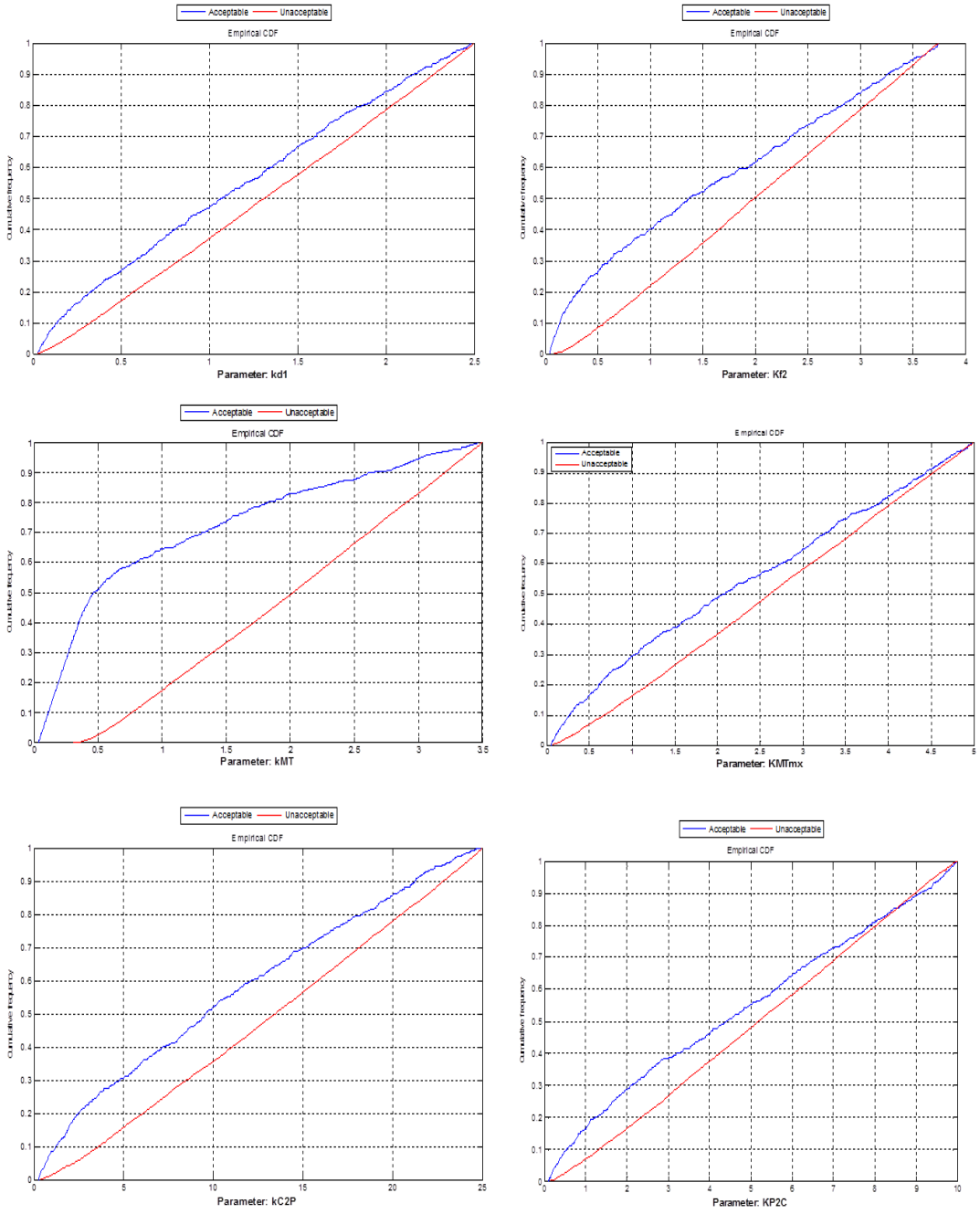

<u>Figure 5.1</u>. Cumulative frequency distributions of the MPSA with respect to the most sensitive parameters in the model. The maximum vertical difference

between the two curves (acceptable = blue, non-acceptable = red) is the K-S statistic for the parameter.

5.3.2. **Bistability of FAK activation**

A deeper analysis of the effects of PIP2 on the dynamics of FAK activation was performed following the MPSA prediction. Using the rate of PIP2 degradation as a bifurcation parameter, the model suggested that a bistability in FAK activation existed in response to changes in PIP2 degradation rate (**Figure 5.2**). FAK activation exhibited a bistability, which implies that FAK may settle into either a low or a high activation state, when PIP2 degradation rate was between 0.2592 and 0.4768. Monostability in FAK activation was predicted at other values of PIP2 degradation rate, a stable high FAK activation state (rate <0.2592), and a stable low FAK activation state (rate>0.4768).

The rate of PIP2 degradation can be directly linked to the cellular concentration of PIP2. In order to provide an experimental validation of the theoretical prediction, rat hepatocytes grown on matrigel were exposed to an exogenous PIP2/histone carrier complex and the state of FAK activation was probed by flow cytometry. Hepatocyte cultures on matrigel have been shown to induce a very low level of PIP2 accumulation (Kimata T, 2006); therefore, a controlled delivery of exogenous PIP2 may provide an experimental platform to demonstrate the validity of our mathematical prediction. A single cell population, with a low FAK activation level, was observed in hepatocytes that were exposed to the carrier alone.

However, a bimodal distribution of FAK activation levels was observed in response to an exposure to 50 mM of exogenous PIP2, where approximately 22.58% of the gated cell population (Total = 10,000 cells) expressed a higher FAK phosphorylation.

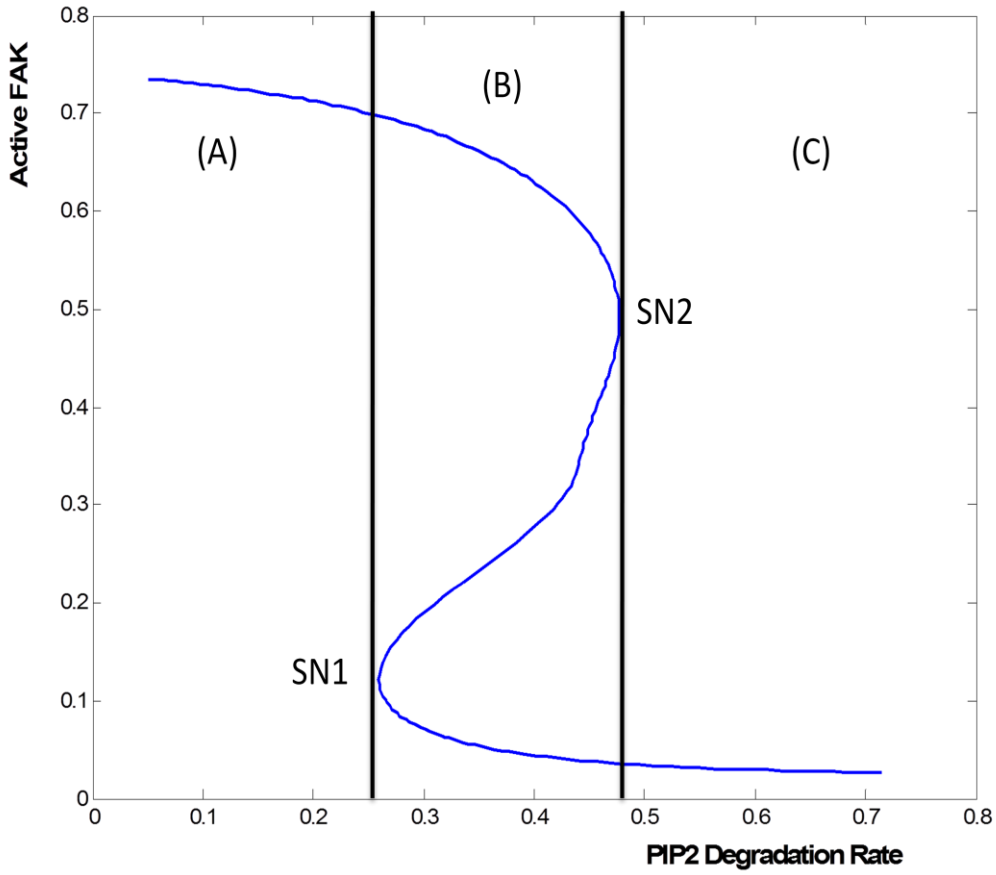

Figure 5.2. **Bifurcation diagram of active FAK in response to changing PIP2 degradation rates**. (A) Monostable high FAK activation (B) Region of bistability (C) Monostable low FAK activation. SN = Saddle node, where SN1 corresponds to PIP2 degradation rate of 0.2592, and SN2 corresponds to a rate of 0.4768.

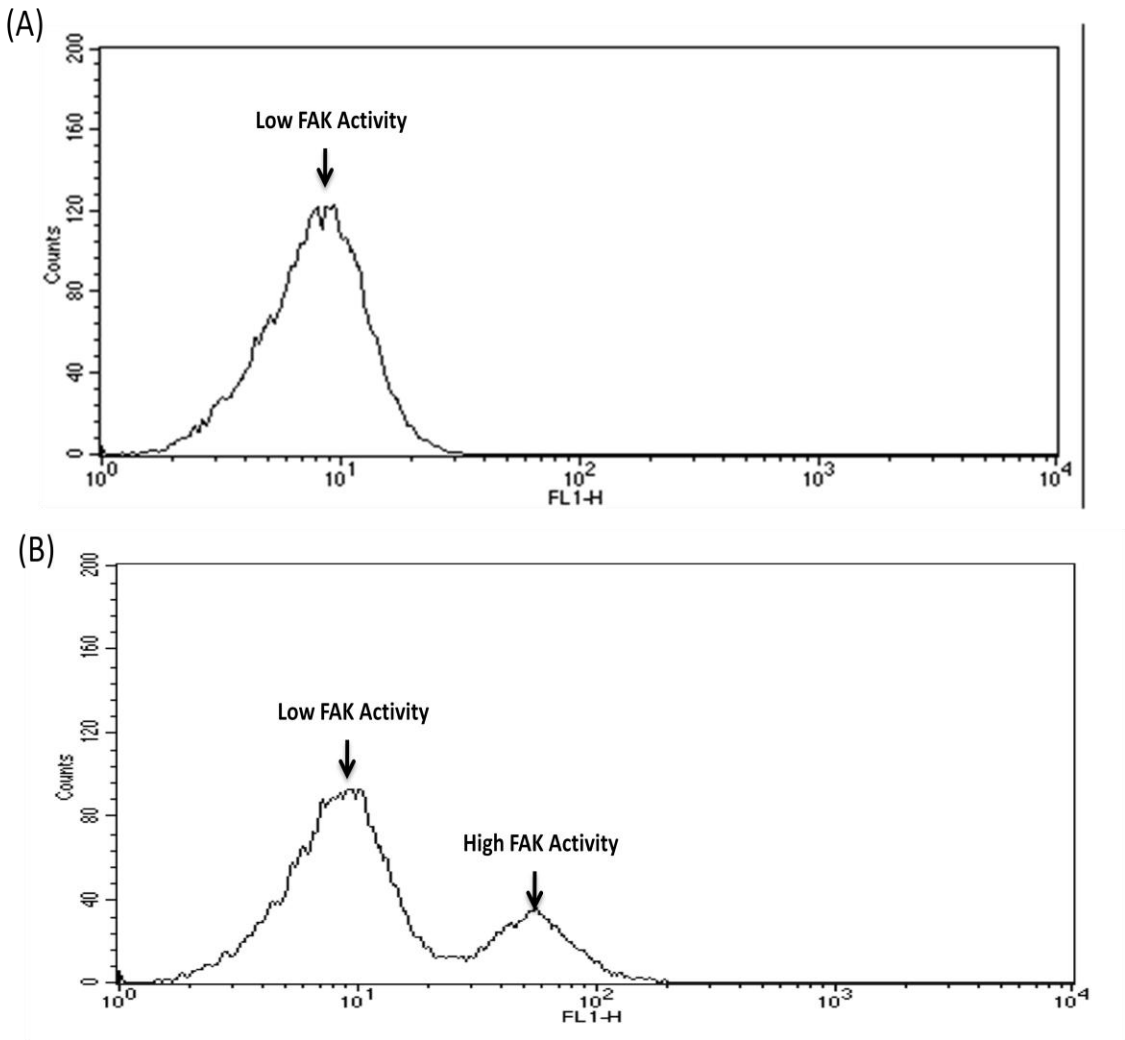

<u>Figure 5.3</u>. **Bistability of FAK activation in response to changing PIP2 concentrations**. Rat hepatocytes were cultured on matrigel for 72 hours. Ten hourly cellular deliveries of PIP2 via a histone carrier were performed, and the levels of FAK phosphorylation ($Y^{576,577}$) were evaluated by flow cytometry after the last delivery. (A) Hepatocytes exposed to the histone carrier alone. (B) Hepatocytes exposed to PIP2/Histone carrier complex (molar ratio= 5:1 with a PIP2 concentration of 50 μM).

A major characteristic of bistable systems is their ability to remain in a modified state long after the removal of the input that induced the modification, a property commonly called hysteresis. Twenty-four hours after the removal of the stimuli (carrier alone, or PIP2/carrier complex), the cells that had been previously treated with the carrier alone remain in a low FAK activation state whereas the two-peak distribution in FAK activation level was maintained in hepatocytes that had been previously exposed to the PIP2/carrier complex, where approximately 12.5% of the gated cell population (Total = 10,000 cells) expressed a higher FAK phosphorylation (**Figure 5.4**).

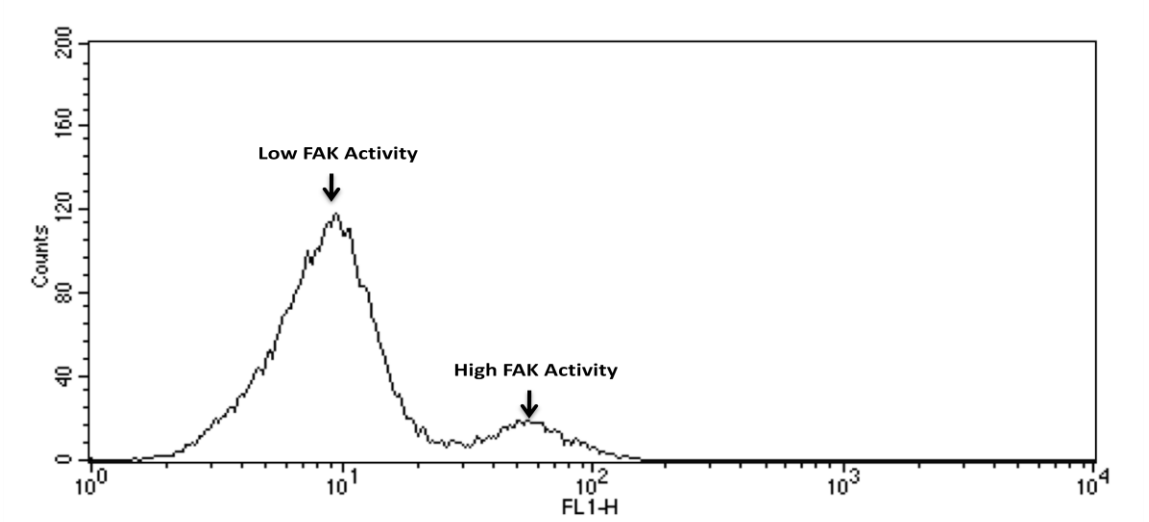

Figure 5.4. Hysteretic behavior of FAK activation in response to changing PIP2 concentrations. Rat hepatocytes were cultured on matrigel for 72 hours. Ten hourly cellular deliveries of PIP2 via a histone carrier were performed, and the cells were left to incubate in normal culture media without PIP2 or carrier after the last delivery. After 24 hours, the levels of FAK phosphorylation ($Y^{576,577}$) were evaluated by flow cytometry.

5.3.3. **Bistability of β-catenin nuclear translocation**

The model also suggests that the cell adhesion pathways may generate a bistability in β-catenin localization in response to changes in PIP2 concentration. Soluble β-catenin levels, which are directly related to the nuclear β-catenin levels, exhibited a bistability within the same interval as FAK activation (0.2592-0.4768). A monostable low soluble β-catenin (none in the nuclei) state at rates that were lower than 0.2592, whereas a monostable high soluble β-catenin (presence of β-catenin in the nuclei) state would occur at rates higher than 0.4768 (**Figure 5.5**).

The delivery of PIP2 into hepatocytes growing in T150 culture flasks is highly impractical. However, given that the PIP2 level can be directly related to the level of FAK activation, and active FAK has been shown to induce the dissociation of the E-cadherin/β-catenin complex at the plasma membrane, which can be simulated using the calcium chelator EGTA. In order to validate the predicted all-or-none switching behavior, β-catenin was measured by flow cytometry in purified nuclei from hepatocytes on collagen that had been exposed to increasing concentrations of EGTA for 6 hours. A bimodal distribution of nuclear β-catenin was observed in cells that had not been exposed to EGTA (**Figure 5.6**), where most nuclei (98.37 %) contained no β-catenin (left peak) and the only a very small fraction of nuclear population testing positive for β-catenin. With increasing concentrations of EGTA, the fraction of nuclear population that stained positively for β-catenin steadily increased (right peak) while the number of nuclei without β-catenin decreased (left

peak). These results suggest that nuclear β-catenin come primarily from the disruption of cell-cell interactions.

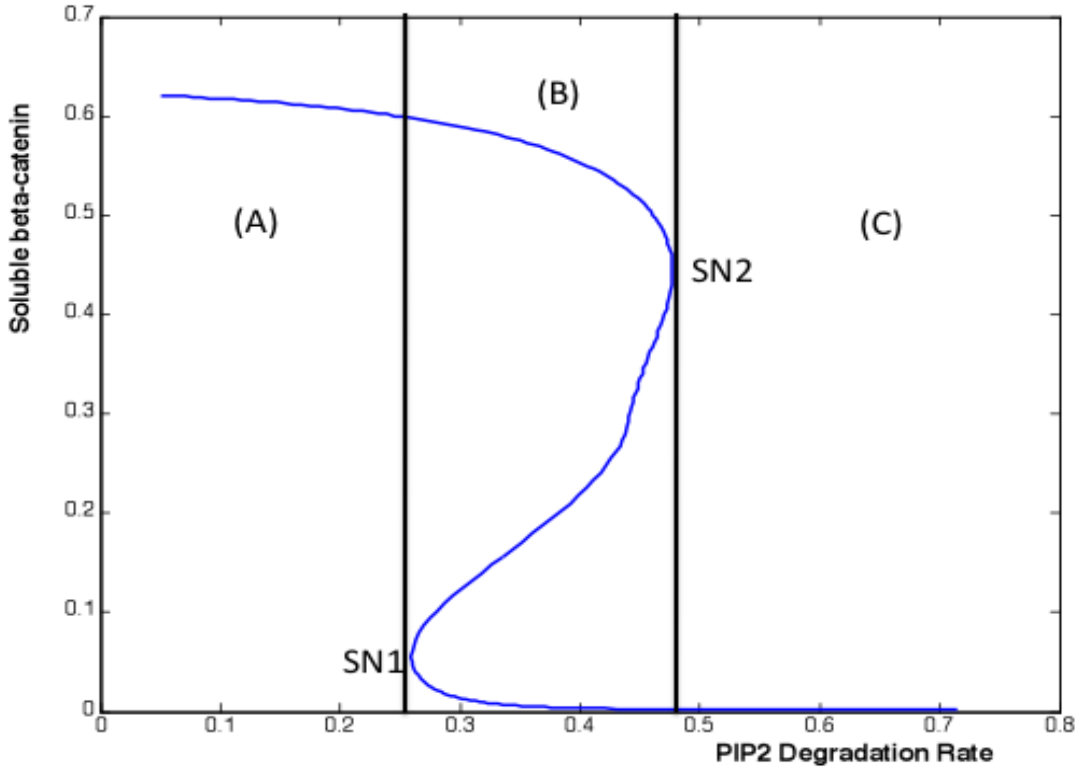

<u>Figure 5.5</u>. Bifurcation diagram of soluble β-catenin in response to changing PIP2 degradation rates. (A) Monostable high soluble β-catenin levels, a high probability of β-catenin translocation to the nuclei (B) Region of bistability (C) Monostable low soluble β-catenin levels, no nuclear translocation of β-catenin. SN = Saddle node, where SN1 corresponds to PIP2 degradation rate of 0.2592, and SN2 corresponds to a rate of 0.4768.

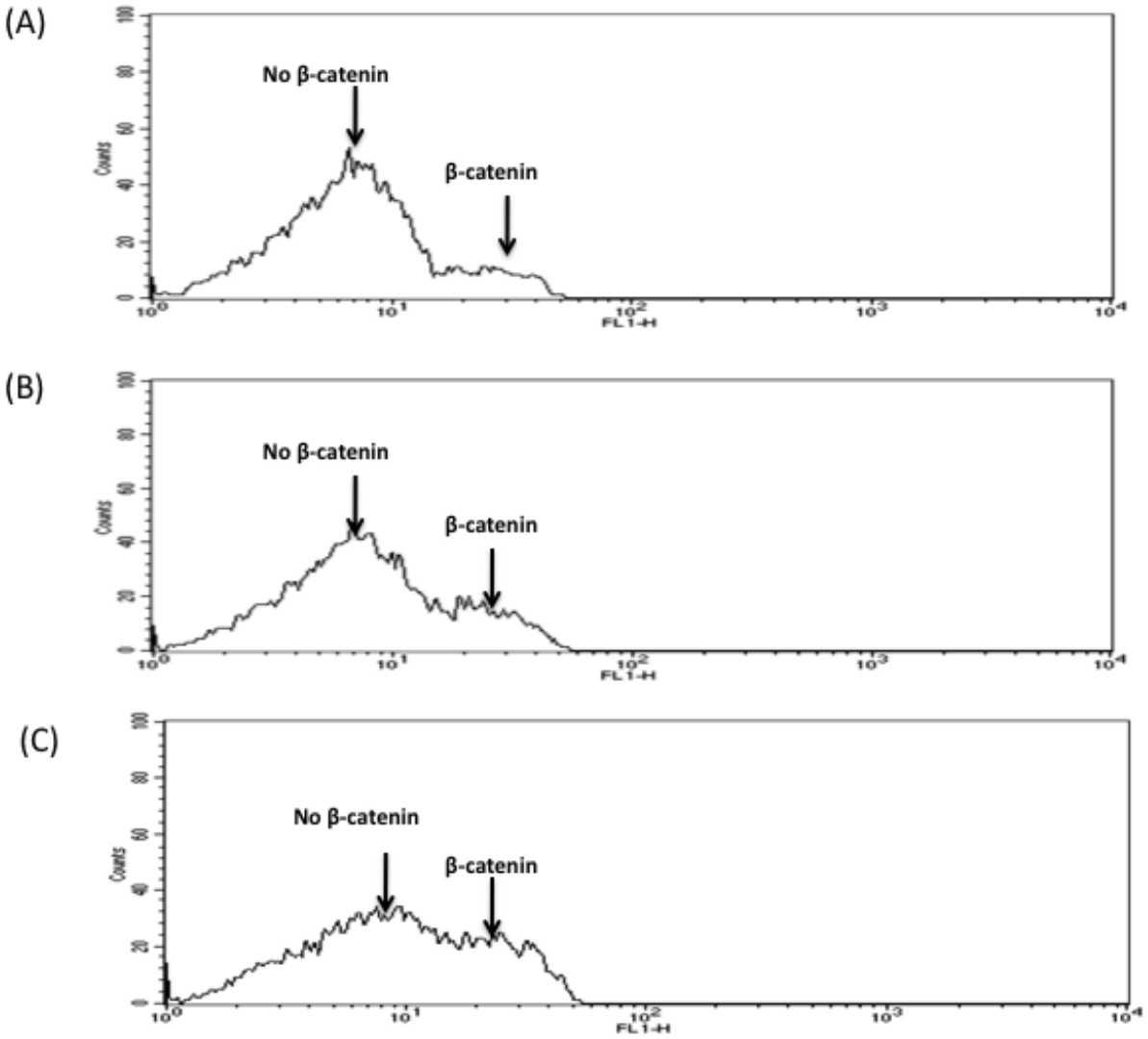

Figure 5.6. Effects of cell-cell interaction on the nuclear translocation of β-catenin. Rat hepatocytes were cultured on collagen in T150 culture flasks for 48 hours, and then exposed to different concentration of EGTA. After 6 hours, the nuclei were purified as described in the materials and methods section, and the levels of nuclear β-catenin were evaluated by flow cytometry. (A) EGTA concentration = 0 mM, β-catenin-positive= 2.63 % (B) EGTA concentration = 0.5 mM, β-catenin-positive= 3.90 % (C) EGTA concentration = 1 mM, β-catenin-positive= 5.86 %.

5.3.4. **Bistabilities of cdc42 and RhoA activations**

RhoA and cdc42 are the focal points in the integration of signals from the integrin and the E-cadherin/β-catenin pathways; therefore, their steady state properties should reflect the activation state of the cell adhesion pathways at equilibrium. The model predicted again bistabilities in the activation of cdc42 and RhoA in response to changes in PIP2 degradation rate. Cdc42 was predicted to be in a high activation steady state at high PIP2 degradation rates (>0.4768); and in a low activation steady state at low PIP2 degradation rates (0.2592). On the other hand, a high activation steady state of RhoA was suggested at low PIP2 degradation; and in low activation steady state at high PIP2 degradation rates. Bistability for either cdc42 or RhoA was predicted within the interval between the values mentioned above (**Figure 5.7**).

The current lack of feasibility in measuring cdc42 and RhoA activities at the single-cell level does not permit the experimental validation of the bistability in their activation. However, the overall changes in the steady state activity within a population of cells, which were exposed to the same condition, should reflect the number of individual cells where the switch between a low to high or a high to low activation states occurred. Hepatocytes in collagen were exposed to different concentrations of FAK inhibitor for up to 6 hours, and then pull-down assays were used to evaluate the levels of cdc42 and RhoA activations. Increasing the concentration of FAK inhibitor caused an increase in total active cdc42, and a decrease in total active RhoA. When compared to hepatocytes in the control group

(no inhibitor, full FAK activation), hepatocytes that were exposed to 0.125 mM of PF-562271 expressed a significant increase in cdc42-GTP levels and a decrease in RhoA-GTP levels (**Figure 5.8**).

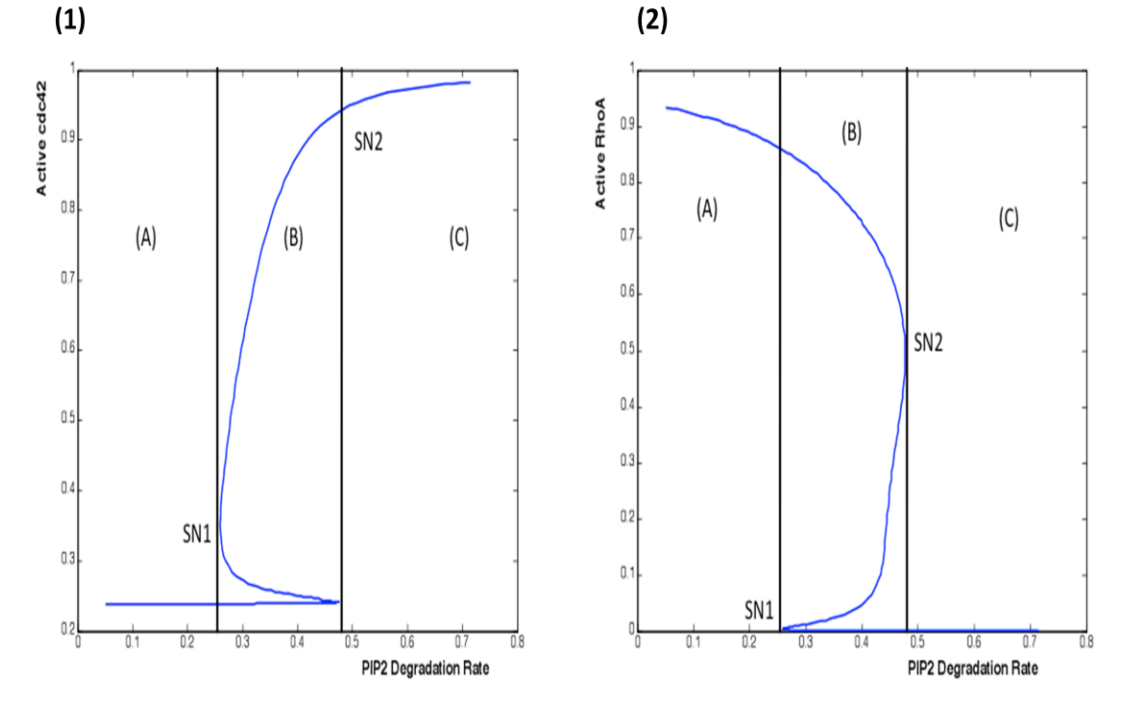

<u>Figure 5.7</u>. Bifurcation diagrams of active cdc42 and RhoA in response to changing PIP2 degradation rates. (A) Monostable low cdc42-GTP/high RhoA-GTP (B) Region of bistability (C) Monostable high cdc42-GTP/low RhoA-GTP. **(1)** Bifurcation diagram of cdc42-GTP **(2)** Bifurcation diagram of RhoA-GTP. SN= Saddle node, where SN1 corresponds to PIP2 degradation rate of 0.2592, and SN2 corresponds to a rate of 0.4768.

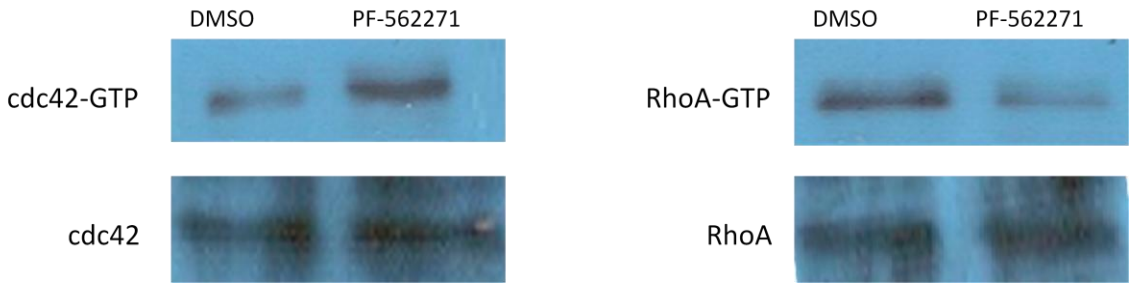

Figure 5.8: **Effects of FAK inhibition on cdc42 and RhoA activations**. Rat hepatocytes were cultured on collagen for 48 hours, and then exposed to 0.125 mM of the specific FAK inhibitor PF-562271. After three hours, pull-down assays were used, as described in materials and Methods, to evaluate the activation levels of cdc42 and RhoA.

5.4. Discussion

In this chapter, we designed a mathematical model of the coupled integrin and E-cadherin/β-catenin pathways to analyze the property of their underlying control system. The mathematical model predicted that PIP2 degradation rate, and the rates of formation and/or disruption of the E-cadherin/β-catenin complex exerted the most significant impact of FAK activation and the nuclear localization of β-catenin.

The model predicted a bistability in FAK activation in response to changing PIP2 rate of depletion, which can be directly related to the cellular concentration of PIP2. The prediction results suggest the existence of critical PIP2 concentration threshold where the underlying control system switches from a low FAK activation (weak integrin-based adhesion) to a high FAK activation (strong integrin-based adhesion). The bimodal distribution of FAK activation levels in hepatocytes on matrigel following the delivery of exogenous PIP2 confirmed the validity of the mathematical prediction. Two distinct hepatocyte populations, which corresponded respectively to cell with low FAK activation level and high FAK activation level, were obtained after exposure to 50 μM of PIP2.

The model also predicted a bistability in β-catenin localization in response to changing dissociation rates of PIP2, which can be correlated with the dissociation of the E-cadherin/β-catenin complex at the plasma membrane. Such prediction suggests that if the number of disrupted plasma membrane E-cadherin/β-catenin

complexes reaches a threshold, a critical accumulation of free β-catenin would happen in the cytoplasm, which would eventually lead to its translocation to the nuclei. The bimodal distribution of nuclear β-catenin in rat hepatocytes, with an increase in the nuclear fraction containing β-catenin when the cells were exposed to increasing concentrations of EGTA, validated our theoretical prediction.

The model also predicts that the steady state level of FAK activity and its potential effects on the E-cadherin/β-catenin pathway would impact the steady state levels of active cdc42 and RhoA. A weak integrin-based/strong E-cadherin-based adhesion (low FAK activity/absence of β-catenin in the nuclei) would lead to high cdc42-GTP and low RhoA-GTP levels. Conversely, a strong integrin-based/weak E-cadherin-based adhesion (high FAK activity/presence of β-catenin in the nuclei) would result into low cdc42-GTP and high RhoA-GTP levels. We confirmed the validity of the prediction by modulating the activity of FAK using its specific inhibitor.

The phospholipid PIP2 is relatively in higher abundance compared to other phospholipids in the plasma membrane (Insall RH, 2001). The net cellular concentration of PIP2 results from the balance between its synthesis and depletion. PIP2 is primarily synthesized from the phosphorylation of C5 on the D ring of the phosphatidylinositol-4-phosphate (PI4P), which is catalyzed by the enzyme phosphatidylinositol 4-phosphate 5-kinase (PIP5K). PIP2 depletion occurs either through its usage in different signaling pathways (e.g. G protein-coupled receptor, PI3K/AKT pathway), or by dephosphorylation via the enzyme Phosphoinositide 5-

phosphatase (Divecha N, 1995). The transmembrane proteoglycan syndecan-4 may play a very significant in the regulation of the cellular concentration of PIP2. Syndecan-4 involvement is necessary for the full activation of FAK (Wilcox-Adelman SA, 2002) and RhoA (Dovas A, 2006), and active FAK and RhoA positively stimulate the activity of the enzyme PI5K (Ling K, 2002) (Weernink PA, 2004). Syndecan-4 also binds to PIP2 and promotes its retention in the plasma membrane (Simons M, 2001) (Kwon S, 2009), most probably by limiting the accessibility to PIP2 of the enzymes that promote its depletion. Full activation of the integrin pathway requires the simultaneous engagement of the integrin receptors and the transmembrane syndecan proteoglycans to the extracellular matrix. Rat hepatocytes in culture secrete fibronectin, which then adsorb to the collagen matrix. Adsorbed fibronectins bind to $\alpha 5\beta 1$ integrin and syndecan-4 and fully activate the integrin pathway, which leads to an accumulation of PIP2 at the plasma membrane and a strong FAK activation.

Active FAK may function both as an activator and as an inhibitor toward cdc42 and RhoA. FAK may upregulate the active form of cdc42 through the FAK-dependent activation of β-Pix (a cdc42-GEF), and as an inhibitor by competing with Nudel for binding to the scaffolding protein paxillin. A paxillin-bound Nudel inhibits cdc42-GAP and thereby works as an indirect activator of cdc42. By displacing Nudel, active FAK relieves its inhibitory effect on cdc42-GAP and thereby functions as a cdc42 inhibitor. Whether FAK works as a cdc42 activator of inhibitor may depend on its level of activation, and a likely difference in the binding affinities of Nudel and active FAK for paxillin . At low FAK activation levels, more Nudel molecules are

bound to paxillin leading to a increase in cdc42-GTP levels. However, Nudel molecules are displaced from paxillin as more and more FAK molecules are activated, which eventually causes a net decrease in cdc42-GTP levels.

The bindings of p190RhoGAP (RhoA inhibitor) and p190RhoGEF (RhoA activator) to active FAK are essential for their activations. Their simultaneous binding to active FAK is unlikely; therefore, we may assume a competitive binding where the final outcomes depend on the level of FAK activation and the presence of other effectors. p190RhoGAP may have a higher affinity to active FAK compared to p190RhoGEF, which may explain the downregulation of RhoA activity at low FAK activation during early culture. As more FAK molecules are activated, more p190RhoGEF are recruited to the focal adhesion and become activated. Moreover, the increase in FAK activation level corresponds to a higher accumulation of PIP2 at the focal adhesion. The affinity of p190RhoGAP for active FAK has been shown to be decreased by the presence of PIP2 (Lévay M, 2009). Therefore, p190RhoGAP is displaced from focal adhesions at high FAK activation levels whereas more and more p190RhoGEF become active through their bindings to FAK. The end result is the net activation of RhoA at high FAK activation levels.

In conclusion, the crossing of the critical FAK/PIP2 threshold constitutes the point of no return where the hepatocyte adhesion network irreversibly switches from a weak integrin-based/strong E-cadherin-based adhesion (below the threshold) to a strong integrin-based/weak E-cadherin-based adhesion (above the threshold). To the best of our knowledge, no report on the bistability of the cell

adhesion network combining mathematical analyses and experimental validations is yet available. Therefore, our model provides a basic framework for the inclusion of additional mechanisms that will improve its analytical and predictive powers. In particular, the accounting of the changes in the expression of the pathway constituents and the effects of the mechanical properties of the extracellular matrix should be addressed in future studies.

5.5. Supplementary information

Model development

The main focus in designing the model was to understand the properties of the control system that regulate the switch between the activation steady states of the cell adhesion network. The adhesion network can be split into two signaling submodules, the integrin submodule (**Supplementary figure 5.1**) and the E-cadherin/β-catenin submodule (**Supplementary figure 5.2**). The crosstalks between the integrin and E-cadherin/β-catenin signaling submodules occur mostly via the activation (or inactivation) of the small GTPases cdc42 and RhoA.

The model consists of a system of ordinary differential equations with 8 state variables, and 32 parameters (**Supplementary table 5.1**). We assumed that the overall concentration of all state variables (with the exception of β-catenin) did not change over time. Fractional terms were used to represent all variables, which rendered the model dimensionless. Most parameter values were either obtained from the literature, or estimated from typical values for similar reaction kinetic processes. The remaining unknown parameters were constrained with the trend of the expression profiles of the state variables, and estimated using the stochastic ranking evolution strategy algorithm (Ji X, 2006), which was implemented using MPI-C++. The parameter values for most simulations in this work, and the MPSA results with respect to their perturbations, are listed in supplementary table 5.2 (reference values).

<u>Supplementary Table 5.1</u>. Reaction Kinetics for the mathematical model

$$\frac{d}{dt}[PIP2] = \left(p_0 + \frac{k_{f1}}{\left(1 + \left(\frac{K_{f1}}{[pFAK]}\right)^n\right)}\right)(1 - [PIP2]) - k_{d1}[PIP2]$$

$$\frac{d}{dt}[pFAK] = \left(f_0 + \frac{k_{f2}}{\left(1 + \left(\frac{K_{f2}}{[PIP2]}\right)^n\right)}\right)(1 - [pFAK]) - PTP\,[pFAK]$$

$$\frac{d}{dt}[Cdc42] = cGEF(1 - Cdc42) - cGAP\,[Cdc42]$$

$$\frac{d}{dt}[R\hbar oA] = rGEF(1 - R\hbar oA) - rGAP\,[R\hbar oA]$$

$$\frac{d}{dt}[MT] = k_{MT}[MT]\left(1 - \frac{[MT]}{K_{MTmx}}\right)$$

$$\frac{d}{dt}[Ecad_s] = -C2P[Ecad_{sol}][Bcat_{sol}] + P2C[EB]$$

$$\frac{d}{dt}[EB] = C2P[Ecad_{sol}][Bcat_{sol}] - P2C[EB]$$

$$\frac{d}{dt}[Bcat_s] = -C2P[Ecad_{sol}][Bcat_{sol}] + P2C[EB] + k_{sBcat}(1 - [EB] - [Bcat_s]) - k_{dBcat}[Bcat_s]$$

Where,

$$PTP = PTP_0\left(1 - \frac{[R\hbar oA]^n}{(K_{RP} + [R\hbar oA]^n)} + k_{EBP}\frac{[EB]^n}{(K_{EBP} + [EB]^n)}\right)$$

$$cGEF = c_0 + k_{f3}\frac{[pFAK]}{(eps + [pFAK]^n)} + k_{EBC}\frac{[EB]^n}{(K_{EBC}^n + [EB]^n)}$$

$$cGAP = k_{d3}\frac{[pFAK]^n}{(K_{d3} + [pFAK]^n)}$$

$$rGEF = c_0 + \frac{[pFAK]}{\left(aR + \left(\frac{rGAP}{K_{rGEF}}\right)^n + [pFAK]\right)}$$

$$rGAP = \frac{[pFAK]}{\left(aR + \left(\frac{[PIP2]}{K_{rGAP}}\right)^n + [pFAK]\right)} + k_{EBR}\frac{[EB]^n}{(K_{EBR} + [EB]^n)}$$

$$C2P = k_{C2P}[MT]\frac{[Cdc42]}{\left(K_{C2P} + \left(\frac{pFAK}{K_{C2PF}}\right)^{n} + [Cdc42]\right)}$$

$$P2C = k_{P2C}\frac{[pFAK]}{\left(K_{P2C} + \left(\frac{Cdc42}{K_{CEcad}}\right)^{n} + [pFAK]\right)}$$

Descriptions of the state variables

- PIP2: Phosphatidylinositol 4,5-bisphosphate
- pFAK: Active FAK
- Cdc42: Active Cdc42 (GTP-bound Cdc42)
- RhoA: Active RhoA (GTP-bound RhoA)
- MT: Polymerized microtubules (Plus ends reaching the plasma membrane)
- $Ecad_s$: Soluble (internalized) E-cadherins
- EB: Plasma membrane E-Cadherin/β-catenin complexes
- $Bcat_s$: Soluble β-catenin (Cytoplasmic and nuclear)

Initial Condition:

[PIP2] = pFAK = 0.001; [Cdc42] = [RhoA] = 0.25; [MT] = 0; [EB] = 0;

$[Ecad_s] = [Bcat_s] = 1$;

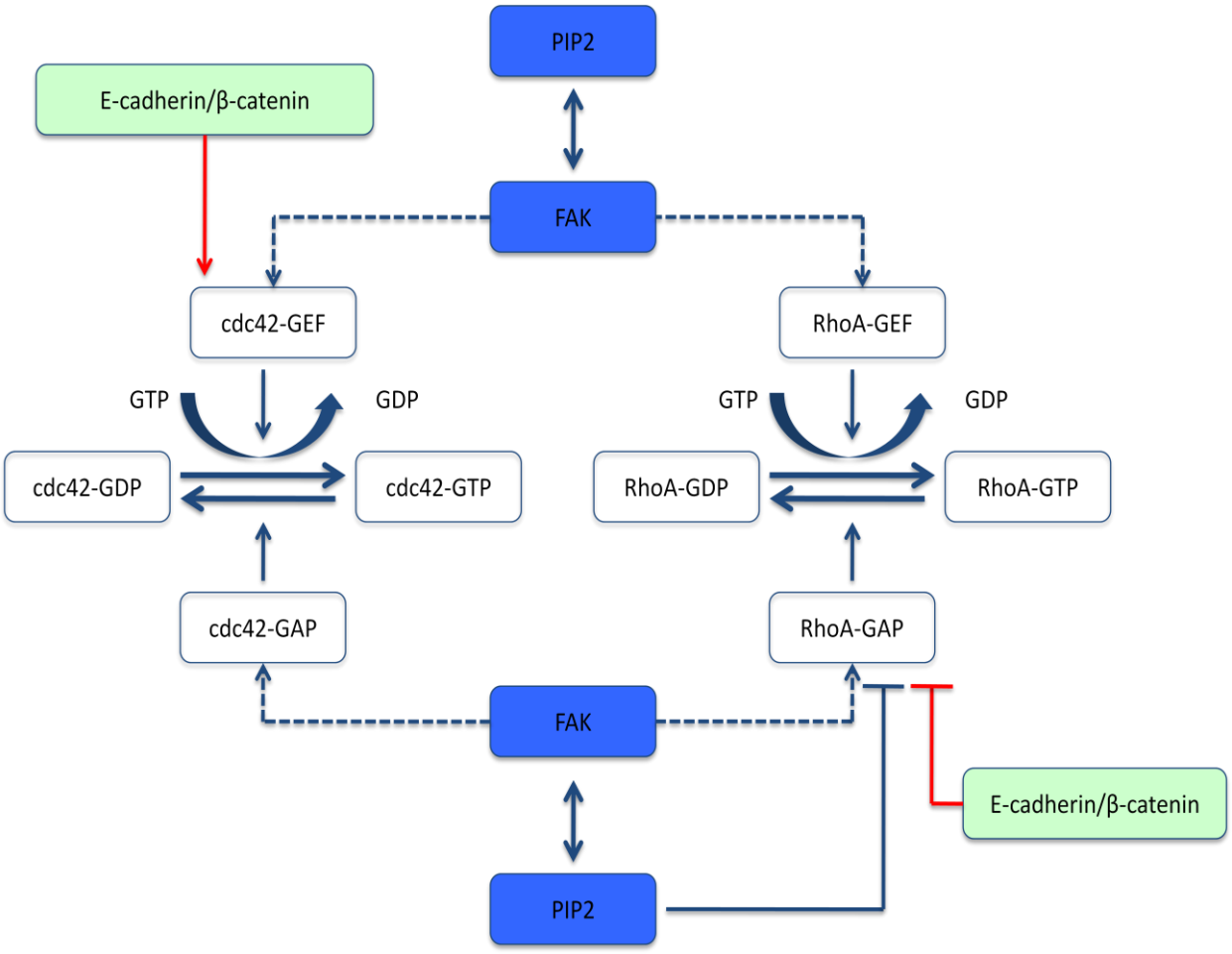

<u>Supplementary figure 5.1</u>. Integrin signaling submodule of the cell adhesion network. Crosstalks with the E-cadherin/β-catenin submodule are depicted in red. Dashed arrows signify that the functional interaction can be either an activation or an inhibition.

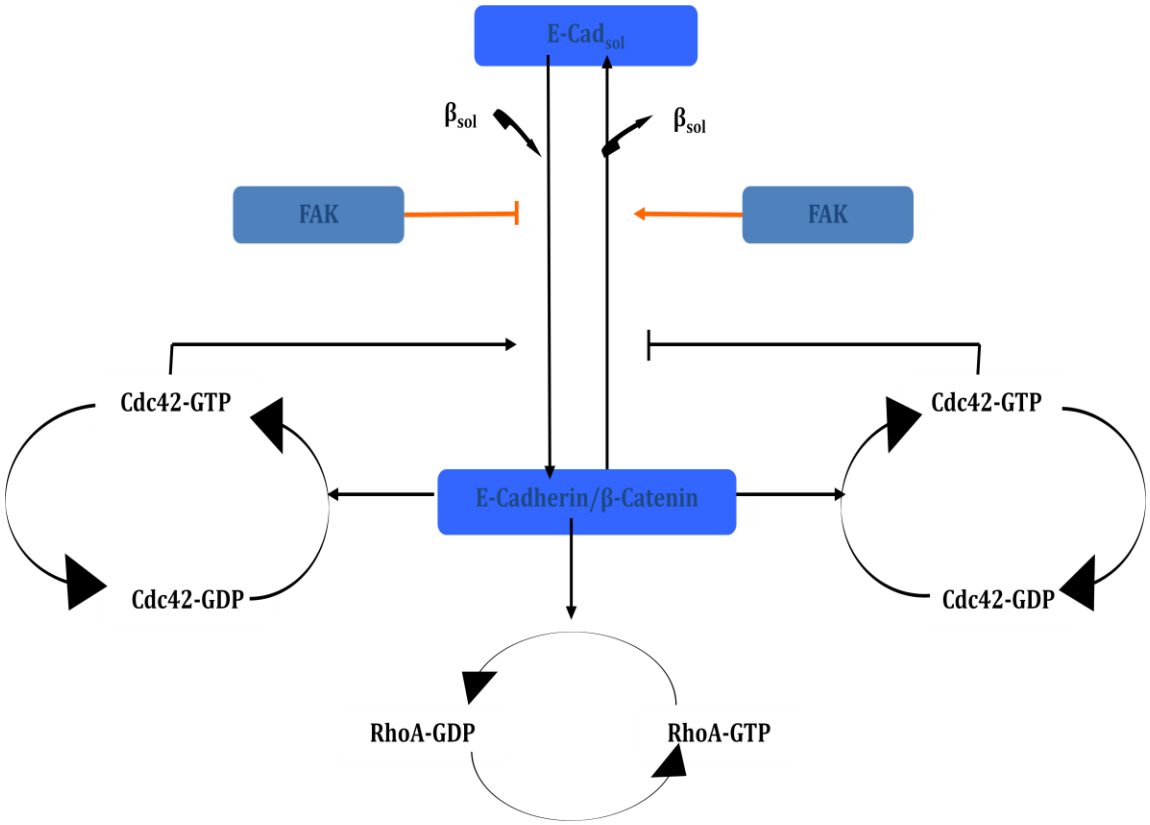

<u>Supplementary figure 5.2</u>. E-cadherin/β-catenin signaling submodule of the cell adhesion network. Crosstalks with the integrin submodule are depicted in red.

Dissecting the effects of FAK on cdc42 and RhoA activations

Active FAK can function either as an activator or as an inhibitor toward cdc42 and RhoA. In order to capture that dual but contradictory role of FAK, we hypothesized that the net effect of FAK on either cdc42 or RhoA depends on its level of activation (**Supplementary figures 5.3 and 5.4**).

FAK can be an upstream Cdc42 activator via β-Pix, and a repressor by competing with Nudel for paxillin binding (Sinha S, 2008) (Shen Y, 2008) (Shan Y, 2009) .

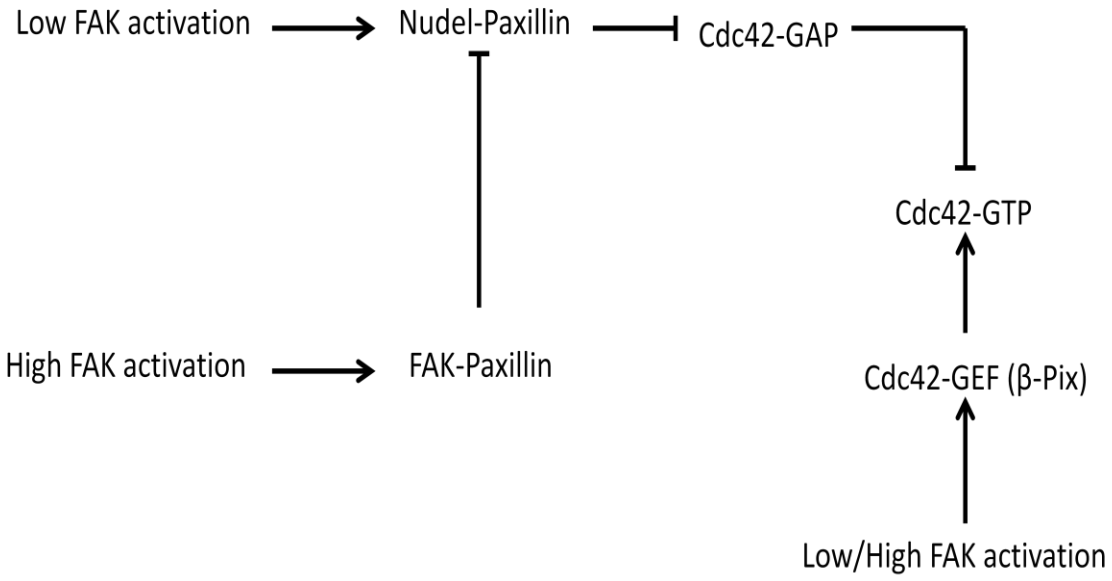

Supplementary figure 5.3: **Hypothetical concentration-dependent effects of active FAK on cdc42 activation**.

Active FAK binds to RhoA-GEF and RhoA-GAP; although it is unlikely that both can bind to FAK at the same time (Tomar A, 2009). We hypothesized that a RhoA-GAP has a higher affinity for FAK than RhoA-GEF. However, the substrate affinity of RhoA-GAP can be modulated by PIP2 (Lévay M, 2009).

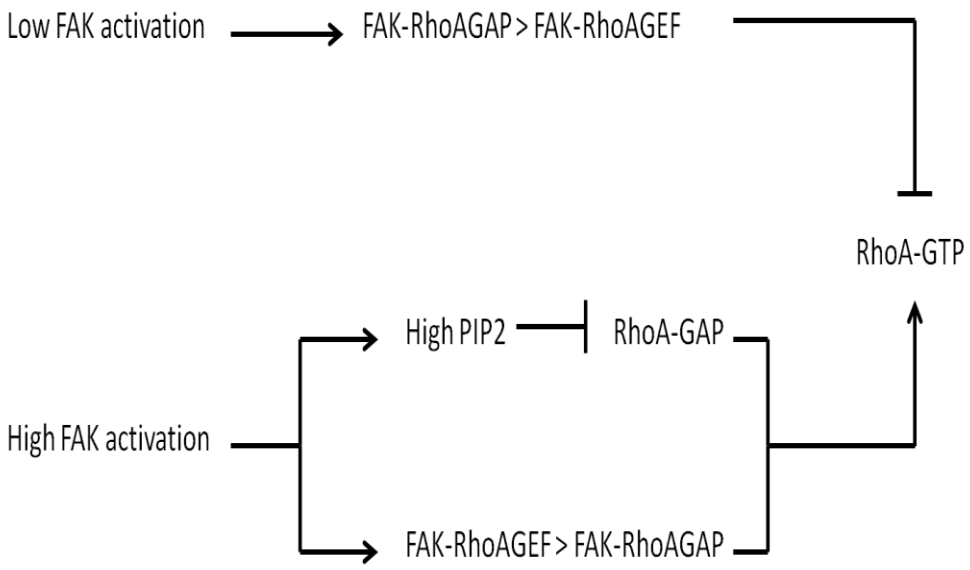

<u>Supplementary figure 5.4</u>: Hypothetical concentration-dependent effects of active FAK on RhoA activation.

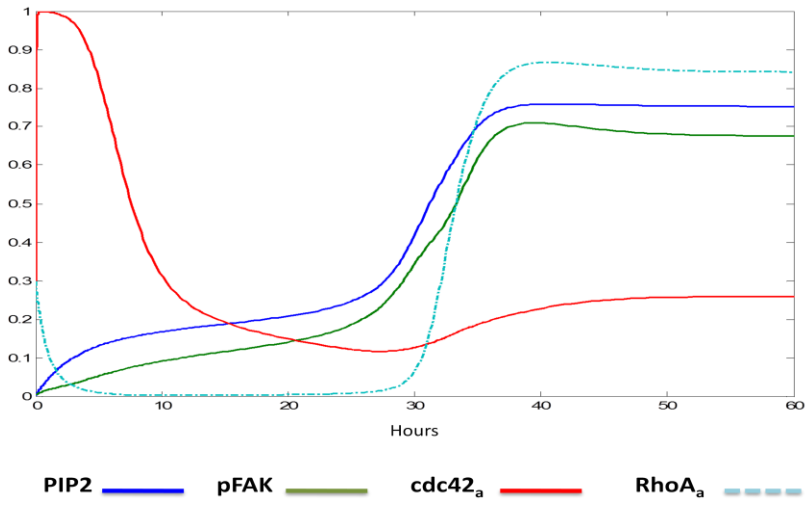

<u>Supplementary figure 5.5</u>. Predicted kinetics of the integrin pathway activation. pFAK = active FAK, $cdc42_a$= active cdc42, $RhoA_a$ = active RhoA.

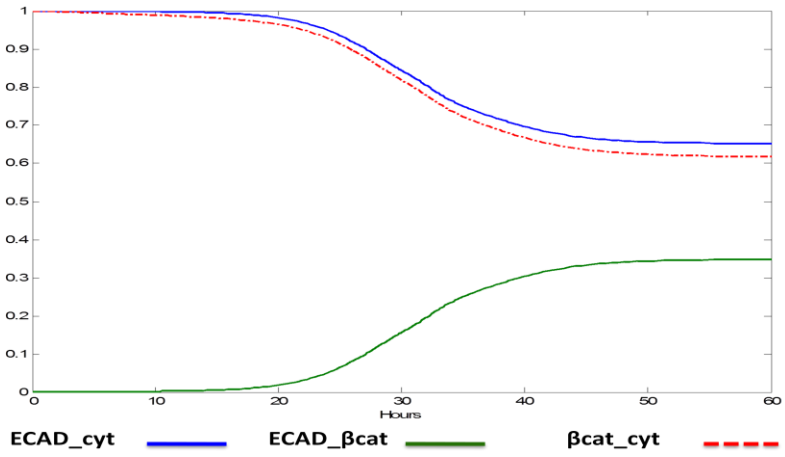

<u>Supplementary figure 5.6</u>. Predicted kinetics of the E-cadherin/β-catenin pathway activation. ECAD_cyt = internalized E-cadherin, ECAD_β-cat = plasma membrane E-cadherin/β-catenin complex, βcat_cyt = soluble β-catenin (nuclear and cytoplasmic).

(A)

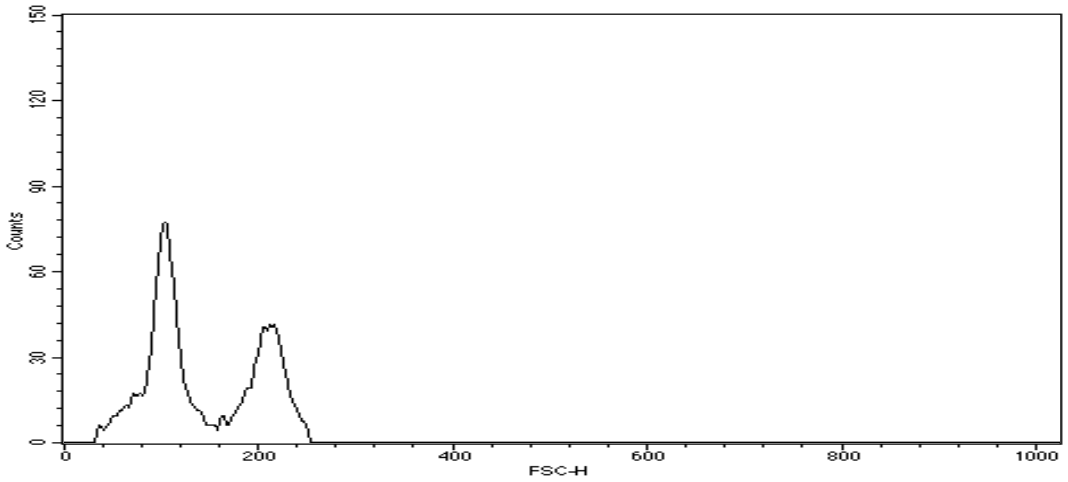

(B)

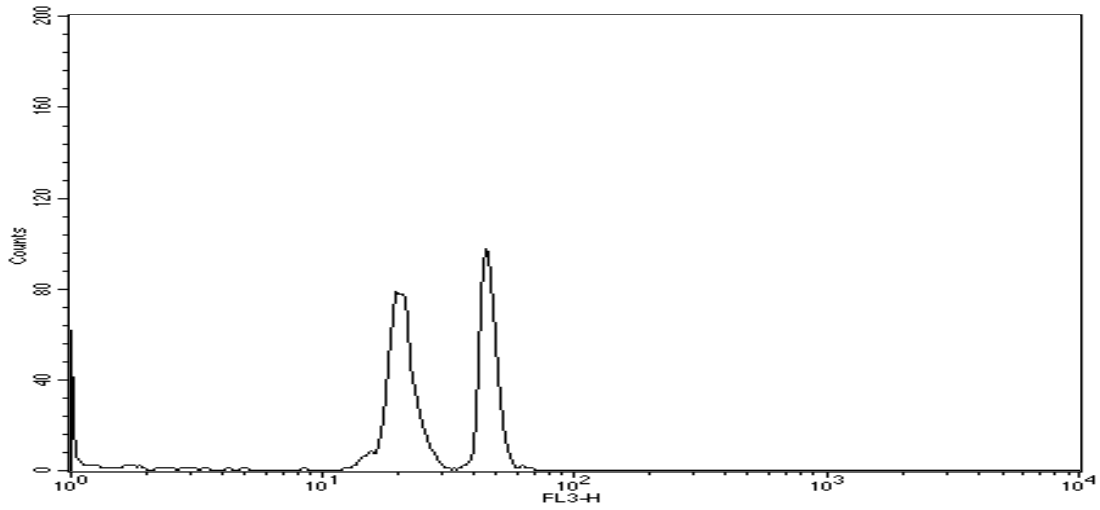

<u>Supplementary figure 5.7</u>. Flow cytometry analysis, histograms of purified nuclei The two peaks correspond respectively to the population of mononucleated and binucleated hepatocytes **(A)** Forward scatter profile of rat hepatocyte purified nuclei **(B)** Propidium iodide staining.

<u>Supplementary Table 5.2</u>: Results of MPSA with respect to variations in the kinetic parameter values of the integrin and E-cadherin pathways

Rate Constant	Description	Reference value	Range of variation	K-S
k_{f1}	PIP2 synthesis	1	0.1-10	0.024
K_{f1}	PIP2 synthesis	0.5	0.05-5	0.048
k_{d1}	PIP2 degradation	0.25	0.025-2.5	0.117
k_{f2}	FAK activation	1	0.1-10	0.070
K_{f2}	FAK activation_PIP2 feedback	0.375	0.0375-3.75	0.202
K_{RP}	FAK phosphatase_RhoA effect	0.25	0.025-2.5	0.049
k_{EBP}	FAK phosphatase_Ecadherin effect	1	0.1-10	0.078
K_{EBP}	FAK phosphatase_Ecadherin effect	0.25	0.025-2.5	0.082
k_{f3}	cdc42GEF_FAK effect	0.001	0.0001-0.01	0.051
k_{d3}	cdc42_GAP	2	0.2-20	0.051
K_{d3}	cdc42_GAP	0.001	0.0001-0.01	0.041
k_{EBC}	cdc42GEF_E-cadherin effect	1	0.1-10	0.061
K_{EBC}	cdc42GEF_E-cadherin effect	0.35	0.0375-3.75	0.039
K_{rGAP}	RhoAGAP_PIP2 related substrate selectivity	0.35	0.0375-3.75	0.023
K_{rGEF}	RhoAGEF_FAK related	0.1	0.01-1	0.031
k_{EBR}	RhoAGAP_E-cadherin effect	0.5	0.05-5	0.043

K_{EBR}	RhoAGAP_E-cadherin effect	0.75	0.075-7.5	0.034
k_{MT}	Microtubule polymerization	0.35	0.035-3.5	0.51
K_{MTmx}	Microtubule polymerization	0.5	0.05-5	0.141
k_{C2P}	E-cadherin/β-catenin formation at the plasma membrane	2.5	0.25-20.5	0.170
K_{C2P}	E-cadherin/β-catenin formation at the plasma membrane	1	0.1-10	0.045
K_{C2PF}	E-cadherin/β-catenin formation_FAK inhibitory effect	0.25	0.025-2.5	0.044
k_{P2C}	E-cadherin/β-catenin disruption at the plasma membrane	1	0.1-10	0.084
K_{P2C}	E-cadherin/β-catenin disruption at the plasma membrane	1	0.1-10	0.134
K_{CEcad}	Cdc42 inhibition of E-cadherin/β-catenin disruption	0.75	0.075-7.5	0.047
k_{sBcat}	Synthesis of new β-catenin	0.01	0.001-0.1	0.037
k_{dBcat}	Degradation of β-catenin	0.001	0.0001-0.01	0.053

Chapter 6

Research Summary and Future Directions

6.1. **Research summary**

This dissertation has been focused on understanding the regulation of control system of the coupled integrin and E-cadherin pathways and its effects on the MAPK/ERK pathway in primary rat hepatocytes. We used an integrative approach combining experimental investigations and bifurcation theory to gain deeper insight into the properties of the hepatocyte adhesion network. The overall purpose of this work was to observe how changes in hepatocyte adhesion, which depend on the nature of the extracellular matrix and/or on cell seeding density, would regulate the switch between its steady state properties and lead to an alteration of the differentiation/proliferation balance. The results from this dissertation suggest the existence of a critical activation level of the integrin pathway, which can be represented by a critical threshold accumulation of the phospholipid PIP2 that would induce the full priming of the MAPK/ERK pathway and would lead to the G1/S progression and the loss of hepatocyte specific functions. This work also has further supported the hypothesis that fibronectin-mediated signaling remains a major factor in rat hepatocyte dedifferentiation. Based on the results we have obtained throughout this thesis research, we can propose the following mechanisms.

Early culture

The early phase of cell attachment does not involve syndecan-4 due to the absence of fibronectin in the extracellular matrix; moreover, the inclusion of syndecan-4 into the focal contacts has been shown to be a late process even in cells

that were seeded on fibronectin (Baciu PC, 1995). Following cell seeding, the focal contact formation is initiated after the binding of the integrin receptors to the extracellular matrix. FAK and the enzyme phosphatidylinositol 4-phosphate 5-kinase (PIP5K) are recruited to the newly formed focal contacts, the two-way positive feedback between FAK and PIP2 accelerates the activation of FAK and the accumulation of PIP2. However, the absence of significant syndecan-4 involvement would cause a rapid depletion of PIP2 and would thereby impede the fast activation of FAK.

The low activation level of FAK also impacts the activation of cdc42 and RhoA. The low activation promotes cdc42 activation while it induces a repression of RhoA. The early cdc42 activation promotes cell attachment to the extracellular matrix through the formation of filopodia and the polymerization of actin filaments, which is required for the translocation of free integrin receptors to the cell-ECM interface (Kawakami K, 2001). The early RhoA inactivation causes the disassembly of the stress, and is necessary for hepatocyte spreading (Arthur WT, 2001). Moreover, a RhoA-dependent inactivation of unknown tyrosine phosphatase has been proposed (Wilcox-Adelman SA, 2002). Therefore, the low activation level of RhoA may contribute to the absence of strong FAK activation during early culture.

The E-cadherin/β-cadherin complex is broken apart following the disruption of cell-cell attachment during the hepatocyte isolation process, and both E-cadherin and β-catenin are internalized into the cytoplasm. The accumulation of free cytoplasmic β-catenin would lead to its nuclear translocation where it induces the

transcription of c-Myc, which explains the similarity in c-Myc gene expressions on all extracellular matrices during early culture. The transport of E-cadherin and β-catenin back to the plasma membrane requires significant microtubule polymerizations, which happen late in hepatocyte culture (Mooney DJ, 1995).

Mid/Late culture

No syndecan-4 involvement

In the continued absence of syndecan-4 involvement (e.g. cultures on matrigel, or on other matrices that do not permit fibronectin adsorption), FAK activation and PIP2 concentration would be kept at low levels. The completion of microtubule polymerizations, which is characterized by the large number of microtubule plus ends reaching the plasma membrane, allow the formation of new adherens junctions and the sequestration of β-catenin at the plasma membrane. The low FAK activation level and the presence of E-cadherin homophilic interactions between neighboring hepatocytes would lead to the increase in cdc42 activation and the sustained downregulation of RhoA activity. Therefore, the hepatocyte adhesion pathways would settle into a state more dominated by cell-cell interaction and less by the cell-ECM interactions (Strong E-cadherin-based /Weak integrin-based adhesions). The weak activation of the integrin pathway in general, and FAK in particular, would not be enough to properly "prime" the cells for a maximal response to EGF, which would lead to the lack of a sustained activation of the MAPK/ERK pathway.

With syndecan-4 involvement

In the presence of syndecan-4 involvement (e.g. cultured on fibronectin, collagen…), the inclusion of syndecan-4 into the focal adhesions would induce the accumulation of PIP2, which would in turn lead to a stronger FAK activation. The characteristics of the hepatocyte adhesion pathways at steady state depend on the nature of the crosstalk between the integrin and the E-cadherin pathways. At low and intermediate hepatocyte seeding densities, there are not enough E-cadherin homophilic interactions to "counterbalance" the effects of the integrin pathway. Therefore, the critical threshold levels of active FAK and PIP2 would be attained and the hepatocytes would irreversibly switch to the state of strong integrin-based/Weak E-cadherin-based adhesions, which promotes the sustained activation of the MAPK/ERK pathway and the ensuing G1/S transition. When hepatocytes are cultured at high seeding density, the increase in the number of E-cadherin homodimers is enough to induce a significant decrease in FAK activity. Nevertheless, the fact that FAK activity is still higher compared to what is observed in the absence of syndecan-4 involvement, and the persistence of the sustained MAPK/ERK activation at high density suggest that the critical threshold of FAK activation is still attained even at high density when syndecan-4 is involved. In conclusion, the inclusion of syndecan-4 in the focal adhesion constitutes a significant turning point in the establishment of the strong integrin-based/Weak E-cadherin-based adhesion steady state in rat hepatocyte culture.

6.2. **Future directions**

Culture on collagen gel

Both the molecular composition and the physical property of the extracellular matrix exert significant impacts on the activation of the integrin pathway, and thereby affect the balance between the pathways in the cell adhesion network. One particular example is the clear difference in rat hepatocyte phenotypes on collagen gel compared to what happens on collagen film. Our results and corresponding conclusions were drawn upon experimental studies using rat hepatocytes on collagen film, and it is completely conceivable that a different balance between the integrin and the E-cadherin would take place on collagen gel. Furthermore, the use of collagen gel allows the establishment of culture conditions closer to *in vivo* conditions and a more efficient control of PIP2 cellular concentrations.

The study of PIP2 effects on the hepatocyte adhesion pathways was seriously limited by the relative inefficiency of PIP2 delivery to hepatocytes on matrigel, a wider range of PIP2 concentrations may have allowed the unraveling of additional hidden properties of the hepatocyte adhesion network. The extensive array of proteins (extracellular matrix molecules, growth factors, enzymes) that are present in matrigel, does not allow a precise determination of the receptors and signaling pathways that might be involved in the regulation of a particular phenotype.

Furthermore, the inefficiency of any type of transfection (gene silencing, plasmid transfection) on matrigel imposes a strict limit on the scope of its usefulness for a more in-depth analysis of the cell adhesion pathways.

Cultures on collagen gel allow the silencing of phosphatidylinositol 4-phosphate 5-kinase (PIP5K), followed by the delivery of PIP2 at wide range of concentrations. The knockdown of PIP5K would create a low PIP2 state, identical to what is observed in hepatocytes on matrigel, the subsequent delivery of different concentrations of PIP2 would allow a more extensive investigation of its effects on the hepatocyte adhesion system.

New extracellular matrix design

The attenuation of the integrin pathway activation is necessary for a better preservation of the hepatocyte differentiation status. In addition, hepatocytes are highly polarized epithelial cells; therefore, any condition that promotes a better preservation of the hepatocyte polarity would be conducive for the preservation of their specific functions. The full activation of the integrin pathway requires the simultaneous involvement of the integrin receptors and the transmembrane proteoglycan syndecan-4, and the integrin receptor engagement to a solid substratum. Therefore, any extracellular matrix that might be capable of attenuating the activation of the integrin pathway should satisfy at least one of the following properties: ability to prevent fibronectin adsorption, and ability to inhibit syndecan-4 involvement.

Use of heparin

The incorporation of heparin, either in the culture medium or attached to the extracellular matrix, may provide a mean to satisfy the aforementioned conditions. Heparin is a highly sulfated glycosaminoglycan, which confers its overall high negative charge. Heparin may prevent the binding of syndecan-4 to the heparin-binding domain of fibronectin. In addition, the high negative charge of heparin would prevent the adsorption of fibronectin onto a collagen matrix due to charge repulsions. At physiological pH (7.3-7.4), fibronectin has a net negative charge (isoelectric point ~ 5 to 5.5) and collagen type I a net positive charge (isoelectric point ~ 8.3 to 9.3).

Addition of soluble heparin in the culture medium has been shown to promote a sustained albumin production (Lin KH, 1995), which is sign of a preservation of the differentiation status, in primary hepatocyte cultures. Data from our group have shown that rat hepatocyte cultures on collagen matrix crosslinked with heparin significantly inhibit FAK activation, and promote stronger gene expressions of some liver-specific transcription factors (**Figure 6.1**).

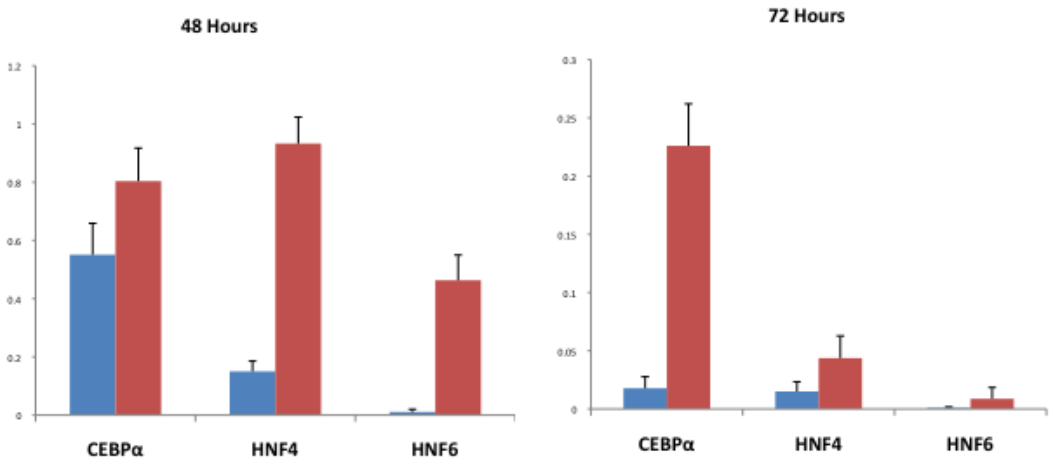

Figure 6.1. Effects of heparin on hepatocyte-specific functions. Rat hepatocytes were seeded on plates coated with collagen (blue bars) or with collagen that were covalently crosslinked with heparin. The gene expressions of the liver-specific transcription factors CEBPα, HNF4, and HNF6 were evaluated by real-time PCR at the indicated time points.

However, some challenges remain with regard to the use of heparin in primary hepatocytes cultures. First, the toxicity of soluble heparin is a factor that cannot be neglected. On the other hand , collagens that are functionalized with heparin cannot be in sandwich cultures, which have been shown to preserve hepatocyte polarity and thereby promote the retention of its specific functions. The immobilization of heparin on soluble collagen is hampered by the premature collagen fibrillogenesis in the presence of heparin. Furthermore, assuming a new method to successfully immobilize heparin onto soluble collagen is developed, the functionalized collagen would still lose its capacity to form a gel due to the presence

of heparin. Therefore, more extensive studies are needed before we can successfully use heparin to functionalize collagen in order to improve the retention of rat hepatocyte differentiation status *in vitro*.

Use of alginate functionalized with cell binding peptides

Alginates comprise a diverse family of polysaccharides that capable to form hydrogels in the presence divalent cations such as calcium, and have been extensively used in various tissue engineering applications (Andersen T, 2012). Very low protein adsorptions can happen on alginates due to its hydrophilicity and its overall negative charge. In order to improve cell attachment, carboxylic groups on alginates can be crosslinked to peptides that bind to known integrin isoforms found in mature hepatocytes (e.g. RGD peptide/$\alpha 5\beta 1$ integrin).

Chapter 7

References

Alt-Holland A, S. A.-L. (2011). Suppression of E-cadherin function drives the early stages of Ras-induced squamous cell carcinoma through upregulation of FAK and Src. *J Invest Dermatol , 131* (11), 2306-2315.

Andersen T, S. B. (2012). Alginates as biomaterials in tissue engineering. *Carbohydr Chem , 37*, 227—258.

Arthur WT, B. K. (2001). RhoA inactivation by p190RhoGAP regulates cell spreading and migration by promoting membrane protrusion and polarity. *Mol Biol Cell , 12*, 2711-2720.

Avizienyte E, F. M. (2005). *Src and FAK signaling controls adhesion fate and the epithelial-to-mesenchymal transition , 17*, 542-547.

Baciu PC, G. P. (1995). Protein kinase C regulates the recruitment of syndecan-4 into focal contacts. *Mol. Biol. Cell , 6*, 1503-1513.

Benaud CM, D. R. (2001). Regulation of the expression of c-Myc by beta1 integrins in epithelial cells. *Oncogene , 20*, 759-768.

Chen R, K. O. (2001). Regulation of Akt/PKB activation by tyrosine phosphorylation. *J Biol Chem , 276*, 31858-31862.

Cho KH, S. S. (2003). Experimental Design in Systems Biology, Based on Parameter Sensitivity Analysis Using a Monte Carlo Method: A Case Study for the TNFα-Mediated NF-κB Signal Transduction Pathway. *Simulation , 79*, 1-14.

Coutant A, R. C.-G. (2002). PI3K-FRAP/mTOR Pathway Is Critical for Hepatocyte Proliferation Whereas MEK/ERK Supports Both Proliferation and Survival. *Hepatology , 36* (5), 1079–1088.

de Rooij J, K. A.-S. (2005). Integrin-dependent actomyosin contraction regulates epithelial cell scattering. *J Cell Biol , 171*, 153-164.

Divecha N, I. R. (1995). Phospholipid signaling. *Cell , 80*, 269-278.

Doedel, E. (1981). AUTO, a program for the automatic bifurcation analysis of autonomous systems. *Cong Numer , 30*, 265-384.

Dovas A, Y. A. (2006). PKCalpha-dependent activation of RhoA by syndecan-4 during focal adhesion formation. *J Cell Sci , 119*, 2837-2846.

Duncan AW, D. C. (2009). Stem Cells and Liver Regeneration. *Gastroenterology , 137*, 466–481.

Elaut G, H. T. (2006). Molecular mechanisms underlying the dedifferentiation process of isolated hepatocytes and their cultures. *Curr Drug Metab , 7*, 629-660.

Evans DR, G. H. (2004). Mammalian Pyrimidine Biosynthesis: Fresh Insights into an Ancient Pathway . *J Biol Chem , 279*, 33035-33038.

Fassett J, T. D. (2006). Type I collagen structure regulates cell morphology and EGF signaling in primary rat hepatocytes through cAMP-dependent protein kinase A. *Mol Biol Cell , 17*, 345-356.

Fassett JT, T. D. (2003). The role of collagen structure in mitogen stimulation of ERK, cyclin D1 expression, and G1-S progression in rat hepatocytes. *J Biol Chem , 278*, 31691-31700.

Fukata M, K. S. (1999). Cdc42 and Rac1 regulate the interaction of IQGAP1 with beta-catenin. *J Biol Chem , 274*, 26044-26050.

Fukata M, W. T. (2002). Rac1 and Cdc42 capture microtubules through IQGAP1 and CLIP-170. *Cell , 109*, 873-885.

García Z, K. A. (2006). Phosphoinositide 3-kinase controls early and late events in mammalian cell division. *EMBO J , 25*, 655 - 661.

Giacinti C, G. A. (2006). RB and cell cycle progression. *Oncogene , 28*, 5220-5227.

Green KJ, G. S. (2010). Intercellular junction assembly, dynamics, and homeostasis. *Cold Spring Harb Perspect Bio , 2*, a000125.

Green, K., Getsios, S., Trovanovsky, S., & Godsel, L. (2009). Intercellular junction assembly, dynamics and homeostasis. *Cold Spring Harb Perspect Biol , 2*, a000125.

Hansen LK, W. J. (2006). Regulation of hepatocyte cell cycle progression and differentiation by type I collagen structure. *Curr Top Dev Biol , 72*, 205-236.

Hatzis P, K. I. (2006). Mitogen-Activated protein kinase-mediated disruption of enhancer-promoter communications inhibits Hepatocyte Nuclear factor 4 α expression. *Mol Cell Biol , 26*, 7017-7029.

Hodgkinson CP, W. M. (2000). Fibronectin-mediated hepatocyte shape change reprograms Cytochrome P450 2C11 gene expresson via an integrin-signaling induction of ribonuclease activity. *Mol Pharmacol , 58*, 976-981.

Holsinger LJ, W. K. (2002). The transmembrane receptor protein tyrosine phosphatase DEP1 interacts with p120(ctn). *Oncogene , 21*, 7067-7076.

Hommelgaard AM, L. M. (2004). Association with membrane protrusions makes ErbB2 an internalization-resistant receptor. *Mol Biol Cell , 15*, 1557-1567.

Insall RH, W. O. (2001). PIP3, PIP2, and cell movement--similar messages, different meanings? *Dev Cell , 1*, 743-747.

Izumi G, S. T. (2004). Endocytosis of E-cadherin regulated by Rac and Cdc42 small G proteins through IQGAP1 and actin filaments. *J Cell Biol , 166*, 237-248.

Ji X, X. Y. (2006). libSRES: a C library for stochastic ranking evolution strategy for parameter estimation. *Bioinformatics , 22*, 124-126.

Kawakami K, T. H. (2001). Dynamics of integrin clustering at focal contacts of endothelial cells studied by multimode imaging microscopy. *J Cell Sci , 114*, 3125-3135.

Kemler R, H. A. (2004). Stabilization of beta-catenin in the mouse zygote leads to premature epithelial-mesenchymal transition in the epiblast. *Development , 131*, 5817-5824.

Kim D, R. O. (2007). A hidden oncogenic positive feedback loop caused by crosstalk between Wnt and ERK pathways. *Oncogene , 26*, 4571-4579.

Kim SH, A. T. (2007). Epidermal growth factor signaling for matrix-dependent cell proliferation and differentiation in primary cultured hepatocytes. *Tissue Eng , 13* (3), 601-609.

Kim SH, L. Z. (2000). E-cadherin-mediated cell-cell attachment activates Cdc42. *J Biol Chem , 275* (47), 36999-37005.

Kimata T, N. M. (2006). Actin organization and hepatocyte differentiation are regulated by extracellular matrix via PI-4,5-bisphosphate in the rat. *Hepatology , 44* (1), 140-151.

Koenig A, M. C. (2006). Collagen type I induces disruption of E-cadherin-mediated cell-cell contacts and promotes proliferation of pancreatic carcinoma cells. *Cancer Res , 66*, 4662-4671.

Kwon S, S. H. (2009). Syndecan-4 promotes the retention of phosphatidylinositol-4,5 -bisphosphate in the plasma membrane. *FEBS Letters , 583*, 2395-2400.

Lévay M, S. J. (2009). Regulation of the substrate preference of p190RhoGAP by protein kinase C-mediated phosphorylation of a phospholipid binding site. *Biochemistry , 48*, 8615-8623.

Lin KH, H. H. (1995). Albumin synthesis by rat hepatocytes cultured on collagen gels is sustained specifically by heparin. *Exp Cell Res , 219*, 717-721.

Ling K, D. R. (2002). Type I-gamma phosphatidylinositol phosphate kinase targets and regulates focal adhesions. *Nature , 420*, 89-93.

Liu F, J. L.-B. (2010). Cadherins and Pak1 control contact inhibition of proliferation by Pak1-betaPIX-GIT complex-dependent regulation of cell-matrix signaling. *Mol Cell Bio , 30*, 1971-1983.

Loyer P, C. S.-G. (1996). Growth Factor Dependence of Progression through G and S Phases of Adult Rat Hepatocytes in Vitro. *J Biol Chem , 271*, 11484-11492.

Luo Y, D. C. (2007). *J Pharmacol Exp Ther , 321*, 884-891.

Maeda Y, H.-V. W. (2006). Tumour suppressor p53 down-regulates the expression of the human hepatocyte nuclear factor 4α (HNF4α) gene. *Biochem J , 400*, 303-313.

Maekawa M, N. E. (2002). Identification of the Anti-proliferative Protein Tob as a MAPK Substrate. *J Biol Chem , 277*, 37783-37787.

Markevich NI, H. J. (2004). Signaling switches and bistability arising from multisite phosphorylation in protein kinase cascades. *J Cell Biol , 164*, 353-359.

McNulty DE, L. Z. (2011). MAPK scaffold IQGAP1 binds the EGF receptor and modulates its activation. *J Biol Chem , 286*, 15010-15021.

Meloche S, P. J. (2007). The ERK1/2 mitogen-activated protein kinase pathway as a master regulator of the G1- to S-phase transition. *Oncogene , 26*, 3227-3239.

Mizuno K, H. O. (1993). Cell density-dependent regulation of hepatocyte growth factor receptor on adult rat hepatocytes in primary culture. *J Biochem , 114* (1), 96-102.

Mooney DJ, L. R. (1995). Cytoskeletal filament assembly and the control of cell spreading and function by extracellular matrix. *J Cell Sci , 108*, 2311-2320.

Mossin L, B. H. (1994). Ploidy-Dependent growth and binucleation in cultured rat hepatocytes. *Exp. Cell Res. , 214*, 551-560.

Murphy LO, S. S. (2002). Molecular interpretation of ERK signal duration by immediate early gene product. *Nat Cell Biol , 4*, 556-564.

Myers JP, R. E.-S. (2012). Focal adhesion kinase modulates Cdc42 activity downstream of positive and negative axon guidance cues. *J Cell Sci , 125*, 2918-2929.

Nakagawa M, F. M. (2001). Recruitment and activation of Rac1 by the formation of E-cadherin-mediated cell-cell adhesion sites. *J Cell Sci , 114*, 829-838.

Nikolaidou-Neokosmidou V, Z. V. (2006). Inhibition of hepatocyte nuclear factor 4 transcriptional activity by the nuclear factor κB pathway. *Biochem J , 398*, 439-450.

Nojima H, A. M. (2008). IQGAP3 regulates cell proliferation through the Ras/ERK signalling cascade. *Nat Cell Biol , 10*, 971-978.

Noren NK, A. W. (2003). Cadherin engagement inhibits RhoA via p190RhoGAP. *J Biol Chem , 278*, 13615-13618.

Noren NK, N. C. (2001). Cadherin engagement regulates Rho family GTPases. *J Biol Chem , 276* (36), 33305-33308.

Oda H, Y. Y. (2007). Cell shape, cell-cell contact, cell-extracellular matrix contact and cell polarity are all required for the maximum induction of CYP2B1 and CYP2B2 gene expression by phenobarbital in adult rat cultured hepatocytes. *Biochem Pharmacol , 75* (5), 1209-1217.

Owen KA, A. M. (2011). FAK regulates intestinal epithelial cell survival and proliferation during mucosal wound healing. *PLoS One , 6* (8), e23123.

Paine AJ, A. E. (2004). Activation of signaling pathways during hepatocyte isolation: relevance to toxicology in vitro. *Toxicol. In Vitro , 18*, 187-193.

Paine, A. (1990). The maintenance of cytochrome P450 in rat hepatocyte culture: some applications of liver cell cultures to the study of drug metabolism toxicity and the induction of the P450 system. *Chem Biol Interact , 74*, 1-31.

Partridge MA, M. E. (2006). Initiation of attachment and generation of mature focal adhesions by integrin-containing filopodia in cell spreading. *Mol Biol Cell* , 4237-4248.

Pfaffl, M. (2001). A new mathematical model for relative quantification in real-time RT-PCR. *Nucleic Acids Res , 29*, e45.

Rameh LE, C. L. (1999). The role of phosphoinositide 3-kinase lipid products in cell function. *J Biol Chem , 274*, 8347-8350.

Ramis-Conde I, D. D. (2008). Modeling the influence of the E-cadherin-beta-catenin pathway in cancer cell invasion: a multiscale approach. *Biophys J , 95*, 155-165.

Ren JG, L. Z. (104). IQGAP1 modulates activation of B-Raf. *Proc Natl Acad Sci U S A , 2007*, 10465-10469.

Rosner M, S. K. (2013). Merging high-quality biochemical fractionation with a refined flow cytometry approach to monitor nucleocytoplasmic protein expression throughout the unperturbed mammalian cell cycle. *Nat Protoc , 8*, 602-626.

Roy M, L. Z. (2004). IQGAP1 binds ERK2 and modulates its activity. *J Biol Chem , 279*, 17329-17337.

Roy M, L. Z. (2005). IQGAP1 is a scaffold for mitogen-activated protein kinase signaling. *Mol Cell Bio , 25*, 7940-7952.

Scheving LA, Z. L. (2006). The emergence of ErbB2 expression in cultured rat hepatocytes correlates with enhanced and diversified EGF-mediated signaling. *Am J Physiol Gastrointest Liver Physiol , 291*, G16-25.

Schorl C, S. J. (2003). Loss of protooncogene c-Myc function impedes G1 phase progression both before and after the restriction point. *Mol Biol Cell , 14*, 823-835.

Schug M, H. T.-R. (2008). Primary rat hepatocytes as in vitro system for gene expression studies: comparison of sandwich, Matrigel and 2D cultures. *Arch. Toxicol , 82*, 923-931.

Seglen, P. (1976). Preparation of isolated rat liver cells. *Methods Cell Biol , 13*, 29-83.

Semler EJ, M. P. (2001). Engineering hepatocyte functional fate through growth factor dynamics: the role of morphological priming. *Biotech Bioeng , 75*, 510-520.

Serra-Pagès C, K. N. (1995). The LAR transmembrane protein tyrosine phosphatase and a coiled-coil LAR-interacting protein co-localize at focal adhesions. *EMBO J , 14*, 2827-2838.

Servant MJ, G. E. (1996). Inhibition of Growth Factor-induced Protein Synthesis by a Selective MEK Inhibitor in Aortic Smooth Muscle Cells. *J Biol Chem , 271*, 16047-16052.

Shan Y, Y. L. (2009). Nudel and FAK as antagonizing strength modulators of nascent adhesions through paxillin. *PLoS Biol , 7* (5), e1000116.

Shen Y, L. N. (2008). Nudel binds Cdc42GAP to modulate Cdc42 activity at the leading edge of migrating cells. *Dev Cell , 14*, 342-353.

Simons M, H. A. (2001). Syndecan-4-mediated signalling. *Cell Signal , 13*, 855-862.

Sinha S, Y. W. (2008). Cellular signaling for activation of Rho GTPase Cdc42. *Cell Signal , 20*, 1927-1934.

Song G, O. G. (2005). The activation of Akt/PKB signaling pathway and cell survival. *J Cell Mol Med , 9*, 59-71.

Stokes JB, A. S.-D. (2011). Inhibition of focal adhesion kinase by PF-562,271 inhibits the growth and metastasis of pancreatic cancer concomitant with altering the tumor microenvironment. *Mol Cancer Ther , 10*, 2135-2145.

Swat M, K. A. (2004). Bifurcation analysis of the regulatory modules of the mammalian G1/S transition. *Bioinformatics , 20*, 1506-1511.

Symons JR, L. C. (2002). Expression of the leucocyte common antigen-related (LAR) tyrosine phosphatase is regulated by cell density through functional E-cadherin complexes. *Biochem J , 365*, 513-519.

Tamura M, G. J. (1999). PTEN interactions with focal adhesion kinase and suppression of the extracellular matrix-dependent phosphatidylinositol 3-kinase/Akt cell survival pathway. *J Biol Chem , 274*, 20693-20703.

Tinel M, B. A. (2003). Downregulation of cytochromes P450 in growth-stimulated rat hepatocytes: role of c-Myc induction and impaired C/EBP binding to DNA. *J Hepatol , 39*, 171-178.

Tomar A, S. D. (2009). Focal adhesion kinase: switching between GAPs and GEFs in the regulation of cell motility. *Curr Opin Cell Biol , 21* (5), 676-683.

Tyson JJ, C. K. (2001). Network dynamics and cell physiology. *Nat Rev Mol Cell Biol , 2*, 908-916.

Weernink PA, M. K. (2004). Activation of type I phosphatidylinositol 4-phosphate 5-kinase isoforms by the Rho GTPases, RhoA, Rac1, and Cdc42. *J Biol Chem , 279*, 7840-7849.

Wilcox-Adelman SA, D. F. (2002). Syndecan-4 modulates focal adhesion kinase phosphorylation. *J Biol Chem , 277*, 32970-32977.

Woods A, C. J. (1986). Adhesion and cytoskeletal organization of fibroblasts in response to fibronectin fragments. *EMBO J , 5*, 665-670.

Xie Y, Y. J. (2012). IQGAP2, A candidate tumour suppressor of prostate tumorigenesis. *Biochim Biophys Acta , 1822*, 875-884.

Yang L, W. L. (2006). Gene targeting of Cdc42 and Cdc42GAP affirms the critical involvement of Cdc42 in filopodia induction, directed migration, and proliferation in primary mouse embryonic fibroblasts. *Mol Biol Cell , 17*, 4675-4685.

Yeatman, T. (2004). A renaissance for SRC. *Nat Rev Cancer , 4*, 470-480.

Yoshida Y, N. T. (2003). Mice lacking a transcriptional corepressor Tob are predisposed to cancer . *Genes Dev , 17*, 1201-1206.

Yun MS, K. S. (2005). Both ERK and Wnt/beta-catenin pathways are involved in Wnt3a-induced proliferation. *J Cell Sci , 118*, 313-322.

Zegers MM, F. M. (2003). Pak1 and PIX regulate contact inhibition during epithelial wound healing. *EMBO J , 22*, 4155-4165.

Zi Z, C. K. (2005). In silico identification of the key components and steps in IFN-gamma induced JAK-STAT signaling pathway. *FEBS Lett , 579*, 1101-1108.